POLITECNICO DI TORINO

Dipartimento di Scienza Applicata e Tecnologia

Dottorato di Ricerca in Ingegneria Chimica
XXVII ciclo (2012-2014)

CARRIER ASSISTED DYEING OF
m-ARAMID FIBERS

Candidato: **Francesco Aimone**
Matricola: 189145

Relatori   Controrelatore
Prof. Giorgio Rovero   **Prof. Giuseppe Rosace**
Prof.ssa Ada Ferri

Coordinatore del Corso di Dottorato
Prof. Marco Vanni

Abstract

The excellence in quality of Biella wool fabric, provided from the last 40 years one of first position in all over the world for the "Biella textile district". In the last decade competition of developing countries became ruthless regarding the common textile like wool for a lot of reason, first of all cheaper labor. Industries started to move production over there but, fortunately, the know-how has remained here. For these reasons, since the past 10 years the world of textile, especially in Europe and USA, is moving to another kind of textile and garments dimension: the Technical Textile. Aramids are, since 90's, the most important technical textile for protection garments, and in Biella district a lot of factories started to handle them. Since some factories started to produce yarn and fabric for protective garments, the need to dye them has come. The market nowadays requires, even for protective goods, not only the conventional coloration with which the fiber is produced in large scale by manufacturers, but all the typical color ranges of other common textile fibers. Nomex® fiber is probably the most important m-aramid used for this scope and its dyeing recipes are well known. However, Nomex® is not easily available for factories due to particular commercial agreements, and is very expensive. Other branded m-aramid fibers exist on the market having same technical properties of Nomex® but, unfortunately, not exactly the same dyeability. In 2010 a regional research project called FILIDEA was born between Politecnico di Torino and Marchi&Fildi Company. One of the 6 research working packages was thought to overcome the difficulties in dyeing a m-aramid fiber called X-Fiper® and produced by a Chinese company called SRO. From this project, since the important results obtained in the first two years of research work, a Ph.D. project was born in 2012. Therefore, the aim of this Ph.D. project is to investigate the dyeing process of this particular fiber starting from the examination of its properties. In this thesis, Chapter I gives a general description of aramid fibers, including also its typical applications. In the second Chapter the crucial role of a carrier, that swells the fiber during dyeing, has been discussed. The main part of the thesis is certainly Chapter 3, in which the thermodynamic and kinetic aspects, of the carrier assisted X-Fiper® dyeing, have been evaluated. Chapter 4 gives a starting point in using ultrasounds in pretreating the dyeing liquor, aiming to increase the dispersion of a disperse dye. Finally, in the last chapter, the capillary electrophoresis technique was applied in wastewater treatment to separate basic dyes mixtures. This last part of the experimental work was carried out during the period abroad of this Ph.D., at the University of British Columbia, Vancouver, Canada.

Contents

Contents

Chapter 1

1. The Aramid Fibers, an introduction

This chapter will provide the concept of aramid fiber with the description of the most important member or this class of technical fiber. Structure, physical and chemical properties as well as product applications will be discussed to give the reader the basic knowledge and useful information for the comprehension of next chapters.

Aramids are synthetic fibers deriving from wholly aromatic polyamides, particular polymers in which at least the 85% of the amides groups are linked between 2 aromatic rings. These kinds of polymers were discovered and synthesized in the first years of the 40s.

Aromatic polyamides can be divided into AB and AABB types, where A stands for the aminic group (-NH-) and B stands the the carboxylic group (-CO-).

Using as monomer for the synthesis 3-aminobenzoic acids or similar the AB type is obtained; otherwise, using di-acids (chloride is better then di-acid for chemical synthesis) and di-amines the AABB type is obtained:
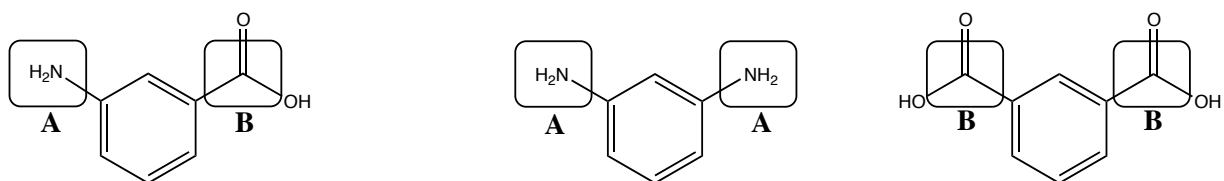
Figure 1. Example of monomers used for AB or AABB polymer synthesis of aromatic polyamides

The molecular structure of aromatic polyamides is responsible of the peculiar chemical and physical properties such as solubility, transition temperature, thermal stability, and crystallization rate as

well as fiber properties. Modifications of polymer composition are often required modify critical polymer properties.

These modifications consists of changing or applying some functional groups to the aromatic rings (AB type or AABB type), or employing spacer group between polymer chains [1a,1b].

Wholly aromatic polyamides are called aramids or aramid fibers to identify them as a new class of materials and to distinguish them from aliphatic polyamides such as nylon and aromatic-aliphatic polyamides.

Aramid fibers had the highest strength-to-weight ratio of any commercially available fiber at the time of their first commercial introduction in the early 1970s. The first commercial aramid fiber, the poly(*m*-phenylene isophthalamide), was produced in the laboratories of Du Pont in Delaware in the middle of the 60s and it took the trade name of Nomex.

After a few years the correspondent para linked fiber, poly(*p*-phenylene terephthalamide), was produced and called Kevlar.

Aramids are well known for their thermal stability and chemical resistance. They also exhibit higher glass transition and melt temperature than aliphatic polyamides.

Hundreds different aramids exist and is very difficult to classify them, so they are often simply divided in two big categories, meta-linked and para-linked one. After Du Pont, many companies all over the world began to produce these fibers due to their outstanding properties. The most commercialized m-aramid fibres are: Nomex from Du Pont (USA), Conex from Teijin (Japan), NewStar from Yantai (China) e and X-fiper from SRO (China). The most commons p-aramid fibers are Kevlar from Du Pont, Twaron and Technora from Teijin.

The focus of this thesis is in m-aramids, which are described in paragraph 1.2. For the sake of completeness, a short description of p-aramids is given in the next paragraph (1.1).

1.1 p-Aramid fibers

The earliest p-aramid fiber was produced by Du Pont under the trade name of Kevlar and was initially targeted at reinforcement of tires and plastics. The characteristics of lightweight, high strength and high toughness have led to development of applications in composites, ballistics, tires, reinforcements, ropes, cables and asbestos replacement.

The chemical composition of Kevlar is poly para-phenylene terephthalamide (AABB polymer type). This fiber, also known as PPD-T, is made from the condensation reaction between paraphenylene diamine and terephthaloyl chloride. The chemical reaction is shown in the figure below (Figure 2).
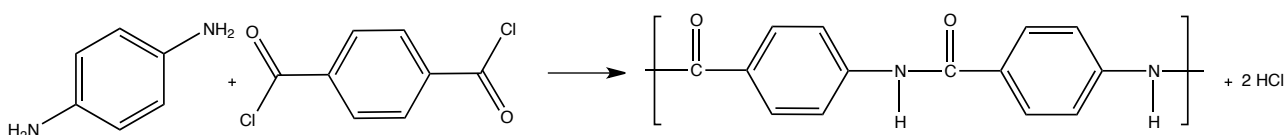
Figure 2. Reaction between *p*-phenylene diamine and terephthaloyl chloride giving *p*-phenylene terephthalamide

The aromatic ring structure contributes to its high thermal stability. The high strength and modulus are due to the para configuration giving stiffness to the polymer. Para aramid fibers belong to the liquid crystalline polymer class (LCP) of material for some reasons. First, these polymers are very rigid and rodlike, and in solution they can aggregate to form ordered domains in parallel arrays [2].
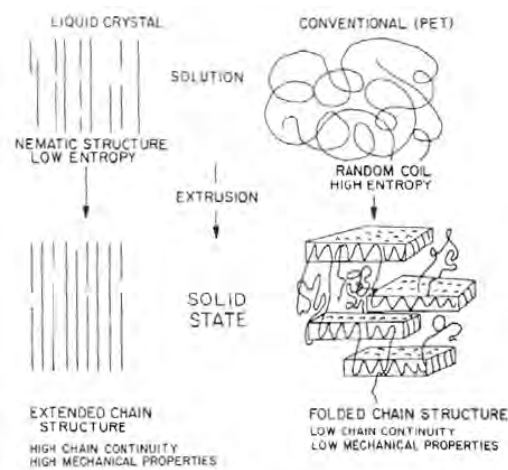
Figure 3. Space disposition of p-aramid fibers in solution.

Unlike conventional polymers that can bend and entangle forming random coils, when PPD-T solution (using concentrated sulfuric acid as solvent) is extruded, the liquid crystalline domains can

3

orient and align in the direction of flow. The degree of alignment is exceptional: straight polymer chains parallel to the fiber axis. This kind of structure is highly anisotropic and gives much higher strength and modulus in the fiber longitudinal direction then in the radial direction. Post process operations, like high-temperature processing under tension, can further increase the crystalline structure orientation raising the fiber modulus [3].

1.1.1 Fiber form and applications of p-aramid fibers

Kevlar is available as continuous filament:
- Yarns
- Rovings
- Woven fabrics

and discontinuos
- Staple and spun yarns
- Fabric
- Pulp

Because p-aramid yarn and rovings are relatively flexible and nonbrittle, they can be processed in most conventional textile operations, such ah twisting, weaving, knitting, carding and felting. Applications include missile cases, pressure vessels, sporting goods, cables, and tension members.

The principal aramid form used in composites is aramid Kevlar woven fabric. Generally, fabrics made of a very fine size of p-aramid are thin, lightweight, and relatively costly, and they are used when ultra lightweight, thinness and surface smoothness are critical. Applications for high-modulus p-aramid fabrics include commercial aircraft and helicopter secondary composite parts, particularly facings of honeycomb sandwich construction, boat hulls, electrical and electronic parts, ballistic systems and coated fabrics. Textured aramid can be processed through a high-velocity air jet to attain filament loops in the continuous filament yarns. The yarns are used in asbestos replacement to give the composite a higher resin-to-aramid ratio and in protective apparel to achieve superior textile aesthetics. Although the continuous filament form dominate composites applications, the use of aramid in discontinuous or short fiber form is rapidly increasing. One reason of this increase is that the inherent toughness of aramid allows the creation of fiber forms not readily available with other reinforcing fibers. Spun yarns formed in this way are not as strong or as stiff as continuous aramid filament yarns, but are bulkier, pick up more resin and have tactile characteristics similar to cotton or wool. They are used in asbestos replacement for clutch facings, and as sewing thread. The shorter aramid fibers are used to reinforce thermoset, thermoplastic and elastomeric resins. Applications include automotive, truck brake, clutch linings, gaskets, electrical parts and wear resistant thermoplastic parts. Woven and knit fabrics from discontinuous filament are used in asbestos replacement and in protective apparel because of their resistance to cutting, puncture,

abrasion, or thermal exposure. Felts are also available in this form and are used as well as in asbestos replacement then in ballistic armor and marine laminated. Also available in pulp form, Kevlar and p-aramid in general, can be easily mixed into resins formulations and is used extensively in replacing asbestos in gaskets, friction products, sealants, caulks and coating [4].

1.1.2 p-Aramid properties

The properties of Kevlar as representative example of p-aramid fiber will be discussed in this paragraph. The most important properties of this fiber are summarized in Table below.
The tensile modulus of p-aramid fibers is a function of molecular orientation. Kevlar fiber exists in three different configurations, having different tensile modulus. Every type of fiber has different properties (Table 1).

Material	Density (g/cm^3)	Filament Diameter (um)	Tensile Modulus (GPa)	Tensile Strength (GPa)	Tensile Elongation (%)
Kevlar 29	1.44	12	62	3.6	4.0
Kevlar 49	1.44	12	131	3.6-4.1	2.8
Kevlar 149	1.47	12	179	3.4	2.0

Table 1. Properties of p-aramid fiber.

Kevlar 29 (called high toughness p-aramid fiber) has tensile modulus (62 GPa) slightly lower than tensile modulus of E-glass (69 GPa). Heat treatment under tension increases crystalline orientation and the resulting fiber, Kevlar 49 (high modulus p-aramid fiber) has a modulus double if compared with Kevlar 29 (131 Gpa). Kevlar 149 (ultrahigh modulus) has an even higher modulus, 179 GPa.
The tensile strength of p-aramid fiber is in the range of 3.7-4.2 GPa. If we consider the same property of conventional organic fiber such as Nylon 66, p-aramid has more then twice the strength. Other important features are tensile properties in hot/wet conditions. High modulus yarns show a linear decrease of both tensile strength and modulus when tested at elevated temperatures in air. However, this decreasing is slight and more then 80% of these properties are retained at 180 °C. The effect of moisture on these properties, at room temperature, is lower then 5%, and at elevated temperature appears to be reversible. Yarn conditioned for 3 weeks at 180 °C with 95% relative humidity and tested at high temperature had essentially the same behavior as dry yarn. Besides, test of yarns while immersed in hot water suggested a loss of 10% of tensile strength due to the water alone [5].
The creep rate of p-aramid fiber is very low and similar to glass fiber one but less vulnerable to creep rupture. Although p-aramid fiber responds very elastically in tension, under compression it

exhibits a ductile behavior. If a certain compression strain is applied, a formation of defects has been observed and called kick bands. Kick bands are probably related to compressive bulking of the molecular structure. For this reason the use of this fiber in application subjected to compressive or flexural loads is limited.

Probably, the best characteristics of the p-aramids (and aramid fibers in general) are their thermal properties. The high degree of thermal stability is due to the aromatic structure of the polymer. PPD-T doesn't have a literal melting point or glass transition temperature (Tg) like other synthetic polymer, Tg for example is estimated to be around 375°C. PPD-T decompose in air at 425 °C and is inherently flame resistant. It is possible to use p-aramid fiber in the range of -200 - +200 °C but usually is not used with temperature above 150 °C for the oxidation. The thermal conductivity is low ( ); p-aramid is even an electrical insulator with a dielectric constant of circa 4.0 (measured at 60Hz). The index of refraction is 2.0 parallel to the fiber axis and 1.6 perpendicularly.

Finally, Kevlar and p-aramid fibers in general show a very strong chemical resistance to organic solvent and diluted acid and bases. However, p-aramids are degraded by strong acid and bases, using strong acid such as concentrated sulfuric acid it is possible to dissolve it. Ultraviolet radiation also degrades p-aramid fiber. The degradation depends on materials thickness because p-aramid is self-screening [6-7].

1.2 m-Aramid fibers

The other category of aramids includes all fibers in which the amidic group is bonded in *meta* position with the two aromatic rings. The founder of this family is certainly Nomex, it was developed in the laboratories of Du Pont and commercialized the first time in 1961. The first name of this fiber was Nomex Nylon for its chemical similarities with aliphatic polyamides, but in 1972 its name changed in Nomex Aramid. Nomex is used in many high temperature applications such as thermal protective clothing, electrical application, honeycomb structures for aircraft and industrial filtration [8-10].

Nomex and all m-aramid fiber are based on wholly aromatic polyamide and chemically known as poly(m-phenylene isophthalamide) or MPD-I (AABB polymer type). The reaction of polycondensation of m-phenylenediamine and isophthaloyl chloride take place at low temperature using and amide solvent as shown in Figure 3.
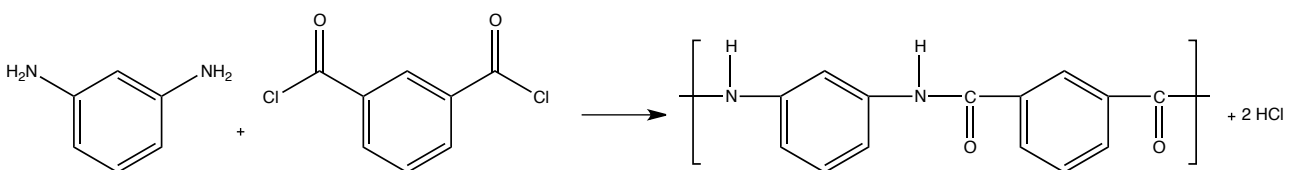
Figure 4. Reaction between *m*-phenylene diamine and isophthaloyl chloride giving *m*-phenylene isophthalamide

Some of the solvents, in which reagents are dissolved, for low temperature condensation are: dimethylacetamide (DMA), dimethylsulfoxide (DMSO) and N-methylpirrolidone. Some salts are added into the reaction solution: for example, to increase the polymer solubility in the polymerization solvent, a basic metal salt such as lithium chloride or hydroxide must be used. Calcium hydroxide is even used to neutralize hydrochloric acid generated during the reaction.

Unsubstituted polymer (MPD-I) exhibits density of 1.43-1.46 g/cm^3 and a glass transition temperature (Tg) of about 280 ºC. Other polymers containing pendant substitutions can show a bit lower Tg (255-260 ºC).

Increasing polymer chemical of physical properties, copolymerization is also possible. Teijin reported a synthesis of a copolymer formed by 75% of repeated unit of MPD-I and segments of diamine alkyl-substituted, that improve dyeability and thermal stability [11]. Another example of copolymer is reported in the studies of Fujie, that synthesized a polymer containing 95% of MPD-I and some organic phosphorous compounds, used to improve the polymer flame resistance [12].

The molecular weight of the polymer formed is generally affected by the monomer stoichiometry, the salt concentration, impurities and reaction temperature. Many studies have been published in this regard. For example Zhizdyuk and Vladimirova discovered that, adding diacid chloride to the solution of diamine and DMA, promotes high polymer molecular weight. Polymer M.W. is also incresed if the temperature is raised near the end of the reaction [13]. Preston observed that the inherent viscosity (viscosity related to the weight average molecular weight of a polymer) of MPD-I increase if the concentration of monomer in DMAc is up to 0.5 M [14].

1.2.1 Fiber Preparation and Products

MPD-I under normal reaction condition remains soluble into the polymerization solvent. This mixture can be extruded directly to form fibers or may be isolated from the reaction mixture and re-dissolved in other amide solvents forming a homogeneous solution for fiber spinning. Using low boiling point solvents like DMAc alone or in hydrocarbon mixture, either dry or wet spinning method can be used to prepare fiber deriving from MPD-I. However, most of the recent literature appears to be more favorable to the wet-spinning method. During spinning, other processes such as drawing and heat treatment are necessary to achieve high fiber strength, homogeneity, good tensile strength and thermal stability. These processes could be also carried out adding other molecules such as pigments, obtaining colored fibers. In addition to drawing and heat treatment, it's possible to treat chemically MPD-I to enhance some functional properties. Treating MPD-I with a solution of tertiary amines, seems to impart dyeability under atmospheric pressure [15].

Nomex and m-aramid fibers are produced in the form of staple, continuous filament yarn and industrial paper. Nomex staple can be converted in all fabric types and can be used for industrial gas filtration. Nomex exhibits better performance, in acid or nonacid condition, then polyester. However is not recommended to use m-aramids with high concentration of hydracids deriving from halogens. Thanks to its outstanding thermal resistance and low flammability, m-aramids are used in all over the world in protective fire clothing, military and sports uses. Continuous filament yarns are used for high temperature applications but, since aramids are not considered dyeable fibers, continuous filament has the disadvantage of not being blended. Nomex industrial paper is available in different thickness and density depending on the end use of the product. Papers are mainly used for electrical application such as: wire wrap phase insulation, end laminates, armature slot insulation, crossover tubing or end caps in motors and generators. They are also used in military and aerospace applications [16].

1.2.2 Fiber properties

Thanks to the abundance of bibliography about Nomex, key properties will be discussed as example of m-aramid fibers properties [17-23].

Color
All undyed m-aramid fibers have intrinsic coloration that depends on the product type. This coloration varies from nearly white to yellowish white.

Density
Measured at 21 °C, Nomex present a density of 1.38 g/cm^3, a bit lower than Kevlar p-aramid fiber.

Tensile properties
Typical tensile properties of Nomex (conditioned at 65% humidity) are around 44 cN/tex (gram per denier), circa 885 cN/tex of initial modulus and 20-30% of elongation to break. All these properties depend on the type or fiber. An example of stress/strain curve of Nomex 430 at ambient temperature is reported in Figure 4.
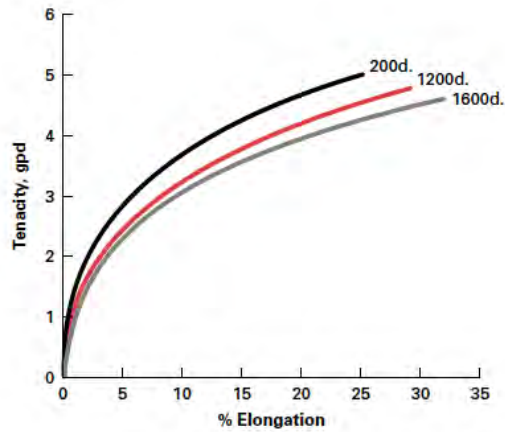
Figure 4. Typical stress/strain curve of Nomex 430 Yarn; 3 TPI, 10" gauge length, 12 in/minute extension rate. 200d = 200 denier.

The breaking tenacity and modulus of Nomex fiber increase with increasing strain rate under impact-loading conditions. After exposure to various temperatures in dry air, the fiber tenacity and modulus decrease increasing the exposure temperature, while the elongation to break increase, increasing temperature (Figure 5).
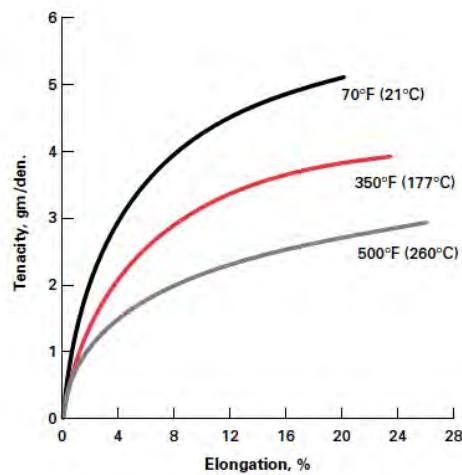
Figure 5. Stress/Strain Curve for 200 Denier type 430 NOMEX® Tested at Various Temperatures after 5 Minute Exposure (100-filament yarn with 3 TPI, 60%/minute extension rate)

As shown in graph above, Nomex is able to retain its tensile properties after short exposures at 260 ºC, the melting temperature of nylon 66.

9

Thermal properties

The thermal stability of m-aramid is probably its best physical property, which allowed Nomex and m-aramid to be the most popular choice in technical fibers.
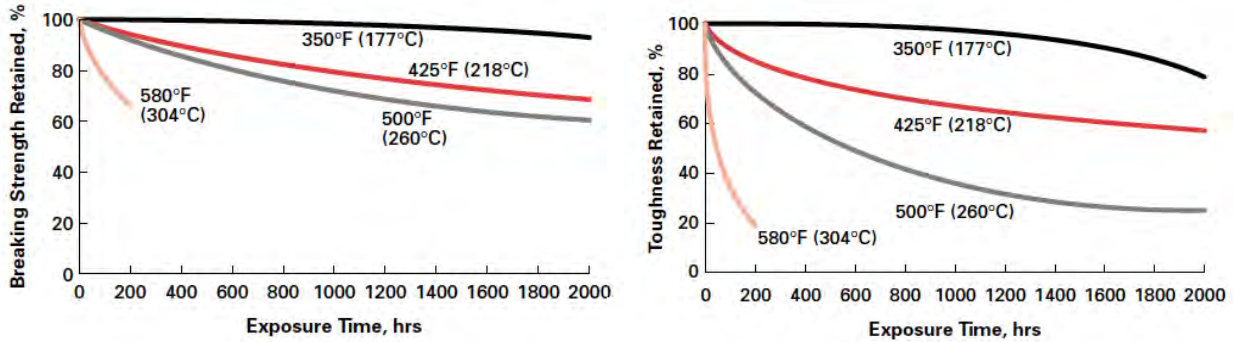
Figure 6. Strength and toughness retained by Nomex type 430 after prolonged exposure to hot, dry air.

The effect of prolonged exposure to hot air is shown in Figure 6.

After exposing Nomex type 430 to dry air at different temperature for 2000 hours and then returning it to room temperature, Nomex retain circa 65% of its ambient (21 ºC tested) breaking strength after exposure for 1000 hours at 260 ºC, and approximately the 35% of the initial toughness that exhibited before exposure.

Moreover, Nomex does not melt and is very stable at elevated temperature. However the fiber starts to degrade rapidly after 370 ºC, but there is not a defined melting point as shown in DSC (differential scanning calorimetry) graph of Nomex type 450 (Figure 7). It is also possible to see the typical "Tg stair" around 260-270 ºC.
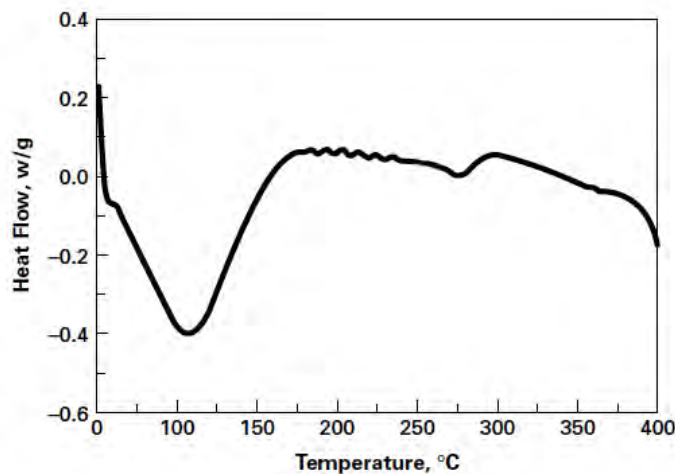
Figure 7. Differential Scanning Calorimetry of Nomex 450 under nitrogen.

Thermogravimetric analysis (TGA) of Nomex type 455 (Figure 8) shows less then 10% of weight loss up to 400 ºC both in nitrogen and air. It's even possible to see that thermal oxidation in air is time/temperature dependent. Fiber charring can occur in just 30 seconds at 350 ºC in air. Obviously, increasing the temperature, the time to form chair is decreased.
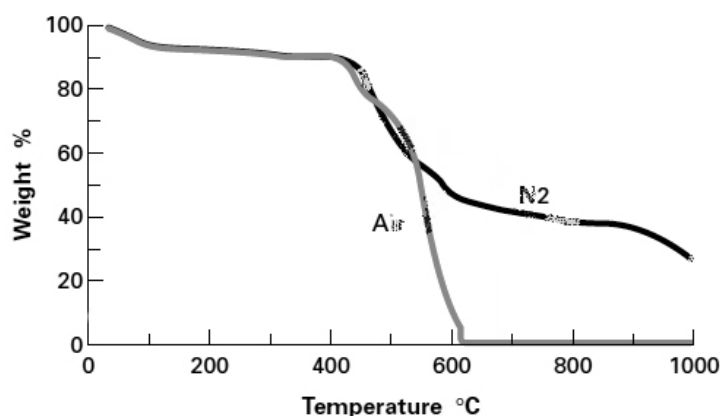
Figure 8. Thermogravimetric Analisys of Nomex 455 under nitrogen and air.

Nomex fiber has a specific heat of 0.29 cal*g^{-1}*ºC^{-1}.

Flex and abrasion resistance
Flex resistance of Nomex is totally comparable to flex resistance of polyester fiber or nylon 66. Testing single filament bent repeatedly in a 180º arc around a 3 mm diameter wire, Nomex gave a flex life of about 50000 cycles.
Abrasion resistance is an important parameter to be taken into account in both protective apparel and filtration applications. Abrasion from wear and laundering is the primary cause of garments failure, while abrasion from dust exposure often leads to filter bag failure. Abrasion resistance of m-aramids is very good, is about equal to that of 2 dpf (denier per filament) of polyester and nylon 66 [17].

Chemical resistance
Nomex, and in general all m-aramid fibers, exhibits very good resistance to many chemicals. It is highly resistant to most hydrocarbons and organic solvents. It shows very good hydrolytic resistance to acids and bases at room temperature, more then nylon 66 but not as good as polyester. However it can be degraded and dissolved by strong acids and bases or diluted acid and bases at elevated temperatures. The chemical resistance during exposure in use and to chemicals and solvents used in cleanings contributes to the excellent durability and wear life of textile and garments. Moreover, Nomex shows a good resistance to sodium hypochlorite bleach with a

moderate strength loss. m-Aramids are very resistant to degradation by fluorine containing elastomers, resins and refrigerants even at high temperatures, more then glass fibers.

In the table below there are some data of chemical resistance at different time and exposures to some organic solvents, acids and bases.

Chemical Substance	Concentration %	Temperature (ºC)	Time (hours)	Effect on Break. Strength*
Strong mineral acids				
Hydrochloric	1	70	10	Slight
	10	70	10	Appreciable
	37	70	10	Degraded
Sulfuric	10	20	100	None
	10	120	100	Appreciable
	70	20	100	None
	96	20	100	Degraded
Nitric	1	20	100	Slight
	10	20	100	Moderated
	70	20	100	Appreciable
Organic acids				
Acetic	99.9	20	100	None
	99.9	100	100	None
Formic	88	20	100	None
	88	100	100	Moderate
Strong bases				
Ammonia	28	20	1000	None
Sodium hydroxide	10	20	1000	None
	10	100	100	Degraded
	40	20	100	None
	40	120	10	Degraded
Oxidizing and Reducing				
Sodium hypochlorite	0.01	20	100	Slight
	0.4	20	100	Slight
Hydrogen Peroxide	0.4	20	1000	None
	0.4	70	100	None
Organic solvents				
Acetone	100	60	100	Slight
Benzene	100	20	1000	None
Carbon tetrachloride	100	80	100	None
Chloroform	100	20	1000	None
DMF	100	120	1000	None
DMSO	100	80	100	Moderate
Petroleum ether	100	20	1000	None
Ethyl acetate	100	20	1000	None
Ethyl alcohol	100	80	100	None
Ethylene glycol	50	100	1000	Slight

Gasoline	100	20	1000	None
Methyl alcohol	100	20	1000	None
Mineral oil	100	100	10	None
Tetrachloroethane	100	20	1000	None

Table 2. Chemical resistance of Nomex 430 type filament yarn.

*None	→	0 to 10% strength loss
Slight	→	11 to 20% strength loss
Moderate	→	21 to 40% strength loss
Appreciable	→	41 to 80% strength loss
Degraded	→	81 to 100% strength loss

When exposed to chemicals that cause degradation, the more crystalline the fiber, the higher is the resistance to degradation. Generally, spun yarns have lower chemical resistance than filament yarns. Finally, it is worth noting that the chemical resistance reported above is the resistance of the fiber to degradation by specific chemicals and not the resistance of m-aramid fabric to penetration by those chemicals. Resistance to penetration is given by specially designed laminated or coated fabric that is applied in protective apparel when protection to chemical penetration in required.

The resistance of Nomex to vapors degradation is a very important parameter in hot gas filtrations. Gases of acids such as HCl, NO_x or SO_2 can reduce significantly the service life of the filter bags. Organic solvent gases have generally a little effect on Nomex.

Light stability and radiation resistance

As other kinds of synthetic fiber, m-aramids are damaged by prolonged exposure to UV radiation (ultraviolet), even if the radiation is generated by artificial light sources. Nomex fiber tends discolor forming a deep bronze coloration. This color change is not necessarily indicative of fiber degradation. Nevertheless, extended exposures also cause a loss of mechanical properties depending on radiation wavelength, exposure time and intensity. To cause fiber degradation, sufficient energy must be supplied to break chemical bonds. Nomex fiber absorbs its maximum energy at approximately 360 nm, where the relative intensity of UV component of most light sources is greatest (because is closer to visible region). Figure 9 shows the strength behavior of Nomex type 430 (200 denier) under laboratory UV light exposure conditions (Xenon arc light, Wheater-Ometer).
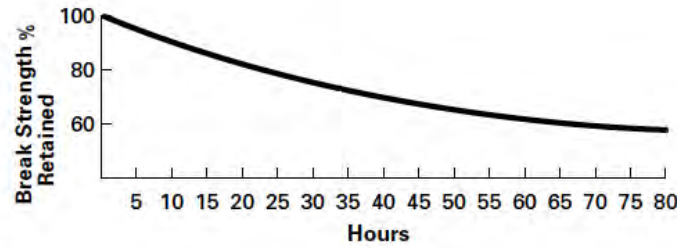
Figure 9. Break strength ret.% of Nomex Type 430 after xenon arc light exposure using a Wheter-Ometer instrument.

The fiber retains circa 70% of its initial strength after 40 hours of exposure and 55% after 80 hours. The strength is reduced under these conditions, but the inherent flame resistance remains unaffected.

Nuclear power plants like other high-energy radiation operations require using fiber products capable of withstanding the deteriorating effects of gamma and ultraviolet radiation. The resistance of Nomex to degradation by such radiation (illustrated in table 3 and compared with Nylon 66) is very high but, however, doesn't provide protection against radiation [18].

		% of breaking strength retention	
Radiation type	**Level**	**Nomex**	**Nylon 66**
As received	/	100	100
Gamma	1.72×10^8 rads	100	30
Ultraviolet	6.04×10^{-2} W/in2	80	80
Ultraviolet + Gamma	4.07×10^{-3} W/in2	100	70
	6.88×10^6 rads		
Ultraviolet + Gamma	1.2×10^{-2} W/in2	95	5
	1.72×10^8 rads		

Table 3. Resistance of Nomex type 430 yarn to some radiation degradation.

In table 4, other interesting are reported data about the degradation of Nomex in the presence of radiation. The breaking strength retention of polyester, nylon 66, and Nomex fibers after exposures to different wavelength ray radiations has been compared. Nomex exhibit outstanding resistance to these radiations.

| | **% of breaking strength retention** | | |
Radiation	Nomex Aramid	Polyester	Nylon 66
Beta radiation – Van de graaf			
200 Mg reps	81	57	29
600 Mg reps	76	29	0
Gamma radiation – Brookhaven Pile (50ºC			
200 Mg reps	70	45	32
2000 Mg reps	45	Radioactive	Crumbled
X-ray (50 kV)			
50 hrs	85	22	/
250 hrs	49	0	/

Table 4. Breaking strength retention % after some radiation exposure.

Flame resistance

Flame resistance is an essential characteristic of m-aramid fibers. Unlike Natural fibers and most synthetic fibers, m-aramid does not ignite and burn in air nor melt and drip. Nomex fiber is also self-extinguishing. Nomex fiber, when exposed to flame at room temperature in a normal environment, will not continue to burn when the flame is removed. At temperatures above circa 427 ºC the fiber carbonize and forms a tough char. The actual chemical structure of the fiber itself is not flammable, aromatic poly-condensed polymers generate low quantities of smoke when burning. They form protective chars readily which help to improve their flame resistance. Therefore, flame resistance of these polymers is built into the fiber. Garment produced with m-aramid fiber acts as a protective barrier helping reduce injuries.

The high temperature integrity of Nomex results from a unique mechanism in the fiber: the intumescence. When exposed to intense heat, the fiber carbonizes and becomes thicker, forming a protective barrier between heat source and skin of operators. This layer remains flexible until it cools, giving the wearer some extra seconds of protection.

Nomex helps to reduce burn injuries in three ways:

1) Fiber itself absorbs heat energy during the carbonization process.
2) Fiber swells and seals opening in the fabric, decreasing air movement and the associated convective heat transfer.
3) Both fiber and fabric thicken increasing the insulating barrier and reduce the conductive heat transfer.

Figure 10. Carbonization and thickening of Nomex when exposed to flame and heat.

LOI is defined as the percentage of oxygen in an environment for a material to sustain combustion. LOI values give an idea of the flame resistance but do not necessarily correlate with it. The flame resistance may be controlled by the chemistry and physics of combustion rather than oxygen content in a normal environment [19].

Table 5 compares Limiting Oxygen Limit (LOIs) of MPD-I and other fibers. The limiting oxygen index of Nomex is approximately 28.

Polymer	LOI
MPD-I	28.5-29.0
PPD-T	28.5-29.0
Nylon 66	20.8
PET	17.1
PE	16.5

Table 5. Limiting Oxygen Index of some different polymers.

Abrasion

Resistance to abrasion is a very important characteristic in both filtration and apparel applications. The abrasion from wearing or laundering is one of the primary cause of garments failure as well as abrasion from dust exposure and cage wear leads to filter bag failure. Woven fabrics made from spun staple yarns of m-aramid fiber exhibit a resistance to abrasion often superior to comparable or even heavier constructions of polyester/cotton blends and 100% cotton fabrics. The graph below shows the resistance to abrasion using a modified wyzenbeek abrasion test[1] for protective apparel fabrics of Nomex III (particular Nomex type) and workwear fabrics of polyester/cotton blend and 100% cotton. The results are given in number of cycles to failure.

[1] The Wyzenbeek abrasion test (ASTM D4157) was originally developed to determine the ability of automotive tires to withstand road abrasion. this test is used to determine the abrasion resistance of fabrics when rubbed against a standard abradent or a wire mesh screen with a backward and forward motion over a curved surface. This abrasion testing method has been modified to test all types of materials against abrasion. In its various iterations, the test can be used to test clothing textiles, leather, upholstery fabric, automotive tires and floor covering [20].
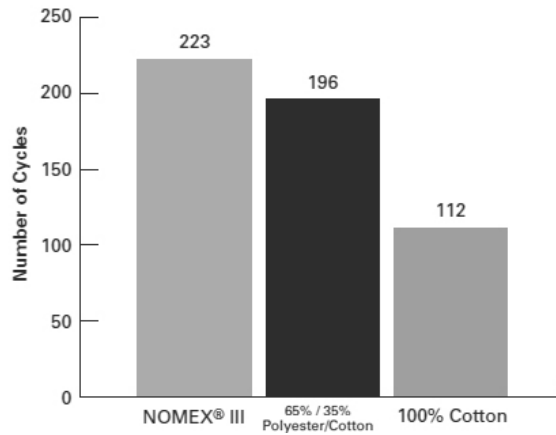
Figure 11. Modified wyzenbeek abrasion test comparing

Moisture regain and dimensional stability

Moisture regain is the tendency of fibers to pick up or give off ambient atmospheric moisture until the equilibrium moisture content is reached. Relative humidity plays a significant role on the rate of moisture absorption and equilibrium level. The moisture regain of m-aramids and in particular of Nomex is about 4.5% in normal ambient conditions. Moisture regain of Nomex fiber is affected by relative humidity. The higher the relative humidity, the faster Nomex absorbs moisture during the initial phase of moisture gain, and the higher the final equilibrium level.
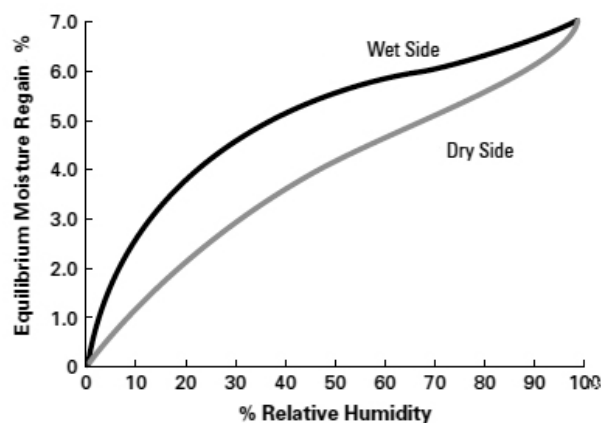
Figure 12. Equilibrium moisture regain of Nomex type 430 tested at 21 ºC.

The fiber is tested in accordance with ASTM D-2654 at 21 ºC, 65% RH, Nomex fabrics contain 5-5.5% of moisture at equilibrium levels. The moisture regain of this fiber is greater than that of polyester, slightly higher than that of nylon and less than that of cotton.

The effect of moisture in terms of small amounts of water vapor in air has no apparent effect on the strength properties of m-aramids, even at elevated temperatures. Variations in RH from 5 to 95% have no measurable effects on the strength of the fiber at room temperature.

Nomex fiber has a low shrinkage. Its length is virtually unaffected by relative humidity but is slightly affected by the temperature. When exposed to dry air at 260 ºC Nomex shrinks only 1% in length within a few seconds. Longer exposure at this temperature has no effect on fiber shrinkage. Moisture and heat cause greater relaxation of internal fiber stresses and produce greater shrinkages than dry heat at same temperature. The relationship between heat shrinkage tension and exposure temperature for Nomex fiber is shown in figure 13 [17, 21].
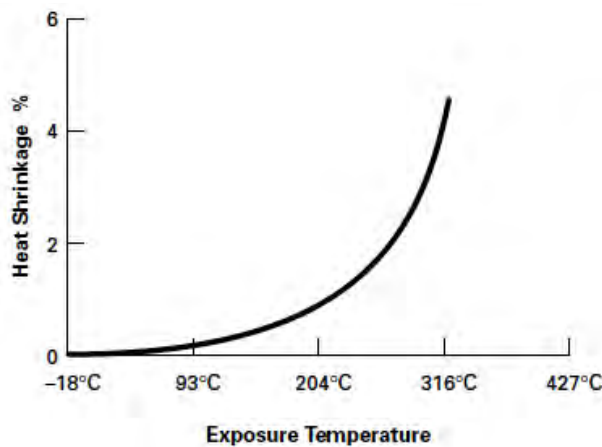
Figure 13. Shrinkage of Nomex type 430 yarn in hot, dry air after 10 minutes at test temperature[2]

---

[2] Approximately 60% of the total shrinkage takes place in the first few seconds of exposure. An additional 0.7% shrinkage occurs within the first 10 minutes of exposure, time within 100% shrinkage takes place.

1.2.3 Fiber products applications

Thanks to their excellent thermal and physical properties, m-aramids are used in a wide variety of applications. Starting from industrial coated fabrics, including ironing or pressing machine covers, rubber hose reinforcement, felt scrims, electrical insulation, filtration, thermal resistant furnishings and, last but not least, thermal protective apparel [24].

Industrial filtration

Nomex aramid fiber, and in general m-aramids, has demonstrated outstanding performance in a wide range of industrial hot gas filtration. It provides services at high temperatures while maintaining his high strength, abrasion resistance and good dimensional stability. Filter bags of m-aramid fiber offer excellent dust release properties and good resistance from chemicals attack

deriving from industrial smoke and fumes. The fiber is used in industrial processes such as aluminum, asphalt, carbon black, cement, crushed stone, coke, ferrous and nonferrous metals, electric arc furnaces, hog fuel boilers and product drying. Several variables are considered in the proper selection and design of a fabric filter system, including:

1) Type of fume
2) Cleaning system
3) Temperature of effluent
4) Concentration of particles
5) Chemistry of gas steam
6) Particle size

These variables may dictate the use of Nomex for service reliability and cost advantages [25].

Electrical insulation

Nomex papers are broadly used in electrical equipment applications. Nomex type 410, for example, is a calendered insulation paper, used in almost every known electrical insulation application. The same Nomex, uncalendered, is widely used in motor phase insulation and transformer coil end filler applications, where high bulk is of prime importance [26].

Honeycomb structures

Honeycomb of Nomex is widely recognized as a highly versatile honeycomb core material. It is extensively used in aircraft interior structures and exterior surfaces to save weight and improve fuel economy. When Nomex core is bonded between two surfaces, the resulting sandwich structure has exceptionally high strength-to-weight and rigidity-to-weight ratios, as much as 9 times stiffer per unit weight than solid steel. Modern jets use Nomex honeycomb in a variety of interior panels such as flooring, storage bins, partitions, etc… It is also used for helicopter blades because of its resistance to high impact, corrosion and fatigue [27].

Thermal protective apparel

Thanks to its unique combination of textile and thermal properties, m-aramids are used in a broad range of thermal protective apparel applications wherever the risk of a fire (firemen) or electric arc exposure is present. These applications include industrial work wear for petroleum, petrochemical and chemical operators, as well as electricians and mechanics. m-Aramids and Nomex are also used by race car drivers, by military and astronauts as well as rocket fuel handlers. Nomex is used when there is an expectation that the worker will be exposed to flames, for example in firefighter turnout

coats and station wear. Garments of m-aramids can even be used for protection against molten metal splatter under certain circumstances.

In selecting woven fabrics of m-aramids for thermal protective clothes, several design varaiables should be taken into account, for example:

1) Required protection level
2) Maximum exposed temperature and time
3) Nature of high temperature hazards
4) Fabric style
5) Basic weight of fabric
6) Function and comfort of apparel
7) Fabric color or print

Clearly, the right selection and design of thermal protective apparel is very important to personnel safety. In many high-risk applications, it's necessary to build prototypic apparel in a high temperature or burning environment for its performance.

A more detailed description of m-aramid protective apparel will be done according to the kind of application [17].

Industrial application

Flame resistant clothing for worker protection, where a flash fire or electric arc hazard is present, are nowadays worldwide adopted in safety guidelines. Chemical, petrochemical and utility workers wear clothing of m-aramid as a protective barrier against the intense heat from flash fires and electrical arcs and to give the wearer a few second to escape in case of fire accident. The range of available garments is very big: from shirts, pants and sweatshirts to rainwear and coats.

Military and aerospace application

The first army started using Nomex was U.S. army in 1960s. Military fibers are colored with pigments incorporated during the fiber-spinning process, for improved consistency in appearance and fastness to light. The biggest applications is the flight suit, but is also used for combat vehicle crews and shipboard engineering crews. m-Aramids are also used in selected applications in gloves, underwear and cold weather gear. The NASA, for example, uses Nomex fabrics for the outer layer of astronaut launch and re-entry suits and as component of its extravehicular activity suits.

Fire fighting and car racing applications

Blends of Nomex and Kevlar (meta+para aramids) are used in firefighters protective apparel. As already explained in the previous paragraphs, their inherently flame resistant materials provide thermal protection in turnout gear, station uniforms, hood, gloves and boots.

m-Aramid are also used in sewing thread for this items. Also racing car driver wear clothing of Nomex to protect themselves from fires, which often accompany crashes on the track and in pit accidents. They wear protective suits as well as underwear, socks and gloves, all in Nomex.

Molten metal applications

A particular type of Nomex, called Nomex III and IIIA, provide thermal protection from molten metal splatter, where small drops of metal are generated during light welding or where portions of the conductor melt in an electric arc discharge. This kind of fabrics must be heavier than the other (used for other applications), not only for thermal protection but also for garment life.

References.

[1] a: H.H. Yang, Handbook of Fiber Science and Technology: Volume III, High Technology Fibers – Part C
b: P.W. Morgan, Condensation Polymers by Interfacial and Solution Methods, Polymeric Reviews, Vol. 10, Wiley Interscience, New York, 1965.

[2] P.J. Flory, Molecular Theory of Liquid Crystals, in Advances in Polymer Science, 1984, Vol. 59, pag. 1-36

[3] S.L. Kwolek, P.w. Morgan, J.R. Schaefgen, L.W. Gulrich, Macromolecules, Vol. 10, 1977

[4] "Kevlar brand pulp in adhesives, sealants, coatings and fiber reinforced plastics", E.I. Du Pont de Nemours & Co., Inc., March 1999

[5] N.J. Abbot et al., "Some Mechanical Properties of Kevlar and Other Heat Resistant Nonflammable Fibers, Yarns and Fabrics", AFML-TR-74-65, Part III, Air Force Material Laboratory, March 1975

[6] H.H. Yang, Kevlar Aramid Fiber, John Wiley & Sons, 1993

[7] Karl K. Chang, E.I. Du Pont de Nemours & Company, Inc., Aramid Fibers

[8] H.H. Yang, Aromatic High-Strenght Fibers, Wiley-Interscience, New York, 1989

[9] W.B. Black and J.Preston, Man Made Fibers, Vol. 2, Fiber Forming Aromatic Polymides, Wiley-Interscience, New York, 1968

[10] A. H. Frazer, High Temperature Resistant Polymers, Wiley-Interscience, New York, 1968

[11] Teijin Ltd., Jap. Pat. Appl. 19933, 1980.

[12] H. Fujie, O. Kai, E. Masunaga, E. Sumitani, A. Shimamai, U.S. Pat. 4,196,118, 1980.

[13] M.P. Vladimirova, B.I. Zhizdyuk, Khim. Volokna, Vol. 3, 1980, pag. 13.

[14] J. Preston, Polym. Eng. Sci., Vol. 15, Issue 3, 1975, pag. 199.

[15] J. Preston, W. L. Hofferbert, Textile Res. J., 49 (5), 1979, pag 283.

[16] E. I. Du Pont de Nemours & Co., Inc., product information.

[17] E. I. Du Pont, Technical Guide for NOMEX® Brand Fiber, H-52720 Revised July, 2001.

[18] G. Hargreaves, J. H. Bowen, Jr., Textile Res. J., Vol. 43, 1973, pag. 568.

[19] J. Preston, Polym. Eng. Sci., Vol. 16, Issue 5, 1976, pag. 298.

[20] www.sdlatlas.com/product/195/Wyzenbeek-AbrasionTester; placetextiles.com/abrasion-testing

[21] Absorption and Desorption of Water by Some Common Fibers, John F. Fuzek, Eastman Kodak Company, Kingsport, TN 37662.

[22] Bulletin NX-17, Properties of Nomex Aramid Filament Yarns, 12/1981.

[23] Yarns and Fabrics of Nomex Aramid Staple and Tow, N-275.

[24] E. I. Du Pont, Technical Guide for NOMEX® Brand Fiber, H-52720 Revised July, 2001, pag. 22-28.

[25] Nomex Aramid for Filtration, E-19853.

[26] Bulletin NX-7. Properties and Performance of Nomex Type 410 Aramid Paper, 1977.

[27] Design and Fabrication Techniques for Honeycomb of Nomex Aramid Sandwich Structures, E-50699.

Chapter 2

2.   m-Aramid carrier assisted dyeing and characterization of X-Fiper® fiber

One of the most important m-aramid fiber is called X-Fiper® and is commercialized by SRO Group China. This fiber is the object of investigation of this experimental work. In this chapter the dyeing of m-aramid fiber will be discussed with all the related issues, including the need of a dyeing carrier with which the fiber must be treated to obtain acceptable dyeing results. Physical and chemical characterization of carrier-treated X-Fiper fiber will be examined in the experimental section of this chapter.

2.1   Introduction to m-aramid dyeing

In the previous chapter the wide use of m-aramids in thermal apparel applications has been discussed. Assuming that even the market of technical textile suffers fashion, and for some application specific colors in garments are required, the dyeing of these fibers for manufacturing protective clothes is mandatory. m-Aramid fiber are very difficult to dye for the high point of crystallinity of its polymer chains as well as the high orientation degree of the macromolecular structure [1]. MPD-I polymers exhibits a very high glass transition temperature, impossible to reach in common dyeing processes [2]. Another aspect concerns the intrinsic yellowish coloration of the undyed fiber due to the aromatic rings into the polymer molecular structure [3]. Two different approaches are possible to dye m-aramids: one is bulk dyeing, the other is wet exhaustion dyeing. Moreover some fabrics printing applications exist in literature.

Dyeing during fiber-spinning process

This process, called solution dyeing but also known as dope or spun dyeing, is the procedure of adding pigments or insoluble dyes to the spinning solution before the solution is extruded through the spinneret. This process is commonly used for difficult-to-dye fibers such as m-aramids (very used also for polyester and nylon) to give good to excellent color fastness to wash and rub and high light stability, because dyes and pigments used in the process become part of the fiber. The solution dyeing is the most used dyeing process of m-aramid producers (Du Pont, Teijin, SRO, ecc…). Only m-aramids producers can easily apply the spun dye process due to the large scale production, in fact this process is very expensive since all the equipment has to be cleaned every time the color change. Thus, the variety of colors and shades produced are limited, the production must be in big stock, and the purchasing of these big stocks is mandatory for small second user factory. For these reasons this type of dyeing is not usually used for apparel yarns or fabrics dyeing [4].

Printing processes

Another way to dye fabrics of m-aramid fiber is to print them. Printing processes are not extremely common, especially if compared with spun dyeing processes. Printing consists in applying a colored paste composed by a solvent, that shows affinity with the textile substrate, and a dye (usually organic dye solvent soluble) or a pigment. Afterwards the impregnation of the fabric into the paste, the fabric is dried and cured at the operative temperature. The following example concerns the printing process of m-aramid fabrics suggested in 1986 by Samir Hussamy.
The printing paste was composed by a variety of anionic or cationic dyes, a very polar solvent such as DMSO (Dimethylsulfoxide), DMA (N-N-dimethylacetamide) or N-Methyl-2-Pyrroldone and a thickening agent compatible with both. Before printing, the fabric is subjected to a special treatment that allows the subsequent dyeing paste penetration. Then, the fabric is dried at high temperature and steamed under pressure to penetrate and fix the dyestuff into the fiber [5].

In next paragraph the wet dyeing processes of m-aramids will be examined, taking into account the most important trouble concerning to them: the carrier need.

2.2   m-Aramid dyeing in wet processes, the state of art

Dyeability in wet processes is, mostly, a function of fiber absorption properties, which are determined by: accessibility of the amorphous mass of the fiber that is correlated with its degree of cristallinity; porosity and density of the fiber; diameter of the fiber itself; chemical structure and functional groups existing in it; affinity with the dyes; temperature of the process; presence of other components in dyeing liquor.

Synthetic fibers like polyester, polyamide and aramids, because of their chemical composition and their production process, are fibers in which the molecules are highly oriented in a crystalline reticule with the result that the amorphous mass is very small. This feature, combined with the fact that the number of hydrophilic groups is very limited, means that the swelling of the fiber in contact with water is very little and consequently it is very difficult for the dyes to penetrate [6,7].

Therefore, thanks to its complete hydrophobic nature, m-aramid impregnation in water with subsequent swelling of the fibers and penetration of the dyes results very difficult, since its glass transition temperature is over 250 ºC.

For these particular features, dyeing of m-aramids must be carried out with a high concentration of other components into the dyeing liquor, called dyeing carriers. Ingamells et al. have explained carrier effects in a dyeing process, with the free volume theory. The dye diffusion depends on the segmental mobility of the polymer chains, which depends on Tg of the polymer (being an important characteristic of polymer viscoelastic behavior). Carriers are able to decrease the Tg and consequently act as plasticizing agents favoring the fiber swelling and promoting penetration of the dyestuff into the amorphous phase of the polymer. Therefore, the dye uptake depends on the plasticization state of the fiber [8,9].

The distribution of the carrier between the liquor and the fiber plays a decisive role in decreasing the Tg and depends primarily on the carrier chemical structure, as well as the equilibrium dye uptake since concentration of carrier into the fiber influence the dye diffusion rate.

This statement has been attributed to a specific interaction between the different carriers and dyestuffs into the inner fiber [10-12].

2.2.1   The swelling agent used in m-aramid fiber dyeing

In the past 30 years several works, aiming at improving the limited swelling of m-aramids, have appeared in the literature. Some of the most significant examples will be considered in this paragraph.

- The first work appeared in literature concerning the use of solvent (namely pyridine) during m-aramid dyeing was published by Preston and Hofferbert at the end of 70s. The fabrics were soaked into pyridine for 16 hours at room temperature prior to dye, then 1% of dye was direct applied into the solution and brought to boiling for 2 hours. The fabrics were then washed for 30 minutes under hot water and dried in oven at 110 ºC. Under these very strong conditions, they obtained deep shades and good light fastness keeping unchanged all the tensile properties [13].
- Moore and Weigmann in 1986 focused on the idea of modifying the fiber structure and thereby improving the dyeability. They modified Nomex structure using highly polar solvent such as dimethyformamide (DMF), dimethylacetamide (DMA) and dimethysulfoxyde (DMSO). After a short time treatment of Nomex yarn and after a water washing carried out to remove the solvents they dye the fiber at 100 ºC under atmospheric pressure. They believed that the improved dyeability after solvent treatment is associated with loss of polymer chain orientation or void formation or both. The mechanical properties remain acceptable but not the same as well as fiber shrinkage. This was one of the firsts approaches in using a carrier to improve the m-aramid dyeability [2].
- In 2005 a similar method was developed by Manyukov *et al.*. They pretreated m- and p-aramid with a mixture of the three solvents (DMA, DMF and DMSO). After the pretreatment they washed the fabrics with a solution containing a surfactant and finally they dyed the fiber obtaining some good results using basic dyes [14].
- Various other experimental have been investigates in the last 20 years. A pretreatment method using three different amines was carried out by two Chinese researchers (Wang and Chen). They discovered that pretreatment with amines may rearrange polymer chains of m-aramid fibers through shrinkage, but degradation of polymer chains may occur if the concentration of these carriers is to high [15]. Even liquid ammonia and supercritical carbon dioxide have been used to enhance the dyeing properties of m-aramid fibers. Liquid ammonia seemed to increase the substantivity of m-aramid for basic dyes, while supercritical CO_2 allows limiting energy consumption and is totally environmentally friendly [16, 17].

However, all processes described above were carried out at laboratory scale; in our knowledge, none of them found place in large-scale production or have been patented except for some patent about the use of DMA as solvent.

- The last meaningful example of carrier solvent application in m-aramid dyeing concerns the study of the carrier effect in the fiber/dye/carrier system using benzyl alcohol done by Nechwatal and Rossbach (pioneers in m-aramid dyeing studies) [18]. This carrier, also called swelling agent (because it actually swells the fibers), was in the last decade one the most recommended by fiber manufacturers. They pretreated the fiber in a mixture of benzyl alcohol and water for 60 min. at the temperature of 120 ºC, then the fiber was squeezed and centrifuged keeping away the excess of carrier, then was dyed applying a conventional dyeing recipe using methylene blue. They discovered that the dye uptake is directly correlated to the liquor concentration of swelling agent. Moreover, the pretreatment with swelling agent does not chemically degrade the fiber but only make changes in its tensile strength, elongation to break and modulus when applied, causing the fibers swells thus improving dyeability.

To complete the bibliography research it's correct to mention that, in recent years, physical/chemical surface modifications have been applied to improve the m-aramid dyeability. For example applying UV/O_3 irradiation can degrade the superficial layer of the fiber creating a hydrophilic surface with increased polar groups that can improve fiber wettability. Even plasma can be applied with the same purpose [19,20].

Finally, it is essential to say that swelling agents, from 80s, have found a wide consumption also in industrial processes and not only for research purpose.

2.2.2   The need of a new swelling agent conception

Despite the improved dyeability, using organic solvents in a pretreatment process or directly during the dyeing process, can affect negatively the fiber structure, causing modifications in the tensile, mechanical and chemical properties at the end of the process. Moreover, industrial machineries have to be conceived for the use of these carriers: fumes and vapors treatment, corrosion and toxicity are just some of the problems that may arise. Additionally, swelling agents' biodegradability in the downstream wastewater treatment is questionable for their organic chemical nature [17].

Referring to the research works done from 70s to 90s and to the commercial products have been developed, the aim of this work was to find the best swelling agent for m-aramid fiber considering the following characteristics:

1) It must swell the fiber, so it's chemical structure must be analogue to the monomer structure.
2) The bulk chemical, tensile, physical and thermal properties must be unaffected at the end of the process.
3) It must improve dyeability.
4) The carrier must be environmentally friendly.

After a wide screening of substances, considering carefully the features above, we focused our attention on two different molecules: 1-phenoxy-2-propanol and N-methylformanilide. The first one belongs to the chemical class of aromatic alcohols and is commonly used in commercial dyeing recipes. The second is an aromatic amide and, in our knowledge, is not widely commercialized as m-aramid's swelling agent. The chemical structures are very related to the fiber's monomer, mostly for the N-methyformanilide. Moreover, they both are more environmentally friendly then other products such as benzyl alcohol or acetophenone.
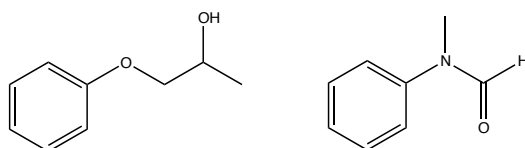

Figure 1. Chemical structures of 1-phenoxy-2-propanol (left) and N-methyformanilide (right).

For simplification, in next paragraphs we will refer to this two product with the name of N-Met for N-methylformanilide and 1-Phen for 1-phenoxy-2-propanol. These two products are easily supplied by Sigma-Aldrich and they present the following characteristics.

Product	Cas. Number	Mol. Weight (g/mol, Da)	Boiling Point (°C)	Density (g/ml) at 20 °C	Intrinsic Coloration	Physical State (Room Temp.)	Water Solubility
N-Met	93-61-8	135.16	243-244	1.095	Yellowish	Liquid	Slightly
1-Phen	770-35-4	152.19	242-244	1.064	Colorless	Liquid	Insoluble

Table 1. Principal characteristics of N-Met and 1-Phen, easily findable in literature.

2.3   X-Fiper® properties evaluation after swelling agents treatment

The aim of this paragraph is to investigate the behavior of a particular m-aramid fiber (X-Fiper) in presence of the two selected swelling agents, studying fiber properties, especially surface properties, when the carrier is used as a pure solvent during a fiber pretreatment. Finally, the mechanical properties of X-Fiper yarns have been investigated to assess whether the probable increased dyeability, given by the carrier, is at the expense of the technical features that characterizing these fibers.

Materials

Yarns and fabrics of X-Fiper® m-aramid fiber are produced by SRO China Group and commercialized all over the world. Our samples were provided by a textile company called Filidea s.r.l.. Unfortunately manufacturers don't give to fiber buyers all the characteristic of their products. The following table shows all the X-Fiper properties provided by the manufacturer.

Property	Value
Fiber fineness	10-20 μm
Tensile strength	>3.5 cN/dtex
Elongation	25-60 %
Tensile modulus	30-70 cN/dtex
Moisture content	5.0 %
Dry heat shrinkage	≤ 1%
Density	1.38 g/cm^3
Glass transition temperature (Tg)	270 ºC
Decomposition point	400 ºC
Limiting oxygen index (LOI)	28-29 %

Table 2. X-Fiper® characteristics provided by fiber manufacturer, SRO [21].

N-methylformanilide and 1-phenoxy-2-propanol were supplied by Sigma-Aldrich.

Fiber Treatment

The m-aramid yarn or fabric was directly dipped into a flask containing N-Met or 1-Phe and left inside for 1 hour, 1 day or 7 days. After immersion process, the samples have been squeezed, washed with water and dried in oven for 2 hours at 80 ºC. This kind of treatment is carried out to simulate the interactions between fiber and carrier in a pre-treatment process before the dyeing, or

the direct contact during dying process, from the mildest (1 hours) to the hardest possible conditions (7 days).

The fabrics or the yarn are washed and dried to simulate the end of a dyeing process in which the end product must have the same properties that the undyed fiber had.

Both samples have been tested in a DSC, one dried and one with 60% of swelling agent still present into the fibre.

2.3.1   Thermal properties

Differencial Scanning Calorimetry

The thermal properties, in terms of glass transition temperature (Tg), were evaluated by differential scanning calorimetry (DSC). The instrument used was a Mettler-Toledo DSC-821e.

All scans were performed with a heating rate of 15 °C/min, under flowing nitrogen at a flow rate of 25 ml/min, reaching the temperature of 350 °C.

Two different tests were carried out on:

1) Fiber used still containing the 60% o.w.f. of swelling agent after a one-week treatment.
2) Fiber dried in oven at 80 ºC after a 168 hours carrier treatment.

The analysis has shown important results regarding the modification of the glass transition temperature, in terms of curve pattern in the zone of the Tg itself. Only DSCs related to one-week treatment are reported, because the DSCs for one-hour and one-day treatment give exactly the same results.

Looking at the graph below it observed that, in the samples with 60% o.w.f. of carrier still inside in comparison with the patterns with the NT (Not Treated fiber) one, the typical Tg stair is almost completely disappeared.

The carrier, swelling the fiber, modifies the macromolecular orientation of the polymer chains. As result of this swelling we can state that the crystallinity of the fiber has changed.

This could mean that the two swelling agents can reduce the energy, necessary for the glass transition step, allowing the fiber swelling and its subsequently improved dyeability. Only when the fiber swells, the dye can penetrate inside the porous of it. This is an important discovery in understanding the swelling behavior of m-aramids; besides, altering this crucial polymer feature, may cause other kind of alteration in other fiber's thermal properties.
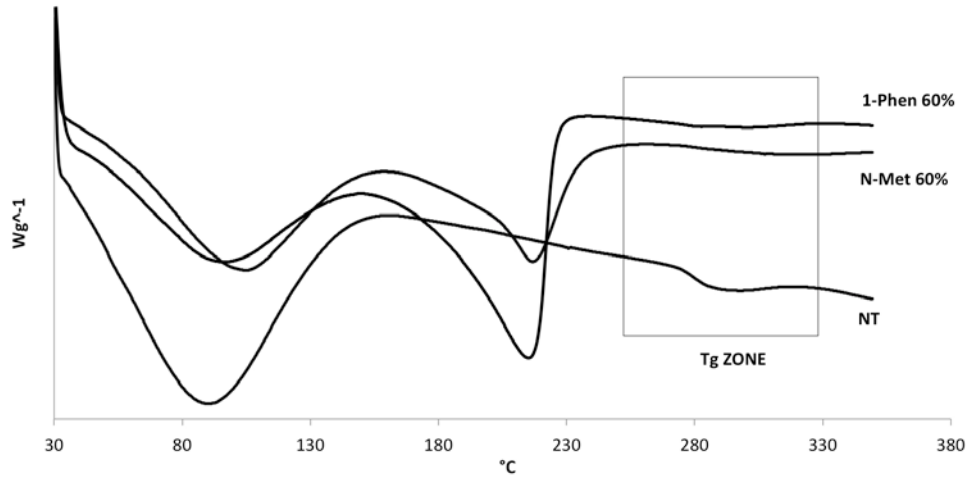
Figure 2. Differential Scanning Calorimetry of fiber in which 60% of swelling agent is still present after one-week treatment.

The DSC of the fabric in which the two carriers have been removed after a one week-treatment is presented in figure 3. It shows the how the Tg pattern is quite modified and the typical stair is not as pronounced as the NT one. However, the "stair" has not disappeared and is possible to find a value of the Tg at circa 280 °C, according to the literature for MPD-I fibers.
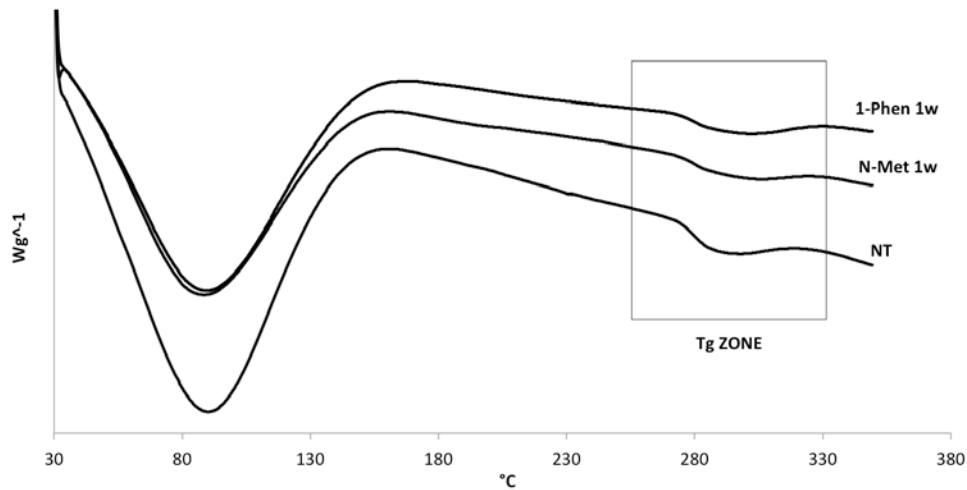

Figure 3. Differential Scanning Calorimetry of fiber washed and dried after one-week swelling agent treatment.

Finally, it's possible to achieve that the alterations produced by the treatment with both the swelling agents is not completely reversible and well visible changes are present in terms of Tg pattern. These changes are more pronounced when the swelling agent is into the fiber at the beginning of the analysis, while when the fiber is dried its effect becomes smaller. Therefore, the most spontaneous conclusion of these statements is that the crystallinity of the fiber is not preserved after both swelling agent treatment.

Thermogravimetric Analysis

All thermogravimetric analysis (TGA), were performed using TA Instruments Thermogravimetric Analyzer TGA Q500. Samples of 10.0 g were heated from 50 ºC to 800 ºC with a temperature ramp of 10 ºC/min in air atmosphere.

The analysis of X-Fiper fiber shows the typical m-aramid thermogravimetric trend found in literature and discussed in chapter one [22]. In air, less then 10% of weight loss up to 400 ºC is reported. After 500 ºC there is a sharp loss of weight due to charring process. Figures below shows TGA of fibers after one-week and one-hour fiber treatment compared with the untreated fiber, one-day results are not shown because very similar to the others.
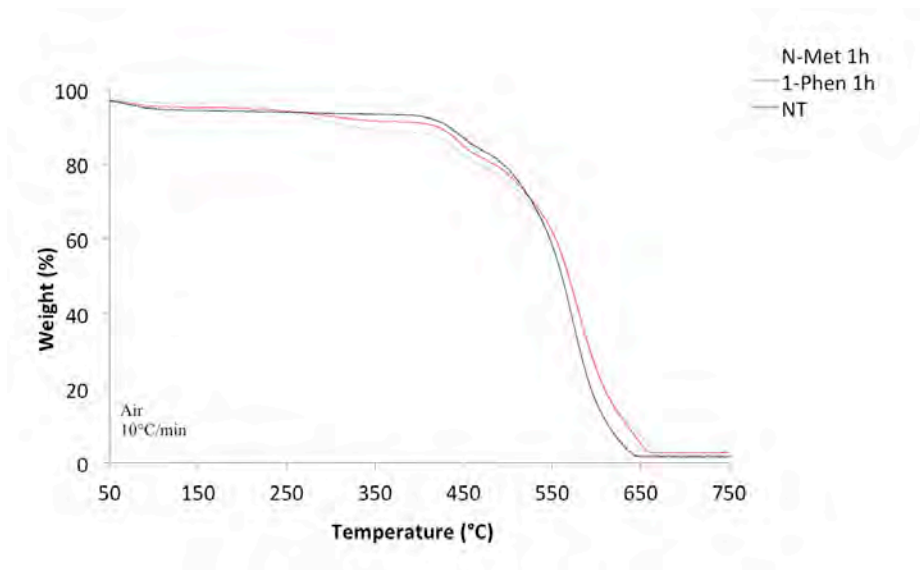

Figure 4. Thermogravimetric Analisys of X-Fiper, swelling agent treated for one hour compared to the untreated one.
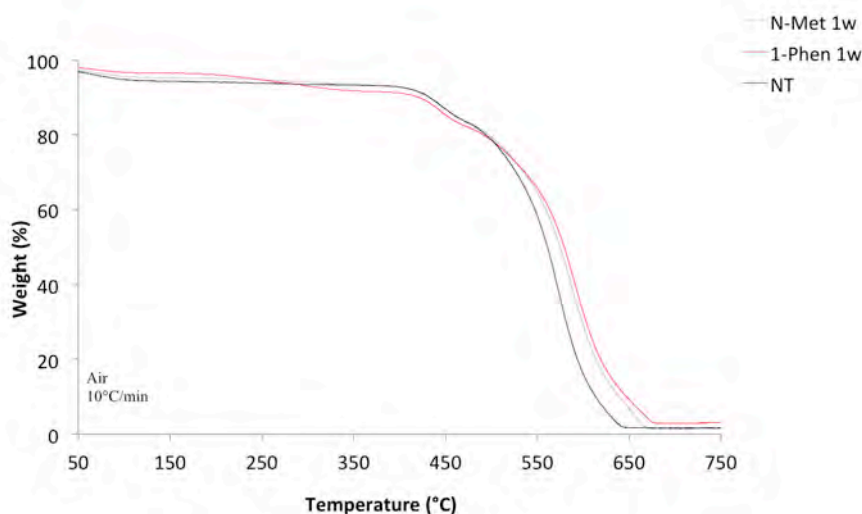
Figure 5. Thermogravimetric Analisys of X-Fiper, swelling agent treated for one week compared to non treated one.

It's immediate to notice that no significant changes occur in terms of temperature/time weight loss between treated and untreated fiber. After one-week fiber dipping the degradation at 500 ºC appears to be less pronounced then after one-hour treatment. However, the decomposition starting point is reduced if compared to with the untreated fiber (data confirmed by producer). Therefore, a prolonged contact between fiber and swelling agent cause a delay in charring, increasing slightly the thermal resistance of the fiber during time. However, treated X-Fiper begins to decompose earlier then the untreated.

2.3.2 Chemical and physical surface modifications

Important information concerned with chemical and physical surface modification after the contact with the swelling agent. In first instance, chemical changes, due to the carrier effect can affect the fine structure of the polymer by forming or breaking molecular bonds, or adding chemical groups. These changes can modify the hydrophobicity of fiber surface thus increasing wettability and finally its dyeability. Chemical changes can even affect the aspect of the fiber modifying its intrinsic coloration.

Moreover, physical modifications of fiber's surface can create a wrinkled layer that can expand the total useful surface during the mass transfer of the dyeing process, consequently increasing the dyestuff adsorption.

Infrared analysis, attenuated total reflectance

Using FT-IR (Fourier Transform Infrared Spectroscopy) with attenuated total reflectance apparatus (ATR) permitted to analyze the surface of the m-fiber after the swelling agent treatment. All the samples were tested in a ThermoScientific spectrophotometer (Nicolet 6700 FT-IR). Studying changes in chemical groups present on the fiber surface, and comparing the results of treated and untreated samples, is possible to classify the chemical surface of X-Fiper and determine if some considerable chemical changes occurred on fiber's surface-layer after the treatments.
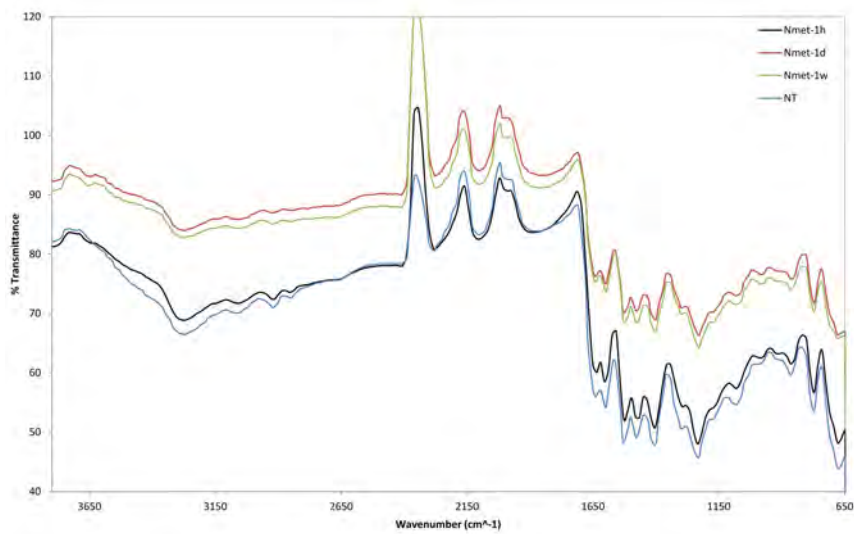
Figure 6. FT-IR spectrum of the three different N-Met treatments compared to the untreated fiber.
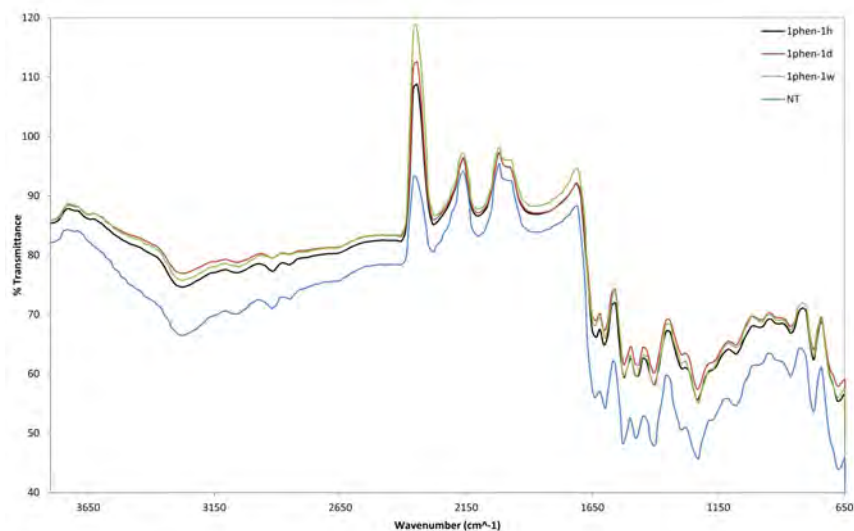
Figure 7. FT-IR spectrum of the three different 1-Phen treatments compared to the untreated fiber.

Looking at the graphs is immediate to denote the typical absorption bands of an aromatic polyamide:

- 1630-1650 cm^{-1} related to C=O stretch and amidic N-H bend
- 3200 cm^{-1} relate to amidic N-H bend
- 1600 cm^{-1} relate to aromatic C=C stretch

No significant variations occurred in absorption spectra of samples kept in a swelling agent for the three different periods. Therefore, the surface chemical properties are completely preserved after fiber treatments. It is finally possible to assess that no considerable chemical changes occur on the surface of the fiber.

Drop Shape Analysis (DSA)

To confirm the results of the infrared analysis, the hydrophilicity of the fiber surface have been tested to check whether the carrier has changed this critical parameter in establishing the dyeability and printability of the fiber. The easiest and most common way to determine the wetting properties consists in measuring the contact angle between a liquid (water) and a solid (fibre), using a Drop Shape Analysis instruments (DSA).
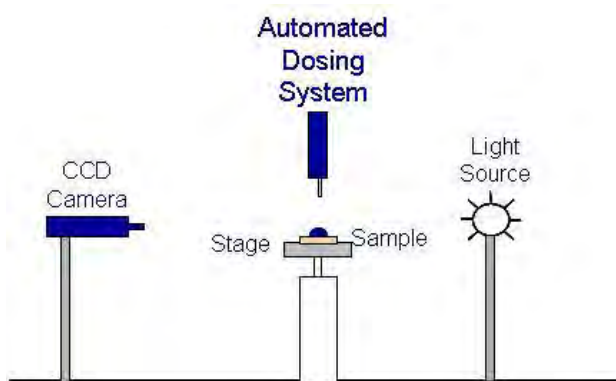A scheme of the instrument is presented in the Figure 8.

Figure 8. Drop Shape Tester, instrument scheme

We measured the contact angle between the fabric (treated and untreated) and a drop of water in the first few seconds of contact. The results represented by θ values are shown in the beneath table.

Entry	Sample Name	Carrier Used	Time of Dipping	Drop/fabric contact angle θ
1	nmet1h	N-Met	1 hour	135.5 °
2	nmet1d	N-Met	24 hours	141.6 °
3	nmet1w	N-Met	168 hours	146.8 °
4	1phen1h	1-Phen	1 hour	137.2 °
5	1phen1d	1-Phen	24 hours	149.8 °
6	1phen1w	1-Phen	168 hours	136.5 °
7	NT	None	None	146.6 °

Table 3. Contact angle between water drop and *m*-aramid fibre fabric.

The organic nature of the swelling agents suggests that, if present on the fiber surface, makes it hydrophobic. Therefore, the fiber has been dried after the treatment in order to completely remove the swelling agent from the fiber surface. The results confirmed the hydrophobic nature of the m-aramid X-Fiper. The wettability of the fiber, after any kind of treatment, remains very poor; this could be a "big trouble" as far as a subsequent dyeing process is concerned.

The figures below show, as an example, the complete hydrophobicity of the fiber after one week into the two carriers in comparison with an untreated sample. No naked eye differences appear looking at the photos.
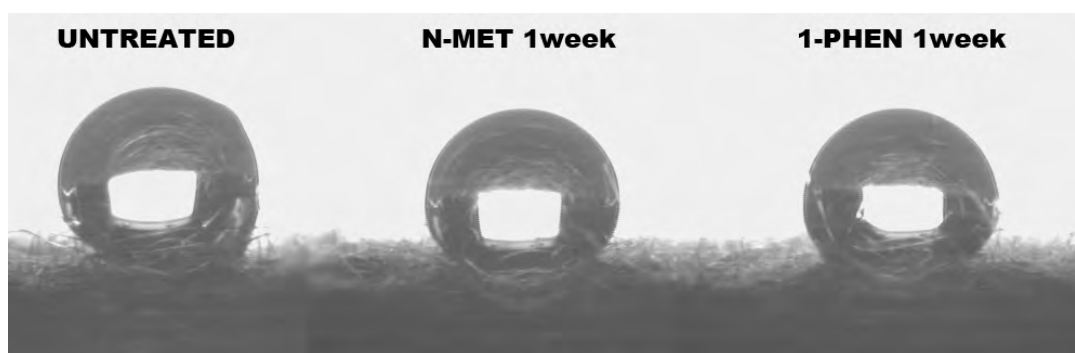
Figure 9. Photos of DSA show the complete hydrophobicity of the m-aramid X-Fiper.

Scanning Electron Microscope (SEM)

One of the most used instruments in studying the morphology of a certain fiber is the scanning electrode microscope, better known as SEM. With SEM is possible to study the macroscopic changes that occur on the surface a fiber as well as, for example, structural modification made by a carrier treatment. Unfortunately, using this kind of instrument, it's impossible to analyze the carrier's impregnated fiber and its swelling behavior because the samples, during the analyses, must be under vacuum. All the analyses were carried out testing the dried samples. The images are presented in two different magnifications (500X and 4500X) for the untreated fibre (NT). Photos of fibers treated with the two carriers are presented with the magnification of 4500X because with 500X alterations would be unremarkable.

Figure 10. SEM images of untreated fiber with magnifications of 4500X and 500X from left to right.

Figure 11. SEM images of N-Met treated fibers, from left to right: 1h, 1d and 1w treatment.

Figure 12. SEM images of 1-Phen treated fibers, from left to right: 1h, 1d and 1w treatment.
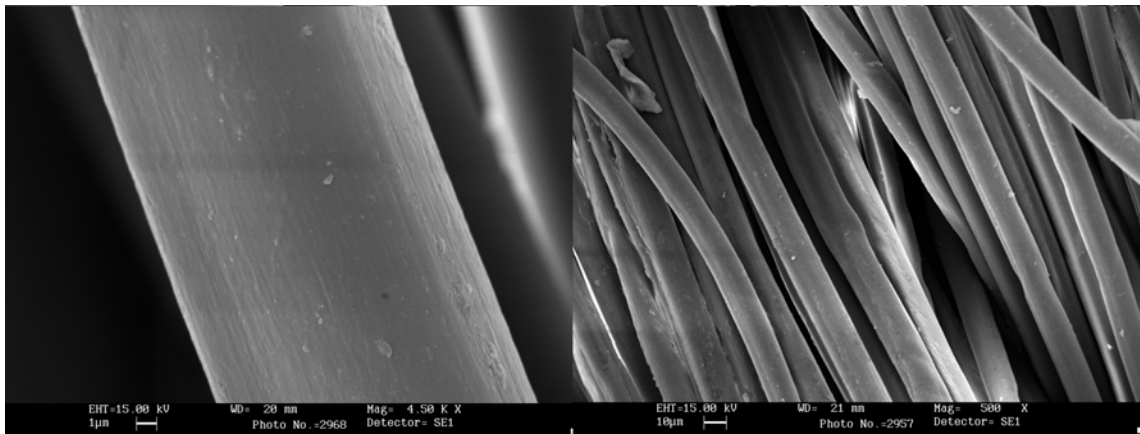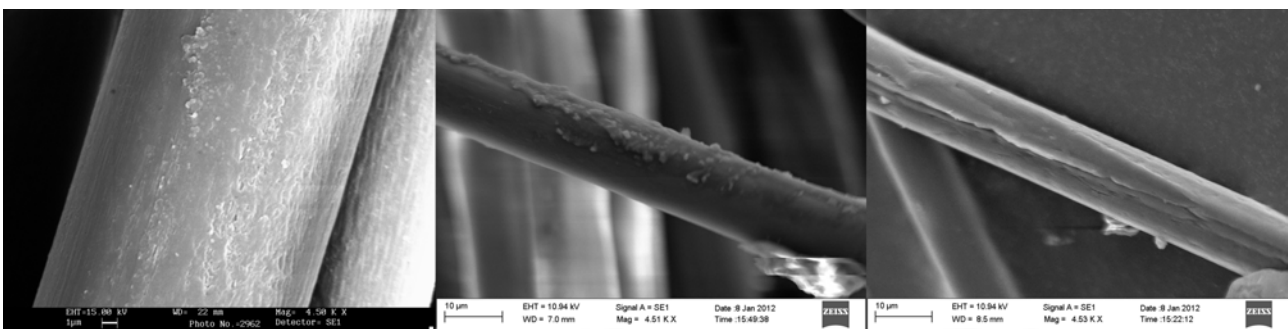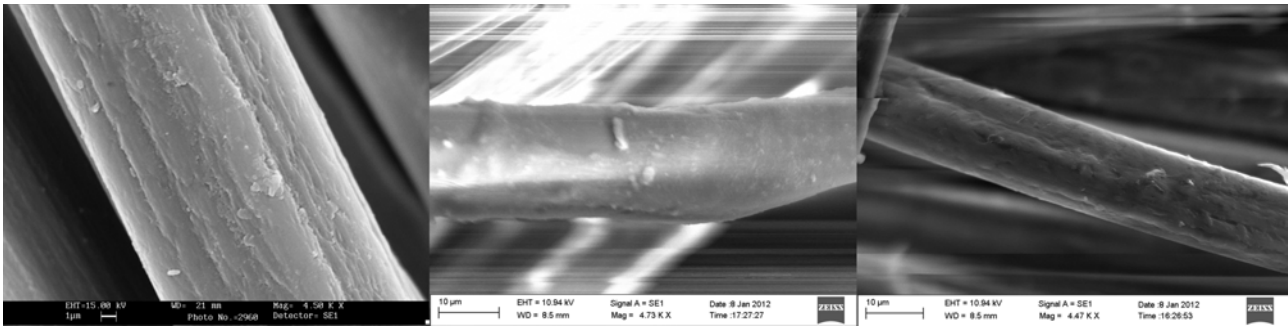
After the treatments, especially with 1phen, the fiber looks rougher and partially damaged. Even though this change is not visible macroscopically (naked eye), and the hand of the fabric remains unaffected, some structural modifications could have occurred. These structural changes can affect negatively the fiber performances. For this reason, checking that the mechanical properties are not varied, some tests are necessary to evaluate the mechanical properties of the single yarn after the pre-treatment process, these evaluations will be discussed in next paragraph.

Color changes

The final coloration of a dyed product is the result of the uptake of a dyestuff (or a mixture of them) giving the textile-desired shade. If, during the dyeing process, some other products are used, is indispensable to know if they can alter or falsify the desired shade. In our case, the presence of a carrier, especially in a pretreatment modality, can modify the intrinsic coloration of the fiber itself. It is worth mentioning that X-Fiper, like almost all m-aramid fiber, presents a yellowish intrinsic coloration that represents itself a serious trouble in dyeing. The analysis performed, using a Datacolor Check II plus spectrophotometer, is a spectrophotometric analysis in reflectance. The results of these analyses, in terms of color difference ($\Delta E_{CMC\ 2:1}$) between untreated (named standard) and treated fibers (dried in oven before analysis, the carrier was completely removed) with both the swelling agents (called batches), are shown in table 3.

Operative conditions of the spectrophotometer:

- Standard illuminant CIE D65
- 10º observer
- Aperture LAV
- Color space CIE L*ab
- $\Delta E_{CMC\ l:c}$ with l=2 and c=1

CIE LabCh D65/10Deg		Brightness	Colorimetric coordinates		Saturation	Hue angle	Change in color
Standard	**Batch**	**CIE L**	**CIE a**	**CIE b**	**CIE C**	**CIE h**	**CIE ΔE**
NT		87.08	-0.03	8.87	8.87	90.19	
	1-Phen 1h	84.85	0.21	9.47	9.47	88.75	**1.01**
	1-Phen 1d	85.90	0.18	9.79	9.80	88.94	**0.96**
	1-Phen 1w	85.24	0.17	9.81	9.81	89.02	**1.09**
	N-Met 1h	83.38	0.54	8.83	8.85	86.52	**1.56**
	N-Met 1d	82.82	0.52	9.34	9.36	86.84	**1.76**
	N-Met 1w	82.51	0.98	9.78	9.63	84.15	**1.99**

Table 3. Colorimetric coordinates found for the different swelling agent treatments

The equations used for the calculation are reported below, colorimetric coordinates C and h are also reported but they don't have been taken into account for the $\Delta E_{\text{CMC 2:1}}$ calculation as shown in the equations below.

$$\Delta E^*_{CMC} = \sqrt{\left(\frac{L^*_2 - L^*_1}{lS_L}\right)^2 + \left(\frac{C^*_2 - C^*_1}{cS_C}\right)^2 + \left(\frac{\Delta H^*_{ab}}{S_H}\right)^2} \tag{1}$$

$$S_L = \begin{cases} 0.511 & L^*_1 < 16 \\ \frac{0.040975L^*_1}{1+0.01765L^*_1} & L^*_1 \geq 16 \end{cases} \quad S_C = \frac{0.0638C^*_1}{1 + 0.0131C^*_1} + 0.638 \quad S_H = S_C(FT+1-F) \tag{2}$$

$$F = \sqrt{\frac{C^{*4}_1}{C^{*4}_1 + 1900}} \quad T = \begin{cases} 0.56 + |0.2\cos(h_1 + 168°)| & 164° \leq h_1 \leq 345° \\ 0.36 + |0.4\cos(h_1 + 35°)| & \text{otherwise} \end{cases} \tag{3}$$

Looking at Table 3 is possible to understand the optical changes, occurred after treatments, in terms of colorimetric coordinates. Treating samples with 1-Phen no significant changes occur on ΔE, meaning that the initial coloration of the fiber is almost totally preserved. However, focusing our attention on the color space La*b* results immediate to see that, brightness, decrease sharply from the untreated samples to the N-Met treated. Moreover, in N-Met treated samples there is a shift on red (a parameter increase).

The ΔE rises increasing the treatment time (Figure 13) and also with one hour treatment is quite high. This effect is very important in terms of a dyeing process and must be taken into account in choosing the dyeing recipe to reach the final desired hue.
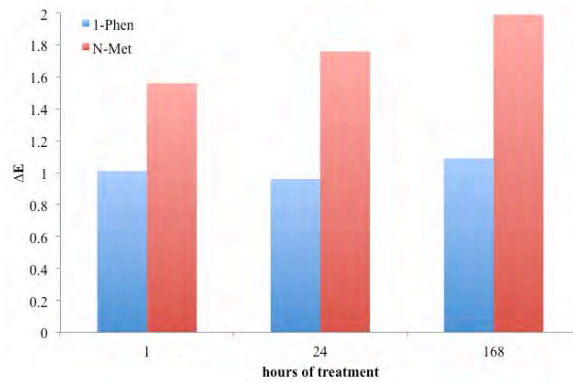
Figure 13. Histogram showing the "ΔE" pattern during time of treatment.

Figure 14 shows an optical point of view of the final color difference after the one-week treatment with N-Met swelling agent. Even at naked eye the color difference is appreciable, especially the red shift.
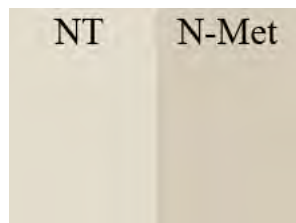
Figure 14. Color difference between NT and 1w N-Met fibers.

Ultra Violet (UV) light exposure behavior

Assessing the behavior of X-Fiber under U.V. light exposure, some tests have been done using both FT-IR (ATR) and Colorimetric analysis after UV exposure.

The samples have been treated under low-pressure mercury U.V. lamp for 10, 20 and 40 minutes.

FT-IR spectrum show that increasing treatment time there's a progressive reducing of the peak at 1630-1650 cm^{-1} (refer to spectrum in previous paragraph) related to the amidic C=O. This phenomenon has been registered for both untreated and treated fiber with the two swelling agents. This is index of a certain polymeric chain degradation occurred on the fiber surface, this fiber damaging acting with reducing processes on carboxylic carbon of the amide groups. No oxidative processes have been registered by the FT-IR analysis.

Assessing the color changes of X-Fiper fiber under UV light, only untreated fiber was tested because it's been considered more appropriate to first understand light behavior of the fiber before

any kind of treatment. Fibers are often stocked under light without any kind of protection. As shown by colorimetric results, the yellowish intrinsic coloration is greatly increased after UV exposure.

CIE Lab D65/10Deg		Brightness	Colorimetric coordinates		Change in color
Standard	**Batch**	**CIE L**	**CIE a**	**CIE b**	**CIE ΔE**
NT		87.10	-0.12	8.78	
	10 min UV treat.	90.74	-0.04	11.58	**1.01**
	20 min UV treat.	92.02	0.87	16.08	**0.96**
	40 min UV treat.	94.00	1.39	20.07	**1.09**

Table 4. Colorimetric coordinates found for the different swelling agent treatments

The time-treatment progressive yellowing is shown in figure below. The coloration of the last sample is completely different from untreated one.
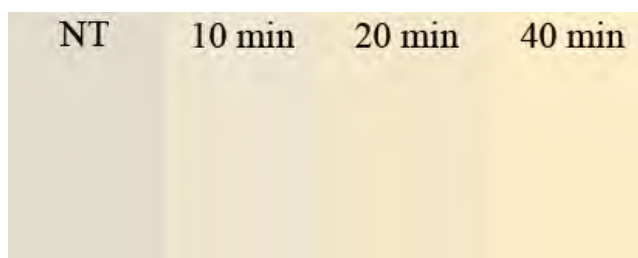

Figure 15. Yellowing from NT to 40 minutes UV exposure.

The exposure to UV light cause serious surface fiber damages especially in changing its coloration. Therefore, it's very important to preserve fibers from both sunlight and artificial light exposure before any kind of pre-dyeing treatments and dyeing process aiming to reach good reproducibility.

2.3.3 Tensile and mechanical properties of X-Fiper® Yarn

Introduction

Measurement of tensile stress-strain properties is the most common mechanical measurement on fabrics and yarns. It is used to determine the behavior of a sample while under an axial stretching load. From this, the breaking load and elongation can be obtained. The principle of tensile strength test is simple: a sample is held in two or more places and extended until it breaks. The tensile properties measured are generally considered arbitrary rather then absolute. Results depend on specimen geometry, fiber type and arrangement as well as on fiber structure.
There are two common types of tensile breaks:
1) Sharp break
2) Percentage break

A sharp break is a sudden drop in load; this test is normally called pull to break. A percentage break is shown as a gradual reduction in the load from its maximum as further extension is applied. A percentage drop from maximum load is often used to define the break point. Modern tensile test instruments can be set up in both break modes. Figures below shows the tensile strength test curve of the two types of break.
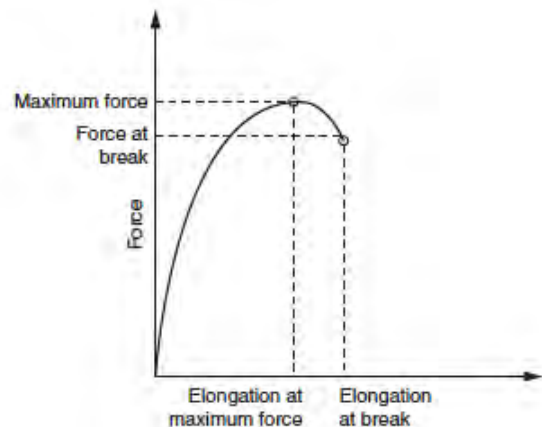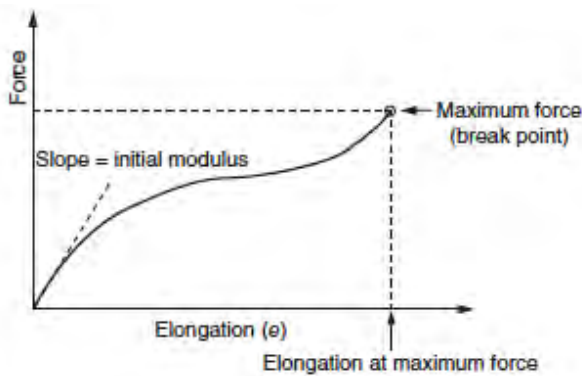
Figures 16 & 17. Tensile strength test curves of sharp (left) and percentage (right) break.

Another important tensile parameter is the extension (or elongation) that is defined as the change in length of a material due to stretching. When a yarn or fabric of original length l_0 is stressed along its axis, it extends an amount dl. The strain in the sample is dl/l_0. The extension is often represented by

the symbol *e* that is referred to elongation. Strain is dimensionless and often reported as a percentage.

Finally, Young's modulus or initial modulus is a measure of the amount of deformation that is caused by a small stress. Materials with high modulus, namely stiff of hard materials, deform very little in presence of a stress. Materials with low modulus, soft materials, deflect significantly. In case of yarn or fabric, initial modulus is related to the fabric handle [23].

Experimental

The effects due to the swelling agent treatment have not to be studied only as far as fiber surface modification is concerned. Mechanical and tensile properties may be changed. Important features that characterize this m-aramid may be disappeared or seriously compromised. Testing these properties on the yarn is one of the most important analyses that must be carried out in choosing the proper swelling agent before testing its behavior during dyeing.

The laboratory equipment used for these tests was a Uster Tensorapid from Uster company. The instrument was used to evaluate the mechanical and tensile properties of untreated and treated m-aramid yarns having a mean linear mass density of 50 tex (1tex = 1g per 1 Km of yarn). The samples were elongated at a constant rate (Constant Rate of Extension principle), 20 different yarns are evaluated for each sample in order to obtain average values.

To facilitate the results reading, in terms of analyzed parameters, a legend has been written:

Time to Break: the time from the start of measurement to the break of the sample.
Breaking Force: maximum force value measured during the tensile test.
Breaking Elongation: elongation at maximum breaking force value.
Tenacity: breaking force in relation to the yarn count of the sample considered (50 tex in our case)
Breaking Work: work done to break (enclosed area below the force/elongation characteristic up to the point of breaking force).

		Time to Break (s)	Breaking Force (N)	Breaking Elong. (%)	Tenacity (cN/tex)	Breaking Work (N*cm)
Sample	**_NT_**					
Average value		11.5	10.35	19.00	20.71	66.28
Std Dev.			0.85	2.27	1.71	13.09
Min. Value			8.78	14.33	17.56	41.86
Max. Value			11.74	22.64	23.49	89.72

Table 5. Tensile properties of untreated X-Fiper yarns.

		Time to Brake (s)	Breaking Force (N)	Breaking Elong. (%)	Tenacity (cN/tex)	Breaking Work (N*cm)
Sample	*__N-Met 1h__*					
Average value		11.8	10.59	19.52	20.73	64.4
Std Dev.			0.58	1.47	1.14	8.39
Min. Value			9.41	15.57	18.41	44.67
Max. Value			11.8	21.27	23.09	75.11
Sample	*__N-Met 1d__*					
Average value		12.5	11.47	20.69	22.95	74.56
Std Dev.			0.59	1.43	1.17	8.46
Min. Value			10.52	18.48	21.03	60.64
Max. Value			12.62	23.27	25.25	88.15
Sample	*__N-met 1w__*					
Average value		12.3	10.38	20.41	21.17	69.26
Std Dev.			0.63	1.55	1.28	8.95
Min. Value			9.25	17.41	18.88	51.75
Max. Value			11.95	23.85	24.38	93.59

Table 6. Tensile properties of N-Met treated X-Fiper yarns.

		Time to Brake (s)	Breaking Force (N)	Breaking Elong. (%)	Tenacity (cN/tex)	Breaking Work (N*cm)
Sample	*__1-Phen 1h__*					
Average value		12.0	10.37	19.80	20.73	66.21
Std Dev.			0.51	1.73	1.02	9.15
Min. Value			9.56	16.77	19.12	52.65
Max. Value			11.31	23.06	22.63	84.51
Sample	*__1-Phen 1d__*					
Average value		12.2	10.98	20.13	21.97	69.9
Std Dev.			0.6	1.84	1.19	10.37
Min. Value			10.11	16.52	20.23	52.21
Max. Value			11.94	23.68	23.89	89.29
Sample	*__1-Phen 1w__*					
Average value		11.1	9.54	18.32	19.39	55.11
Std Dev.			0.77	1.45	1.57	7.68
Min. Value			7.79	14.56	15.83	35.07
Max. Value			11.31	20.6	22.99	68.23

Table 7. Tensile properties of 1-Phen treated X-Fiper yarns.

All the results obtained for treated fiber are included in the standard deviations of those obtained for the untreated samples. We can say that any changes arise in the mechanical and tensile properties of the yarn after the treatment, even if prolonged (7 days). The two swelling agent don't damage the inner fiber leaving unaffected al its key properties.

2.3.4   Chemical resistance properties

As written in previous chapter all m-aramid fibers exhibits very good resistance to many chemicals, including hydrocarbons, organic solvents, strong and diluted acid and bases.

Before testing fibers with other chemicals, chemical resistance of untreated sample in terms of weight loss was evaluated using the two swelling agents. After dipping fabrics into pure chemicals, the fiber was squeezed and dried.

Swelling Agent	Dipping time (hours)	Temperature (ºC)	Weight loss %
N-Met 99%	1	22	<1
	1	120	1<val.<2
	24	22	<1
	24	120	1<val.<2
	168	22	1<val.<2
	168	120	2<val.<3
1-Phen 93%	1	22	1<val.<2
	1	120	3<val.<4
	24	22	3<val.<4
	24	120	5<val.<6
	168	22	3<val.<4
	168	120	7<val.<8

Table 8. X-Fiper chemical resistance, in terms of weight loss, to the two swelling agents.

No significant loss of weight occurs treating the fiber with N-methyl formanilide even if the treatment if made at high temperature (simulating a dyeing process). However, treating the fiber with 1-Phen, especially in prolonged time ad high temperature, cause a more significant loss of weight that reach almost 8%.

The chemical resistance, of treated X-Fiper fabrics, was also evaluated considering weight loss after dipping into the selected swelling agents. For these tests are considered only the fiber treated with

the two swelling agents for one hour. After drying the samples were weighted, then treated with chemicals to test them resistance after swelling agent treatment. Some chemicals have been used and the results are shown in following tables.

Chemical Substance	Concentration %	Temperature (ºC)	Time (hours)	Weight loss %
Strong mineral acids				
Hydrochloric	10	22	2	>10%
	37	22	2	Degraded
Sulfuric	10	22	2	<5%
	96	22	2	Degraded
Organic acids				
Acetic	99.9	22	2	<1%
	99.9	100	2	<1%
Strong bases				
Ammonia	28	20	2	None
Sodium hydroxide	10	20	2	None
	10	100	2	Degraded
Organic Solvents				
DMSO	99%	22	2	<5%
	99%	80	2	>10%
DMSO/Acetic Acid 4:1	/	80	2	<1%
Hexane	99%	22	2	<1%
Petroleum ether	99%	22	2	<1%

Table 9. X-Fiper chemical resistance, in terms of weight loss, after N-Met 1h treatment.

After treatment with N-Met, the chemical resistance of X-Fiper is exactly the same found in literature for all m-aramid fibers (chapter one). It is important to underline the behavior of treated fiber using DMSO and DMSO mixed with glacial acetic acid: with only DMSO, at the temperature of 80 ºC, there is a significant loss of weight. Mixing 4 part of DMSO with 1 part of acetic acid, any loss is registered.
Results obtained for 1-Phen treated samples are very similar, for this reason the table hasn't been shown.

2.4   Final considerations

In conclusion of this chapter it is possible to say that the interactions between the X-Fiper m-aramid fiber and the two tested swelling agents do not cause serious modifications of the fiber surface and structure. Both FT-IR and SEM showed that the surface morphology remains the same with the exception of some roughness appearing after prolonged treatment. Moreover, this roughness does not change the hand of the fabric itself. Thermal properties, in terms of thermogravimetry, have not shown any trend differences between treated and untreated fiber. Besides, DSC showed an important change in transition glass temperature pattern (especially if performed whit carrier still present into the fiber); this fact is probably amenable to the swelling process due to the carriers, confirming they act as plasticizer, increasing chain mobility. The fiber showed a good chemical resistance against the two swelling agent except with prolonged treatment with high temperature using 1-phenoxy-2-propanol. Tensile and mechanical properties of the yarn are even maintained after any kind of treatment. The strongest change occurs, however, on fiber coloration after treatment with N-methyl formanilide. The "red shift" must be taken into account in a successive dyeing process. Like all aramids, also X-Fiper is damaged by UV light exposure; experimental results confirmed that UV light exposure cause a drastic change in color in terms of yellowing. UV light exposure after fiber treatment has not been tested and will be the next step of this kind of experimental work.

Finally, the DSA analysis showed that the hydrophobicity, as expected, has not changed. As consequence, the wettability of the fiber is not increased by the swelling agent treatment, however in terms of dyeability of m-aramids, wettability is not as important as the swelling that these two carriers give to the fiber.

The obtained results gave us the possibility to continue the research work, going to assess the dyeing thermodynamics of the system composed by carrier/dye/fiber in water media to finally understand the complex dyeing mechanism that characterizes m-aramid dyeing.

This part of the research work will be discussed in next chapter.

References

[1] E. A. Manyukov, S. F. Sadova, N. N. Baeva, V.A. Platonov, Fibre Chemistry, 2005, Vol. 37, No. 1, pag. 54-58.

[2] R. A. F. Moore, H. D. Weighmann, Textile Res. J., 1986, Vol. 56, pag. 254-260.

[3] Handbook of Fiber Science and Technology: Volume III, High Technology Fibers – Part C, Nomex Aramid Fiber, Menachem Lewin, July 1996.

[4] Dictionary of Fiber & Textile Technology, KoSa, 1999

[5] S. Hussamy, US Patent Number 4705527, 1987

[6] N. N. Baeva, E. A. Manyukov, S. F. Sadova, L. Y. Konovalova, G.S. Negodyaeva, Fibre Chemistry, 2007, Vol.39, No. 3, 205-209.

[7] J. Cegarra, P. Puente, J. Valldeperas, The Dyeing of Textile Materials, Paravia-Texilia, Torino, 1988.

[8] W. Ingamells, K. V. Narasimhan, J. Soc. Dyers and Colour., 1977, Vol. 93, pag. 306-312.

[9] A. Nechwatal, V. Rossbach, Textile Res. J., 1999, 69, 635-640.

[10] Z. Gur-Arieh, W. Ingamells, R. H. Peters, J. of Appl. Polym. Sci., 1976, Vol. 90, pag. 8-11.

[11] W. Ingamells, A. M. Yabani, J. of Appl. Polym. Sci., 1978, Vol. 22, pag. 1583-1592.

[12] W. Ingamells, J. Soc. Dyers and Colour., 1980, Vol. 96, pag. 466-474.

[13] J. Preston, W. L. Hoffbert, Textile Res. J., 1979, 49, pag. 283.

[14] E. A. Manyukov, S. F. Sadova, N. N. Baeva, V.A. Platonov, Fiber Chem., 2005, Vol. 37, Issue 1, pag. 54-58.

[15] C. C. Wang, C. C. Chen, Textile Res. J., 2003, 73, pag. 395-400

[16] M. Nicolai, A. Nechwatal, J. Soc. Dyers and Colour., 1994, Vol. 110, pag. 228-230.

[17] J. J. Shim, J. H. Choi, J. H. Ju et al., 6th ISSF at Versailles, Apr. 28-30, 2003.

[18] A. Nechwatal, V. Rossbach, Textile Res. J., 1999, 69, pag. 635.

[19] Y. Dong, J. Jang, Color. Tech., 2011, Vol. 127, pag. 173-178.

[20] E. M. Kim, J. Jang, Fibers and Polymers, 2010, Vol. 11, pag. 677-682.

[21] http://www.sro.hk/en/products/x-fiper-meta-aramid-fibers/x-fiper-characterisrics.

[22] E. I. Du Pont, Technical Guide for NOMEX[®] Brand Fiber, H-52720 Revised July, 2001.

[23] Fiber Testing, Jinlian Hu, The Textile Institute, Woodhead Publishing Limited, Cambridge, 2008.

Chapter 3

3.   X-Fiper$^®$ dyeing, thermodynamic and kinetic study of the carrier/dye/fiber system

The aim of this chapter is to study the dyeing behavior of X-Fiper in the complex system water/carrier/dyestuff/fiber. At the beginning, an introduction about the m-aramid common dyeing processes will be done, discussing the state of the art. Then, an introduction about dyeing mechanisms, using cationic and disperse dyes, will be also given. In the experimental section the thermodynamic equilibrium will be analyzed and the absorption isotherms using the types of dyes, cationic and disperse, will be derived. The kinetic of the process will be analyzed as well to find the experimental diffusivity of a particular disperse dye. Moreover, the disperse dye diffusion into the fiber will be simulated by fluid dynamic simulation using COMSOL Multiphysics software. Finally, the quality of dyed materials will be also evaluated in terms of hue and standard fastness to wash and rub.

3.1   m-Aramid dyeing recipes

Not many dyeing recipes of m-aramid fibers appear in literature and they are very similar to each other. Most of these recipes are provided by fiber manufacturer or by dyestuffs producers. Some patents are also present in literature; they suggest some particular recipes about the use of particular dyeing conditions that, in the end, don't show particular differences with manufacturer's recipes or experimental works found in literature. As discussed in the previous chapter, the use of a particular carrier called swelling agent is mandatory for the dyeing of these fibers. Due to their high glass transition temperature, high temperatures must assist the use of carriers; usually m-aramid fibers are dyed in the range of temperature from 120-130 ºC. The most important dyeing component is certainly the dyestuff; m-aramids are worldwide dyed using dyestuffs belonging to the class of Basic (Cationic) Dyes for many reasons that will be discussed afterwards.

Others important dyeing parameters are the pH of the liquor that, using basic dyes, must be maintained acidic, keeping free the positive charge of the cationic dye, and the liquor ratio, that

expresses the quantity of liquid media against the fiber's weight. The liquor ratio depends on the machinery, fiber aspect (tow, tops, yarn or fabric) and kind of process that you want to realize [1-4]. The following is an example of recipe, during a time/temperature diagram (Figure 1), provided by DyStar (1997) for Nomex[®] dyeing.
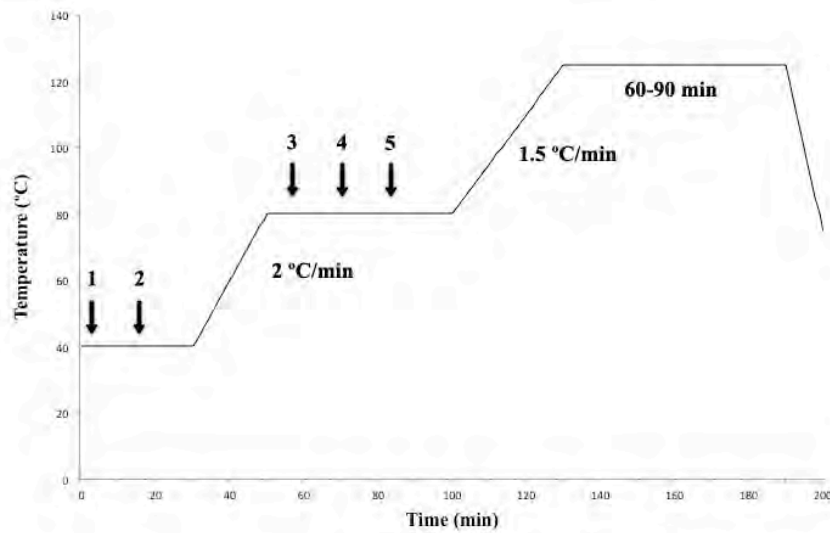

Figure 1. Time/Temperature diagram of DyStar suggested recipe of 1997.

1- Add swelling agent: 20 g/l of acetophenon or 70 g/l of benzyl alcohol or 40 g/l of Levegal C45.
2- Add selected cationic dye from 1% to 5% and adjust pH to 3.5-4.0 with acetic acid.
3- Add 7 g/l of Sodium Nitrate.
4- Add 7 g/l of Sodium Nitrate.
5- Add 7 g/l of Sodium Nitrate.

3.2 Cationic dyes

The most used dyes in m-aramid dyeing are basic dyes. Basic, or cationic dyes are salts of organic bases in which the chromophoric system is linked to the cation, while the anion is colorless. Cationic dyes are very numerous and their chemical structures are very assorted. Due to their positive charges, they present affinities with the acid groups situated into the fiber; their positive charge could be delocalized on the molecule by resonance, or localized. The most used in dyeing of m-aramid possess a delocalized charge. In Figure 2 has the structure been represented of Methylene Blue, which is probably the most famous example of Basic Dyes. It possesses a delocalized positive charge [3].
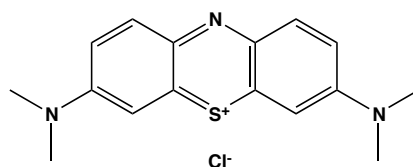

Figure 2. Molecular structure of 3,7-bis(dimethylamino)phenothiazin-5-ium chloride (Methylene blue), in which the positive charge is delocalized on the molecule by resonance.

1) There are many reasons why cationic dyes are widely utilized for m-aramid dyeing. First of all they can interact through anion bonds with the carboxylated (-COO⁻) termination of the polymeric chains; moreover they can interact, using secondary bonding, with the lone pair situated on: the oxygen of the carbonyls (-C=O) of the amidic groups and on the nitrogen of the amidic groups.
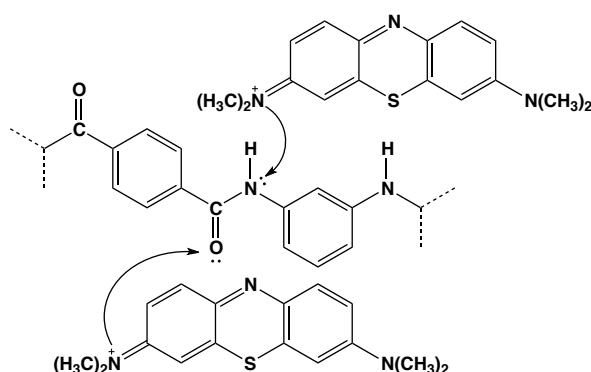

Figure 3. Example of interactions between a m-aramid fiber and a basic dye (C.I.: Basic Yellow 13).

They present a low molecular weight (400-600 amu) that permits an easier penetration into the fiber pores. Additionally, they show a good solubility in water, which is very important in dyeing processes, where water is the media transporting dye molecules into the fiber.

3.3 Disperse dyes

Disperse dyes are usually used to dye synthetic fibers such as PET or polyester. They have an organic, nonionic composition; they are almost insoluble in water but even though they're applied in aqueous dispersion.
Three different categories of disperse dyes exist, as shown in Figure 4:

1) Dyes including "azo" groups (N=N) in their molecules, mainly mono-azo or di-azo. These dyes include a very large range of coloration.
2) Nitro di-phenol amine dyes for yellows and oranges.
3) Dyes possessing an anthraquinone-like structure, for oranges, greens and blues.
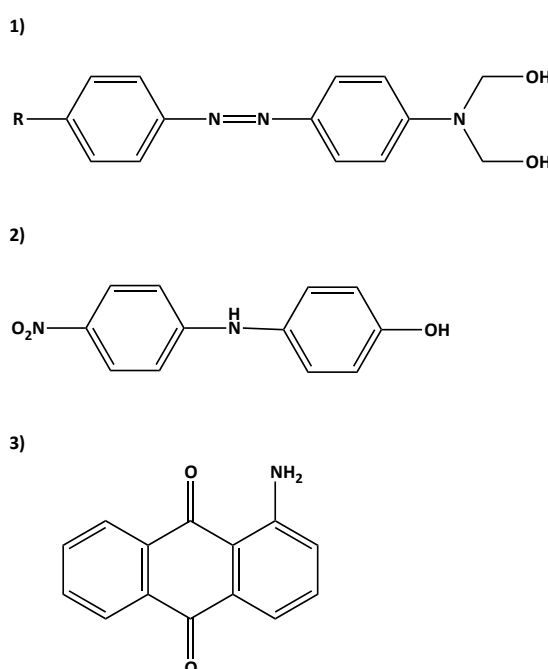
Figure 4. Examples of disperse dye belonging to three different classes.

They represent a novelty in m-aramid fiber dyeing, as no reference has been found in the literature about the dyeing of m-aramids with this class of dye. They present low molecular weight allowing them to penetrate easily into the fiber pores when the fiber is swelled; unfortunately they are not

water-soluble. Furthermore, using insoluble dyes, a dispersant is mandatory during a dyeing process.

3.4   Dyeing Mechanisms

3.4.1   Cationic dyes

Cegarra and Puente in "Dyeing of Textile Materials" give a classic explanation about the dyeing mechanism for acrylic fibers using this class of dyes [3]. The acrylic example was reported as the most similar with m-aramids found in the literature. The only differences with m-aramids mechanism are related to the chemical groups, on the fiber, with which dye molecules are bonded. Acrylic fibers possess both sulfonic and carboxylic terminations. In these terminations, due to the equilibrium in water during the dyeing, can be negatively charged and act as binder for the dye molecules positively charged.
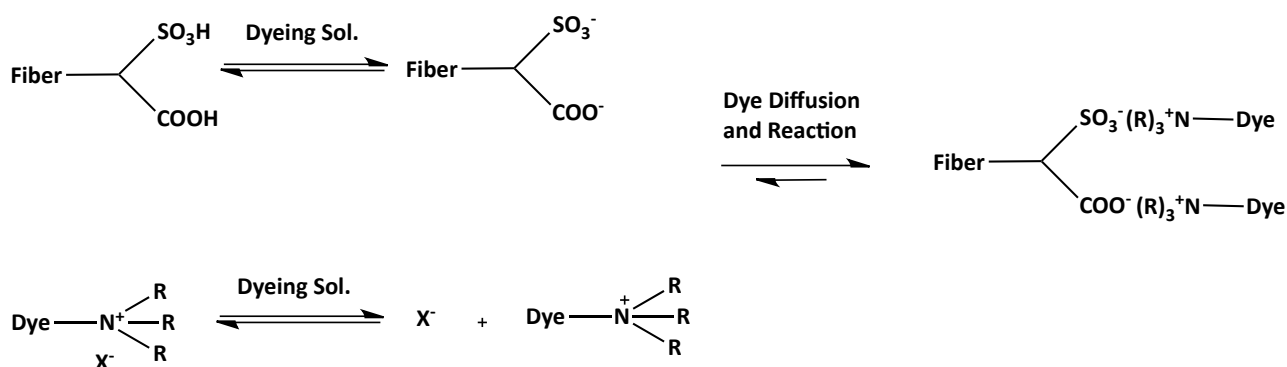
Figure 5. Scheme of the dyeing mechanism of a basic dye with acrylic fiber, namely the diffusion of the dye in the fiber.

All the different equilibrium phases determine the so-called "dyeing equilibrium" in which, normally, the Rate Determining Step or RDS (the slowest step) is the final step (represented in Figure 5). With normal basic dyes, the inverse reaction speed is very low: a reaction between dye and fiber occurs, therefore the migration in practically absent. The typical phases which occur during the dyeing process and which establish the mechanism of the reaction are the following:

1) Adsorption of the dye on the surface of the fiber
2) Diffusion of the dye into the fiber
3) Fixation of the dye in the reactive group of the fiber

The dye diffusion takes place when the structure of the fiber is "opened", this occurs at temperatures greater than Tg. This, as mentioned before, is the slowest phase and represents the RDS.

Obviously, this dyeing mechanism can be influenced by a lot of parameter such as, for first, fiber composition and the presence of one or more carriers, as well as pH, temperature, presence of electrolytes and bath ratio.

3.4.2   Disperse dyes

Disperse dyes are considered water insoluble due to their hydrophobic nature; they do not have ionic groups in their structure. Nonetheless, they do have polar substitutes such as –OH or NO_2, so they present an extremely low solubility that, however, is extremely important for dyeing. In fact, dyeing takes place due to the dissolved dye molecules. Obviously, this poor solubility is further decreased by the formation of dye aggregates into the aqueous system. For this reason, dispersion plays a crucial role during an aqueous dyeing process: for increasing dye dispersion, a dispersing agents play a crucial role.

They break the dye aggregates forming a micelle-like system that increase the pseudo solubility of the dye. During dyeing, dissolved dye molecules come from micelles more easily than from the dye aggregates. The equilibrium can be represented by three different phases of single multiple equilibrium.

Solid DYE

Dissolved DYE   **DYE into Fiber**
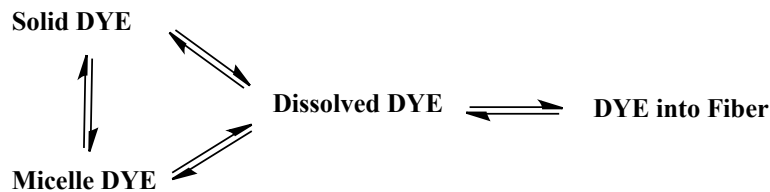
Micelle DYE

Figure 6. Scheme of dyeing mechanism using disperse dyes.

The dispersing agent, as mentioned previously, increase the pseudo solubility of the dyes including them in micelles, that are more easily dissolved in aqueous media than the solid dye present in clusters into the solution. The dye into the micelle can be considered as a reserve that can give up further dye after this has been partially absorbed by the fiber. It's important to choose properly the process parameters, because the equilibrium is very labile; no reaction occur between fiber and dye, and the dyes can go out in same manner they entered into the fiber pores. For example, using a too high concentration of dispersing agent, the equilibrium between dye in the bath and in the fiber can

be shifted toward the bath and dye molecules prefer to remain, or go back, into a micelle system rather than stay, or go, into the fiber.

On the other hand, using too low dispersing agent concentration can cause a poor dispersion moving the equilibrium to the insoluble dye clusters formation. If the dispersion is not stable while dyeing, defective results are very probable [3].

3.4.3   m-Aramid dyeing mechanism in carrier/dye/fiber system

In m-aramid dyeing process, even though the same dyes have been used, the system is quite different. Introducing into the dyeing process, a third component (the swelling agent) acting directly in the rate determining step of the dyeing process (not like the dispersing agent for disperse dyes, which acts on dye dispersion and solubility which is not the slowest phase), complicates more the scenario described previously. The mechanism changes, the thermodynamic equilibrium pathway as well as kinetics appear altered. This new situation must be evaluated experimentally and simulated by fluid dynamics simulations, aiming to comprehend the dyeing mechanism.

Ingamells *et al.* [5] explained the carrier effect by the free volume theory: dye diffusion depends on the segmental mobility of the polymer chains, which in turn depends on the glass transition temperature, being an essential characteristic of the polymer viscoelastic behavior. A dyeing transition temperature "Td" occurs under dyeing conditions. Dye uptake depends on the plasticization state of the fiber and rises sharply at Td. There is a relationship between Td and Tg. The distribution of the carrier between the liquor and the fiber plays a decisive role in reducing Tg and is dependent on the structure of the carrier (as discussed in Chapter 2). Although equivalent concentration of carrier into the fiber influence the dye diffusion rate to some extent, the equilibrium dye uptake depends on the structure of the carrier. This fact has been attributed to a specific interaction between different carriers and dyes in the fiber interior. In some studies on dyeing polyacrylonitrile fibers with basic dyes, Ingamells et al. [6, 7] used the benzyl alcohol as carrier, which is an important carrier also for m-aramid fiber dyeing, as shown by Nechwatal and Rossbach in their studies [8]. They experimentally found a correlation between the concentration of benzyl alcohol into the liquor and final dye uptake into the fiber, using Methylene Blue (cationic) dye.

Regarding the use of disperse dyes, only a paper has been found in literature; Herlinger et al. confirmed the Ingamells' results for a carrier/fiber/dye using PET and disperse dyes [9]. When the dyeing process begins, they say, there are emulsified drops of carrier and disperse dye in the liquor. During the heat-up period, the fibers have already adsorbed a part of the carrier. Because of their high solubility in the carrier, if compared with water, the disperse dyes migrates simultaneously in the carrier drops in the liquor and in the carrier layer on the fiber surface. When the temperature rises, carrier and dye diffuse from the surface layer into the inner fiber.

However, information about kinetics and thermodynamics of disperse dyes/carrier/m-aramid, crucial in understanding the chemico-physical mechanism, are lacking.

For this reason, the goal of the experimental work is to evaluate the thermodynamics aspect of the dyeing process of X-Fiper m-aramid fiber in the system carrier/dye/fiber using both basic and disperse dye. Firstly, the equilibrium time will be found in order to build the absorption isotherms. After that, the diffusivity will be estimated experimentally through kinetics studies. Finally, a simulation model will be built in order to simulate the diffusion behavior of the dye into the complex system.

3.5   Introduction to experimental part

3.5.1   Foreword of the experimental part

Some preliminary test have been done to evaluate the potentiality of the carrier; these tests have demonstrated that, 1-Phenoxy-2-propanol (1-Phen) gives unsatisfactory results in terms of dyeing shade and end product quality. This is due to the fact that its dispersant power against disperse dyes is very poor. For this reason it has been decided to focus our attention on using the N-Met swelling agent. Moreover, N-Met has been considered a novelty in terms of swelling agents, and it has never been tested before in X-Fiper m-aramid fiber dyeing.

Two different dyes have been chosen for this experimental work. These two dyes, one blue cationic and one red disperse have low molecular weight and are easily commercially available. The cationic dye is the C.I. Basic Blue 41 (BB41), while the disperse dye is the C.I. Disperse Red 21 (DR21).
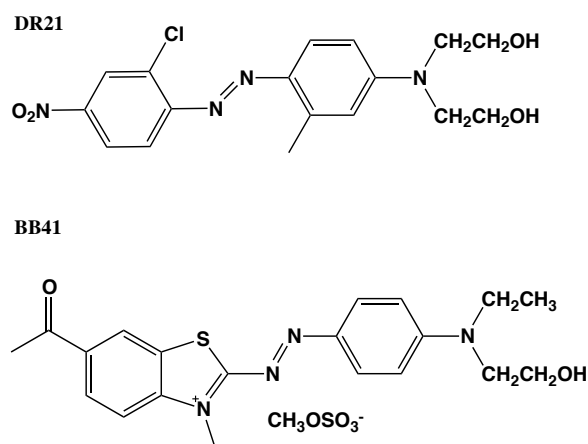

Figure 7. Chemical structures of Disperse Red 21 (upward) and Basic Blue 41 (down).

In Table 1, are given the principal characteristics of the two dyes.

Dye Class	Color Index (C.I.)	Molecular Weight (g/mol)	Water Solubility (g/l)
Cationic	Basic BLUE 41	482.57	90 (90 ºC)
Disperse	Disperse RED 21	378.81	Negligible

Table 1. Principal features of DR21 and BB41.

3.5.2   Dyestuff Extraction

The evaluation of the absorbed dye is normally done indirectly by the analysis of the exhausted bath at the end of a dyeing process. With a swelling agent, that shows poor water solubility but great affinity with dyes, the procedure above described is impossible because at the end of the process small droplets of carrier, emulsified into the water, trap the dye molecules reducing the real dye concentration into the exhausted bath. For this reason the evaluation of dye concentration must be done directly by extracting the dyestuff present into the colored fiber. Obviously, a solvent extraction is necessary to remove easily the reacted or included dye without damaging it. Thanks to the good chemical resistance of m-aramid fiber, a screening of many solvents and mixtures was necessary. Finally, the best extraction mixture has been found to be composed composed by 4 parts of dimethylsulphoxide (DMSO) and 1 part of glacial acetic acid. The organic solvent swells the fiber and extracts the dye molecules, while the organic acid maintains a low pH that helps the dyes going out from the fiber and prevents dyes degradation. A portion of dyed fiber (from 0.5 g to 2.0 g depending on the fiber color intensity) was added to 25 ml of DMSO-acetic acid mixture and heated at 75 ºC for about 20 minutes. The amount of dye uptake (mg/g) was calculated from the equation below:

$$q_t = c_{extr}(\frac{V_{extr}}{W_f}) \qquad (1)$$

where c_{extr} is the dye concentration in the extraction mixture (mg/ml), V_{extr} is the extraction mixture volume (ml) and W_f is the fabric sample weight (g).

The dye concentration in the extraction mixture was determined spectrophotometrically by means of a ThermoScientific spectrophotometer equipped with a xenon lamp working between 400-700 nm with a bandwidth of 2 nm. Basic Blue 41shows an absorbance maximum at 625 nm (λ_{max}), Disperse Red 21 has a λ_{max} = 520 nm. A calibration curve was plotted between absorbance and dye concentration in the extraction mixture, obtaining an extinction coefficient equal to 75.278 for BB41 and 9.7294 for DR21. The R^2 value of both calibration curves resulted higher then 0.99.

In a number of articles [10, 11] BB41 shows the maximum absorption peak around 610 nm. The observed difference in wavelength is due to the organic solvents mixture, which shifts the absorption peak of the molecule. This phenomenon is commonly known as bathochromic shift or red shift.
The calibration curves of BB41 and DR21 in DMSO/AcOH mixture are reported in Figure 8 and 9.
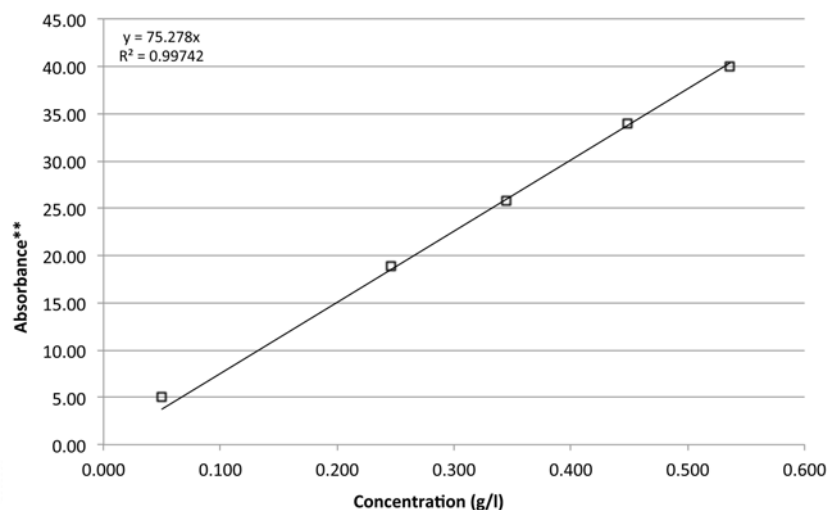

Figure 8. Calibration Curve for BB41 in DMSO/AcOH 4:1.

** The absorbance values were multiplied by 5, 50 or 100 depending on the dilution applied on the initial solution, according to initial dye weighted (that could not be as lower as necessary for calibration, due to the analytical balance limit).
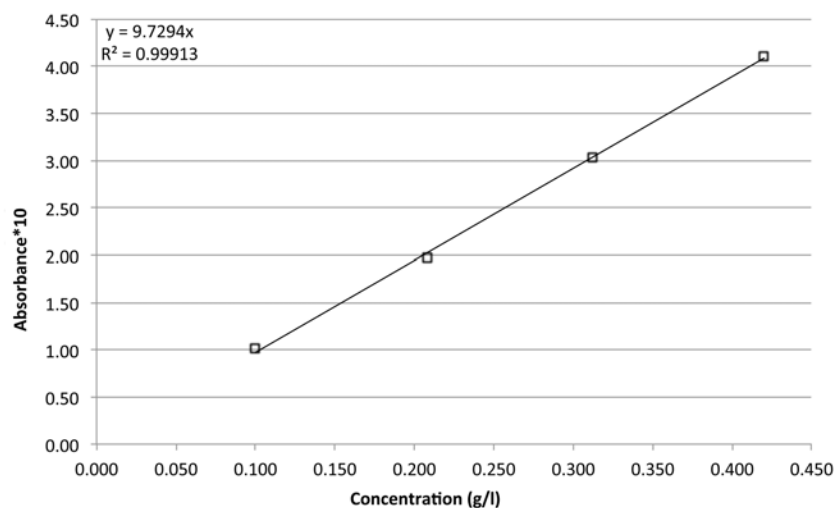

Figure 9. Calibration Curve for BB41 in DMSO/AcOH 4:1.

3.5.3   Fiber scouring

To remove spin finishes and impurities, the fabric was scoured in a solution containing 1g/l of ECE-2 detergent. Scouring was carried out at 50°C for 20 minutes. After scouring, the fabric was rinsed with cold water and dried at 60°C in an oven.

3.5.4   Dyeing Experiments

Dyeing experiments were carried out in a batch system using a Mathis Labomat-BF8 laboratory-dyeing machine. The machine is equipped with 8 sample holders of 250 ml capacity, heated by three infrared lamps and fixed in a revolving disk.

1 – Sealed beaker
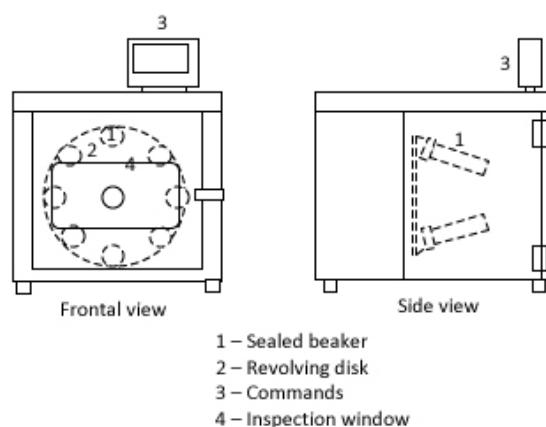2 – Revolving disk
3 – Commands
4 – Inspection window

Figure 10. Machine scheme of Mathis Labomat-BF8.

5 g of fabric sample has been used each test, adding 100 ml dyebath of known dye concentration (bath ratio = 1:20). A desired amount of N-methylformanilide (N-Met) was added and emulsified to the dyeing bath or applied directly on the fiber as a pretreatment (only for DR21). The dye bath pH was adjusted with glacial acetic acid to 3-4. Different initial dye concentrations, namely 0.5%, 1%, 2%, 5%, 10% and 20% o.w.f.% (over fiber weight), and four N-Met concentration, namely 20%, 40%, 60% and 80% o.w.f., where investigated. Time-temperature profile, in figure 7, shows that temperature was raised to 30°C, then the machine was allowed to rotate at "65 rpm left-right" for 10 minutes in order to create the same ambient for all the samples contained in all sample holders. Subsequently, the temperature was raised to 125 °C at a rate of 1.5°C/min. The temperature was held constant for 1.5 hours for BB41 and 2.0 hours for DR21, while the rotation was set at "55 rpm left-right". The two different durations were found from preliminary tests to be long enough for dye-fiber equilibrium to be reached. Temperature was then lowered to 60 °C at a rate of 6°C/min. Subsequently, the fabric was removed from the sample holders. A stripping treatment was performed to remove residual dye and N-Met deposited on the outer fiber surface. This process consists in rinsing the fabric samples with cold water and keeping them in a solution of sodium hydrosulfide

and sodium carbonate (to set the pH to 8.5-9.0) at a temperature of 60 °C for 15-20 minutes. Finally, the fabrics were rinsed again with cold water and dried in a dryer at a temperature of 60 °C for about 1.5 hours.
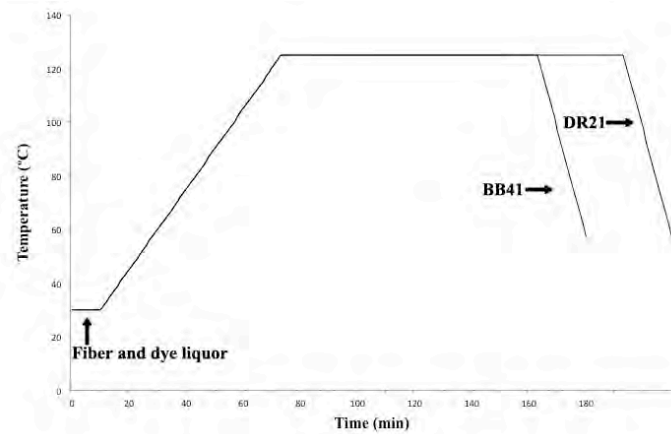
Figure 11. Time-temperature diagram of dyeing processes, using both BB41 and DR21.

The effect of initial dye and swelling agent concentration was evaluated studying the adsorption isotherms of both the considered dyestuffs at the N-Met different concentrations. As mentioned before, the adsorption isotherms have been studied at the thermodynamic equilibrium; preliminary tests have demonstrated that the thermodynamic equilibrium has reached at 1.5 hours for BB41 and after 2.0 hours using DR21, after these times the dyes start their degradation as will be explained afterwards.

3.6 Thermodynamics equilibrium study, BB41

As shown in Figure 12, the adsorption ability of Basic Blue 41 on X-Fiper m-aramid fiber is a function of the initial dye concentration into the dyebath as well as of the concentration of N-Met emulsified into the bath. All the final concentrations values derived from a mean of 3 values and the error is about 0.15 mg/g of fiber.
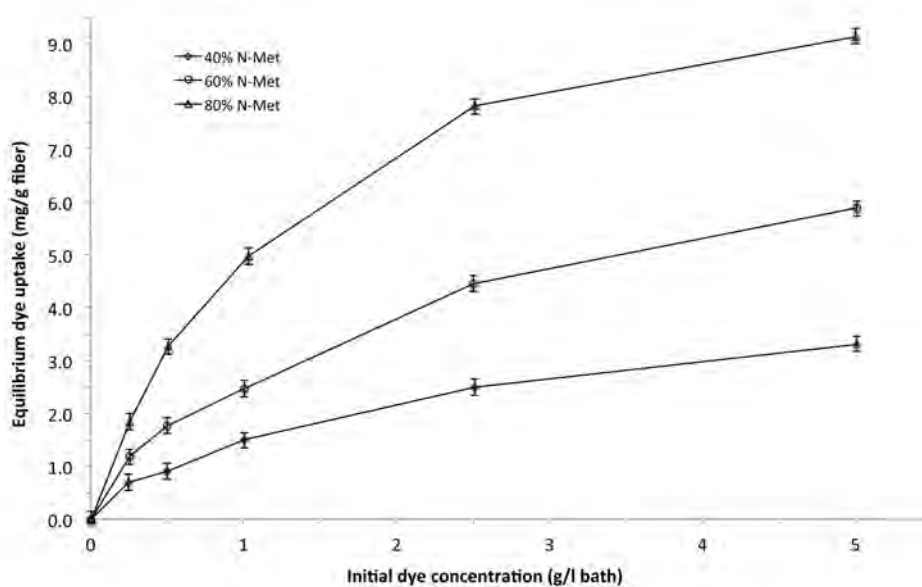

Figure 12. Equilibrium dye uptake of BB41 on X-Fiper at different N-Met concentrations.

	Initial Dye Conc. (g/l)	Eq. Dye uptake (mg/g)
40% N-Met	0.25	0.70
	0.50	0.91
	1.01	1.49
	2.51	2.49
	5.01	**3.31**
60% N-Met	0.26	1.18
	0.50	1.77
	1.00	2.47
	2.50	4.46
	5.01	**5.88**
80% N-Met	0.25	1.84
	0.51	3.27
	1.04	4.97
	2.52	7.81
	5.00	**9.14**

Table 2. Mean Dye uptake results of the dyeing with three different concentrations of N-Met.

As expected, under equilibrium conditions the amount of dye adsorbed on the fiber increases with increasing of the initial dye concentration. This effect is remarkable at all N-methylformanilide concentrations: dye uptake at equilibrium increased by five to six times as the initial dyebath concentration was increased from 0.5% to 10% o.w.f. (from 0.25 g/l to 5 g/l). However, at 40% N-Met concentration, final dye uptake is very low at all initial dye concentrations. Considering, for example, the graph point: 5g/l initial dye, 40% N-Met, only 3.3% of the initial dye is found on the fiber with an uptake (calculated over fiber weight) of 0.33%. This suggests that 40% of carrier is not enough for an adequate dye uptake; the dye consumption is to high respect the final fiber hue. Moreover, using 60% of N-Met is possible to reach the 40% N-Met dye uptake (with 10% of initial dye) only using 3.5% o.w.f. initial dye. Increasing the carrier concentration to 80% o.w.f. the dye uptake, reached with 10% of initial dye at 40% of N-Met, has been reached using 1% of initial dye; 10 times higher than using half concentration of swelling agent. Nevertheless, from an industrial and technological point of view, to obtain an acceptable final hue on m-aramid fabrics, at least 60% o.w.f. of swelling agent and 5% o.w.f. of BB41 dye are needed. Figure 13 was obtained calculating the exact color hues (using Photoshop) by colorimetric coordinates evaluated by a spectrophotometric analysis, using a Datacolor Check II-plus instrument.
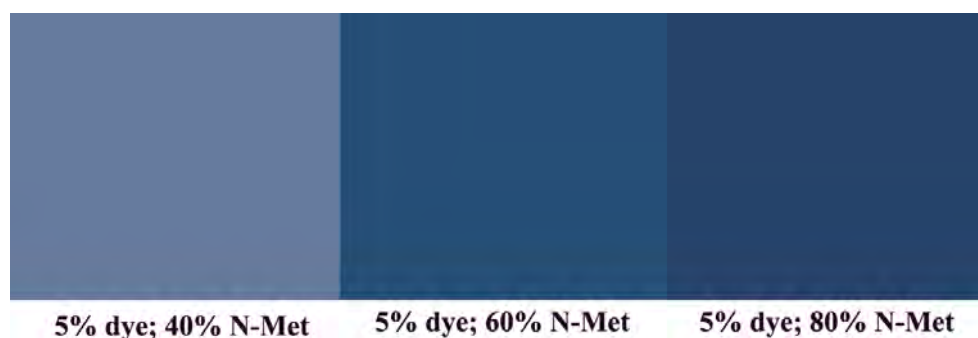
Figure 13. Hues obtained by colorimetric coordinates (Lab*) analysis, using different N-Met concentrations.

Looking at the "dye uptake" graph it's possible to predict a preliminary dyeing mechanism. At all selected concentrations, a part of N-methylformanilide is dissolved in water (it's been calculated that, using BB41, circa 30% owf of N-Met is water soluble) and the rest creates an emulsion with water. The swelling agent droplets solubilize the dye, which is much more soluble in the swelling agent in comparison to water, and transport dye molecules to the fiber (as studied previously, carrier has higher affinity with fiber). Moreover, during the dyeing process, the solubilized carrier helps the solubilized dye molecules reaching the fiber; his affinity towards m-aramid is strongly higher than water. Thus, the swelling agent with solubilized dye is preferentially adsorbed at the fiber surface, forming a surface layer on the fiber. As the temperature increases, the swelling agent and the dyestuff diffuse from the surface layer into the inner fiber, the swelling agent diffusing first. This hypothesis of dyeing mechanism confirms the hypothesis formulated by Nechwatal and Rossbach in their work [8], as described in paragraph 3.4.3. To verify this hypothesis, based on the experimental tests that have been carried out, adsorption isotherms were studied.

3.6.1   Adsorption isotherms, BB41

Two different models of isotherm adsorption have been evaluated: Langmuir and Freundlich.
The purpose of adsorption isotherms is to relate the adsorbate concentration in the bulk and the adsorbed amount at the interface. Langmuir isotherm has been successfully applied to many adsorption processes [12,13]. The basic assumption of Langmuir theory is that sorption takes place at specific sites and adsorbate-absorbent molecules undergo strong intermolecular attractions [14-15]. Thus, Langmuir theory predicts the absorption of a monolayer of adsorbate molecules on the surface, excluding the formation of multilayers. Langmuir isotherm is expressed by the following equation:

$$q_e = \frac{q_m \, K_L c_e}{1 + K_L c_e} \qquad\qquad (2)$$

which can be linearized as follows:

$$\frac{1}{q_e} = \frac{1}{q_m} + \frac{1}{K_L q_m} \frac{1}{c_e} \qquad\qquad (3)$$

Where q_e is the amount of dye adsorbed on the fiber (mg/g) in equilibrium with the dye concentration in the bath c_e, expressed in mg/l. The equilibrium concentration in the bath (c_e) has been obtained from the difference between the initial amount of dye in the bath (c_i) and the amount of dye extracted from the fiber (q_e). q_m is the maximum density of adsorption with complete monolayer coverage on the absorbent surface (mg/g), K_L is the Langmuir constant and is related to the energy of adsorption (l/mg).
The q_m value represents a practical limiting adsorption capacity when the surface is fully covered with dye molecules (saturation concentration), so it assists in the comparison of adsorption performances [16]. The values of q_m and K_L are then calculated from the intercepts and the slopes of the trend lines of the plot of $1/q_e$ versus $1/c_e$.

N-Met Conc. (% o.w.f.)	Initial Dye Conc. (% o.w.f)	Initial Dye Conc. (mg/l)	c_e (mg/l)	q_e (mg/g)
40%	0.5	251	216	0.70
	1.0	500	455	0.91
	2.0	1007	932	1.49
	5.0	2507	2382	2.49
	10.0	5006	4840	3.31
60%	0.5	255	196	1.18
	1.0	503	414	1.77
	2.0	1001	878	2.47
	5.0	2503	2280	4.46
	10.0	5014	4720	5.88
80%	0.5	252	160	1.84
	1.0	506	343	3.27
	2.0	1035	786	4.97
	5.0	2515	2124	7.81
	10.0	4998	4541	9.14

Table 3. Experimental data used for adsorption isotherms, found at different carrier concentrations.

The adsorption data, at the thermodynamics equilibrium, of BB41 on X-Fiper m-aramid fibers were fitted using the Langmuir model. The figure below shows the plot of $1/q_e$ versus $1/c_e$. Where the intercept is equal to $1/q_m$ and the slope is equal to $1/(K_L q_m)$. Values of q_m and K_L are reported in Table 4 for the three different carrier concentrations.
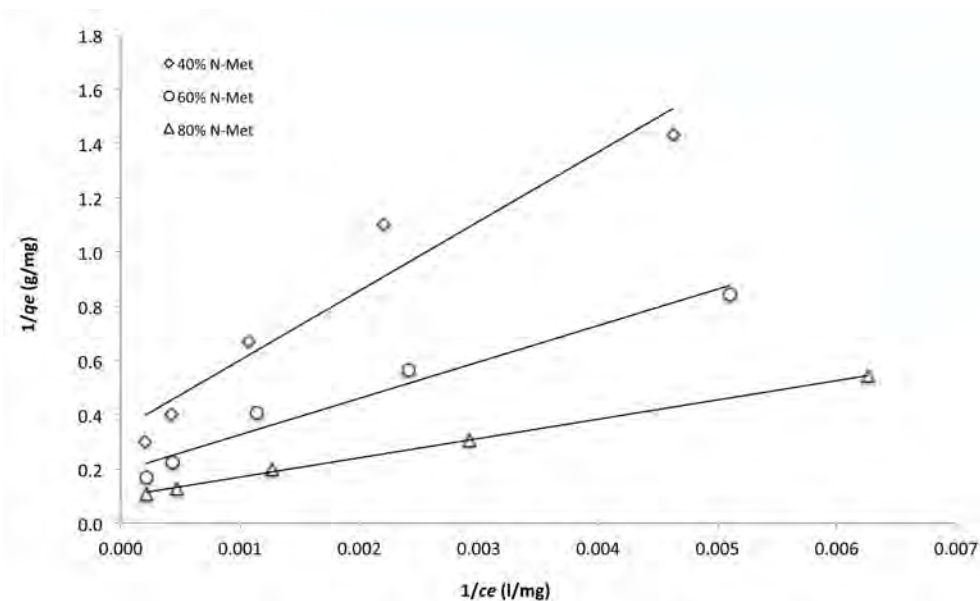

Figure 14. Plot of $1/q_e$ versus $1/c_e$ given by Langmuir linearized equation.

	q_m(mg/g)	K_L(l/mg)	R^2
40% N-Met	2.89	$1.35*10^{-3}$	0.933
60% N-Met	5.21	$1.43*10^{-3}$	0.965
80% N-Met	10.11	$1.39*10^{-3}$	0.998

Table 4. Parameters of Langmuir isotherms plot, including the R^2 of the trend lines.

Using Langmuir parameters, Langmuir isotherms have been built and compared with the experimental measurements.
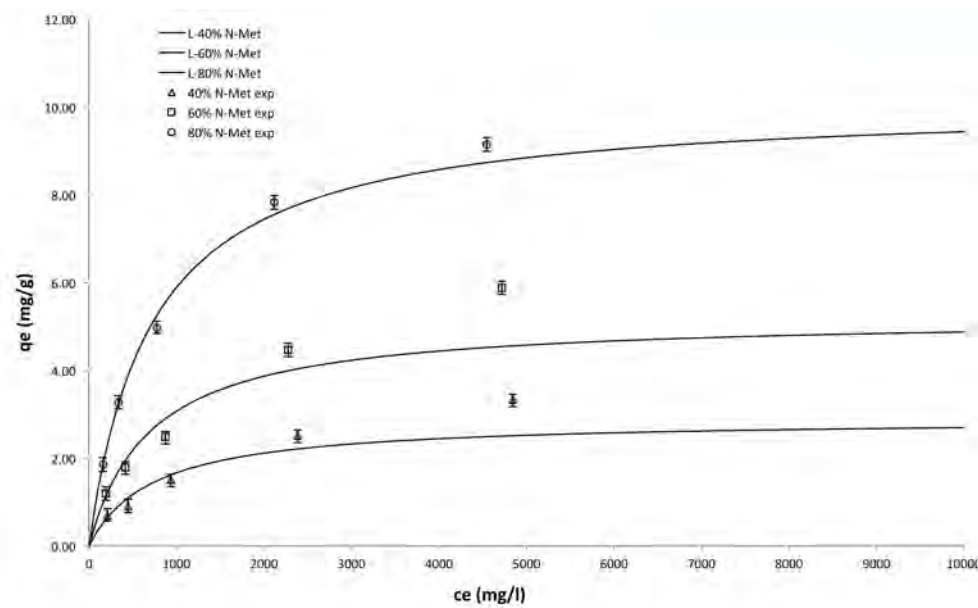

Figure 15. Experimental data compared to the theoretical Langmuir isotherms.

It's immediate to notice that, for 40% and 60% of N-Met, the Langmuir hypothesis of the monolayer is not applicable: the concentration at saturation q_m is lower then the experimental maximum dye concentration (q_e with initial dye concentration of 10% owf). Due to the great excess of dye in the liquor, it is likely that multilayer adsorption takes place. The isotherm of Langmuir fit well only using 80% of N-Met. At this carrier concentration the hypothesis of a monolayer could be applied, even though this hypothesis appears very strange. The question is then: why only using 80% of N-Met the Langmuir isotherm fits the experimental data? The answer will be given further ahead.

The essential characteristic of Langmuir isotherm can be expressed in terms of a dimensionless equilibrium parameter, such as the separation factor or equilibrium factor (R_L) defined in the following equation [17, 18]:

$$R_L = 1/(1 + K_L c_o) \qquad (4)$$

where K_L is the Langmuir constant and c_o is the initial adsorbate concentration in the solution. This parameter indicates that isotherm will be shaped according to the following adsorption characteristics [19].

$R_L > 1$ Unfavorable adsorption;
$R_L = 1$ Linear adsorption;
$0 < R_L < 1$ Favorable adsorption;
$R_L = 0$ Irreversible adsorption.

As given in Table 5, it can be seen that the adsorption of BB41 onto X-Fiper fiber is highly favorable.

N-Met Conc. (% o.w.f.)	c_o (mg/l)	K_L (l/mg)	R_L
40%	251	0.0135	0.2279
	500	0.0135	0.1290
	1007	0.0135	0.0685
	2507	0.0135	0.0287
	5006	0.0135	0.0146
60%	255	0.0143	0.2152
	503	0.0143	0.1221
	1001	0.0143	0.0653
	2503	0.0143	0.0272
	5014	0.0143	0.0138
80%	252	0.0139	0.2221
	506	0.0139	0.1245
	1035	0.0139	0.0650
	2515	0.0139	0.0278
	4998	0.0139	0.0142

Table 5. Equilibrium factor (R_L) calculation for Langmuir adsorption isotherm of BB41.

However, the theoretical Langmuir curves derive from the interpolation of experimental data using a linearization of the Langmuir equation. Moreover, it is possible to find the best Langmuir parameters K_L and q_m without the application of linearization. The consequence results in a better fitting than the previous one that, however, continues to be not completely satisfactory. These results are reported in Figure 16 and Table 6.
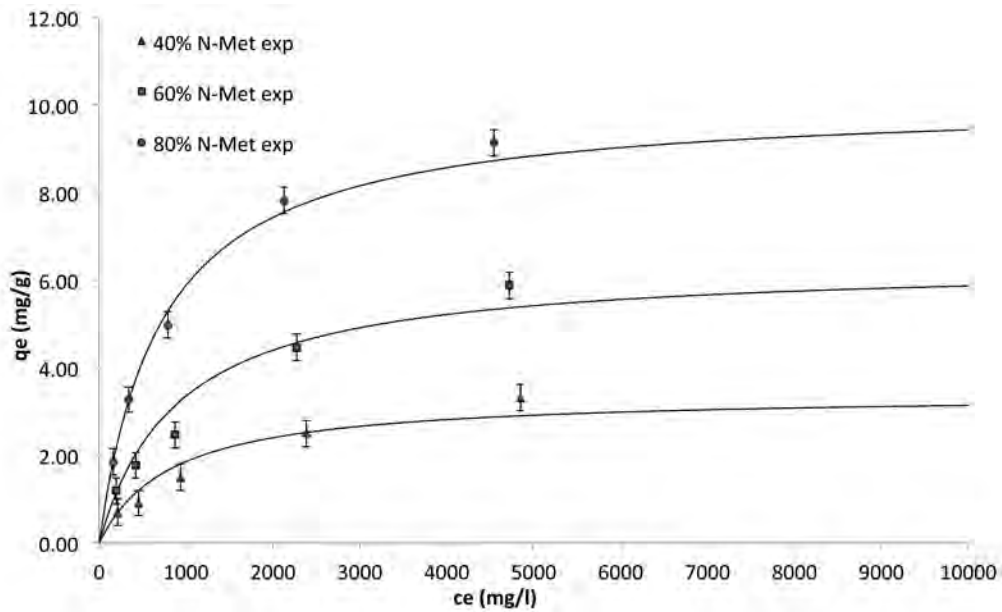

Figure 16. Best Langmuir fitting obtained without the use of linearization.

	q_m(mg/g)	K_L(l/mg)	R^2
40% N-Met	2.89	$1.35*10^{-3}$	0.933
60% N-Met	5.21	$1.43*10^{-3}$	0.965
80% N-Met	10.11	$1.39*10^{-3}$	0.998

Table 6. Parameters of Langmuir isotherms plot, including the R^2 of the trend lines.

The experimental data of BB41 adsorption on X-Fiper m-aramid fiber, at different N-Met concentrations, have been fitted with another adsorption isotherm, given by Freundlich model. The empirical equation is given by the following equation [20]:

$$q_e = K c_e^{1/n} \qquad (5)$$

Freundlich constants K and n are related to the adsorption capacity and adsorption strength, respectively. Although was purely empirical, equation of this type can be derived mathematically from the assumption of a heterogeneous surface. Freundlich equation is then linearized as follows:

$$\ln q_e = \ln K + \frac{1}{n} \ln c_e \qquad\qquad (6)$$

The plot of $\ln q_e$ versus $\ln c_e$ is shown in Figure 17 and the Freunlich constants are given in Table 7. The magnitude of the exponent $1/n$ can give an indication of the favorability and capacity of the adsorbent/adsorbate system, where $n > 1$ represents favorable adsorption conditions. In most literature cases the exponent n results between 1 and 10, in the present experimental study values of circa 2 were obtained for all N-Met concentration, meaning that the adsorption is favorable as well as the system remains the same changing swelling agent concentration [17, 19].
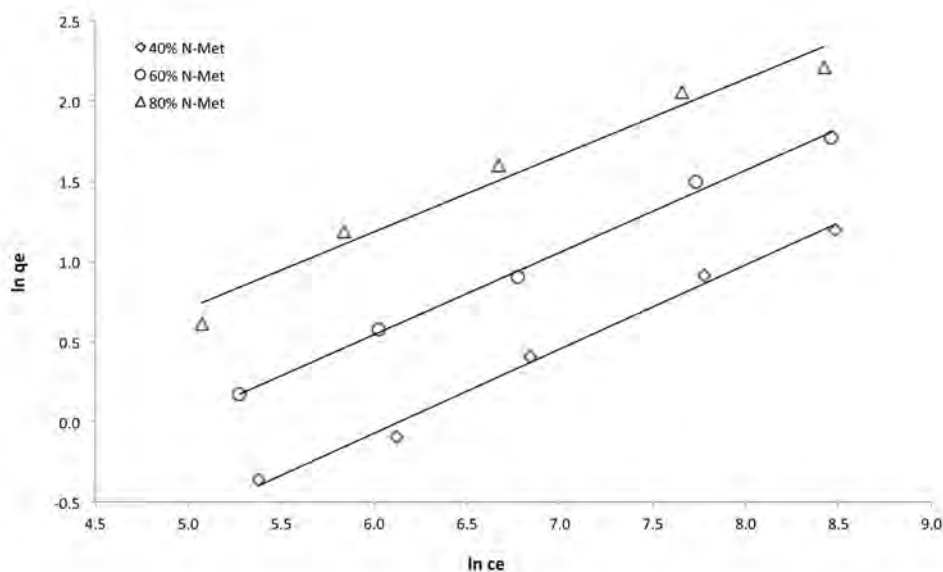
Figure 17. Plot of $\ln q_e$ versus $\ln c_e$ given by Freundlich linearized equation.

K values are calculated as exponential of the value of the ordinate at the origin of the trend line and $n = 1/$(line slope). Values are reported in table below:

N-Met Conc. (% o.w.f.)	K (l/mg)	n	R^2
40%	$3.99*10^{-2}$	1.90	0.992
60%	$7.95*10^{-2}$	1.95	0.996
80%	$1.87*10^{-2}$	2.09	0.967

Table 7. Values of Freundlich constant (K), n exponent and R^2 at different N-Met concentrations.

Using Freundlich parameters, Freundlich isotherms have been built and compared with the experimental measurements.

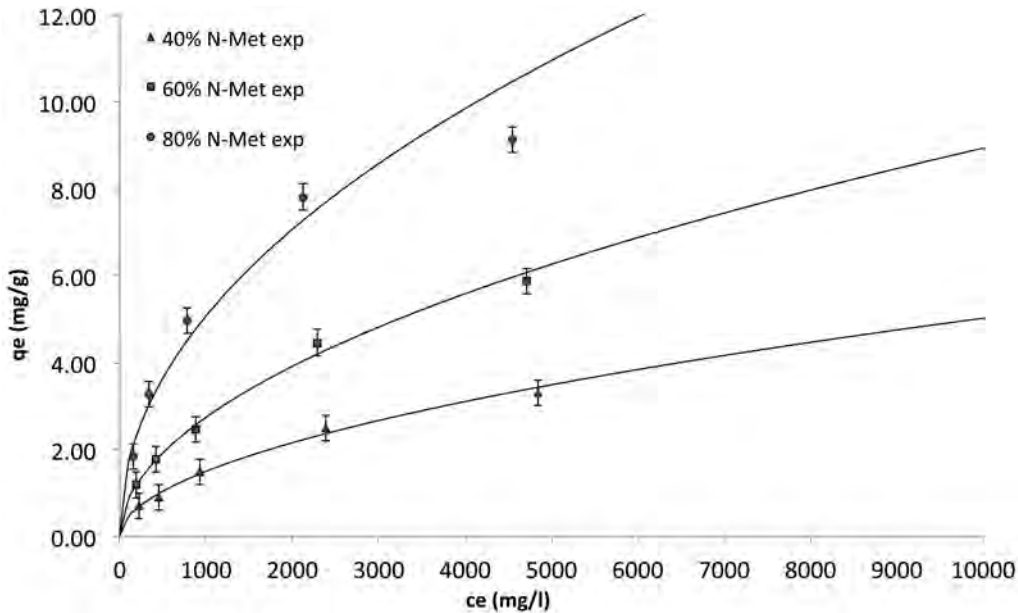Figure 18. Experimental data compared to the theoretical Langmuir isotherms.

Based on the correlation coefficients shown in the previous tables, the adsorption model better describing BB41 adsorption on X-Fiper fiber was the Freundlich one. This result suggests a heterogeneous distribution of the adsorption sites; apparently an uneven arrangement of heterogeneously adsorbed dye would promote the development of local multilayers and aggregates on m-aramid fibers.

To confirm the formulated hypothesis, the visible light absorption spectrum of extracted dye has been analyzed in order to lead a kinetic study. It has been discovered that the basic blue 41 degrade into the dye bath after a certain time at 125 ºC. This degradation is also carrier assisted and, moreover, depends on the initial dye concentration. This phenomenon takes place only at initial dye concentration higher than 5% o.w.f. and with more then 40% o.w.f. of N-Met. Using 60% o.w.f. of N-Met degradation occurred after 1.5 hours and after 1.0 hour using 80% o.w.f. of carrier. Assuming this phenomenon is real, the monolayer hypothesis established for "80% N-Met" is no longer applicable; the experimental q_e, after 1.5 hours and with an initial dye concentration of 10% o.w.f. results from a dye degradation; for this reason, probably, the concentration results to be lower then q_m.

The hypothesis of a multilayer becomes the most accredited, even using 80% o.w.f. of swelling agent. In the end, the carrier helps both the fiber swelling and dye solubilization. Due to the great excess of dye into the bath, the diffusion takes place in first instance into the monolayer; after surface layer is saturated with dye, that bind active sites of the fiber through ionic bonds, swelling agent diffuse into the deeper fiber, followed by the dye excess that couldn't bind the fiber into the

previous layer (due to active sites lack). In this way, the greater q_e found for high initial c_0, if compared to q_m of Langmuir (concentration of saturation), is finally explained.

In Figure 19 the Basic Blue degradation is shown qualitatively comparing the visible light absorption spectrum with the absorption spectra after 1.5 and 2 hours of dyeing use 80% o.w.f. of N-Met with 10% o.w.f. of initial dye.
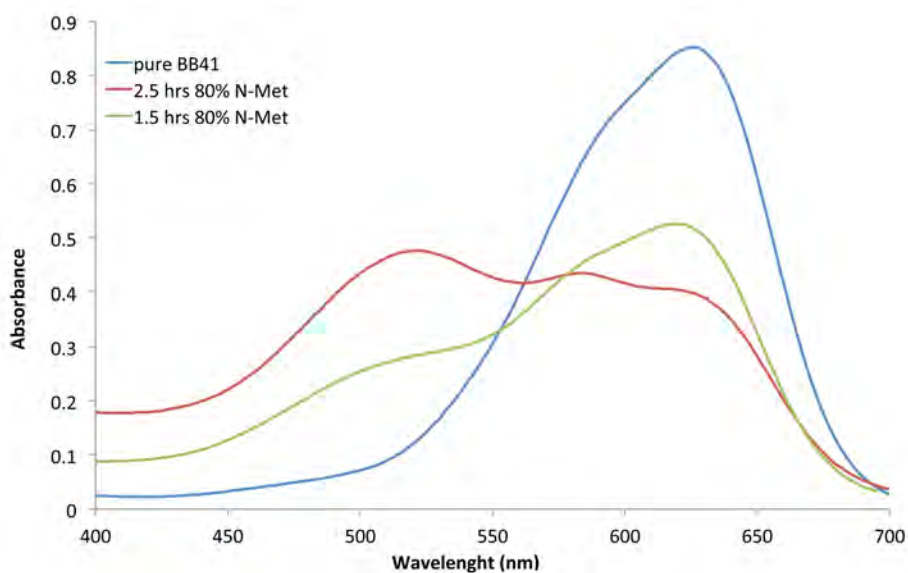

Figure 19. Qualitative comparison between absorption spectra, showing BB41 degradation

3.7   Thermodynamics equilibrium study, DR21

The same experimental approach was adopted for the equilibrium study of the dyeing process of X-Fiper fiber using the Disperse Red 21 (DR21). As discussed before, disperse dyes are less thermo-sensible then basic ones. In order to be sure that DR21 is not degrading after a certain dyeing time at 125 ºC, some preliminary tests have been done. The results of these preliminary tests showed that the thermodynamic equilibrium is reached after circa 2 hours dyeing, and after 3.5 hours dyeing, the equilibrium uptake starts to decrease meaning that the dyestuff has begun to degrade. In this case, two different experimental methods were adopted for the dyeing process. In the first one, the carrier was dispersed in the dyeing liquor creating an emulsion, as shown previously for BB41. In the second one, the fabric samples were impregnated with the swelling agent before being introduced in the aqueous dyeing liquor. The right amount of swelling agent was kept on the fabric by squeezing the excess in a calender at appropriate pressures. In this way, different amount (20%, 40%, 60% and 80% over fiber weight) of N-Met have been put homogeneously on the fiber surface. This kind of treatment was done to have a better indication about the interaction that occur into the fiber/dye/carrier system, in particular to understand which could be the swelling behavior of the fiber in the two different situations:

1) The swelling agent diffuses from the bath to the fiber during the dying process.
2) The swelling agent is already onto the fiber when the process begins.

It will be demonstrated, in next paragraphs, that the dyeing mechanism will suffer intense modifications changing the way with which the carrier is put in contact with the fabric.

3.7.1   Emulsion case

In Figure 20, the dye uptake of DR21 is shown at different initial dye concentration using different quantities of swelling agent. All the final concentrations values derived from a mean of three values and the error is about 0.30 mg/g of fiber.
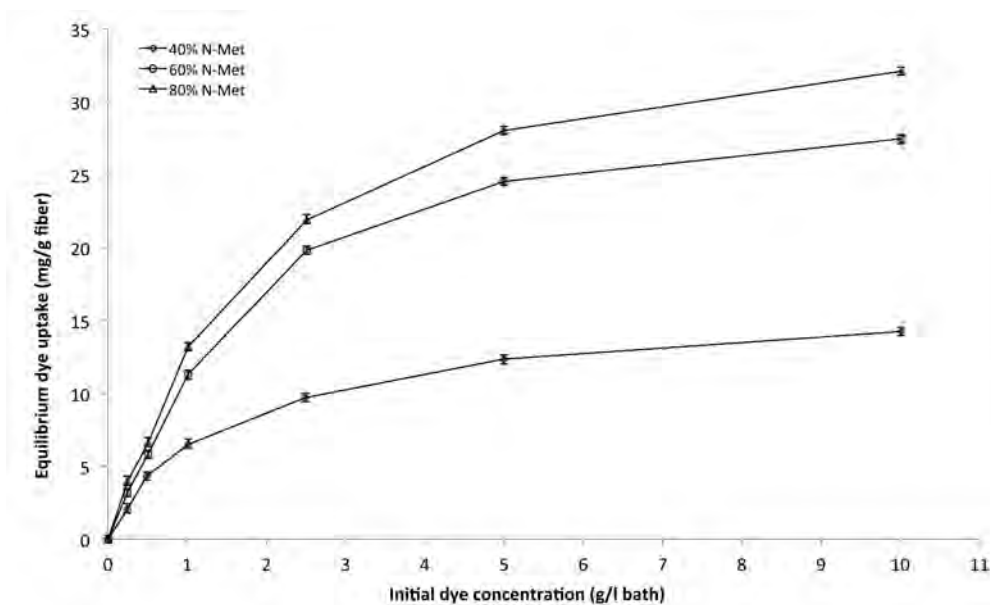
Figure 20. DR21 equilibrium dye uptake onto X-Fiper at different N-Met concentrations.

Comparing the dye uptake using DR21 against the dye uptake with BB41, it is evident that the uptake of DR21 is higher then the one of BB41 at all initial dye concentration as well as at all carrier concentrations. The dye uptake, at maximum initial dye concentration for DR21, is almost five times more than BB41 uptake at all N-Met concentrations, suggesting that the fiber has a greater affinity towards the disperse dye then towards the basic one. Even in this case, under equilibrium conditions, the amount of dye adsorbed on the fiber increases with increasing of the initial dye used. This effect is remarkable at all N-Met concentrations.

	Initial Dye Conc. (g/l)	*Eq. Dye uptake (mg/g)*
40% N-Met	0.25	2.1
	0.50	4.3
	1.01	6.5
	2.50	9.7
	5.01	12.3
	10.01	**14.2**
60% N-Met	0.25	3.2
	0.51	5.8
	1.01	11.3
	2.51	19.8
	5.01	24.5
	10.01	**27.4**

	0.25	4.0
	0.51	6.6
80% N-Met	1.02	13.2
	2.51	21.9
	5.00	28.0
	10.01	**32.1**

Table 8. Mean Dye uptake results of the dyeing with three different concentrations of N-Met.

The N-Met shows good solubilizing power towards the disperse dye, so, during the dyeing process, the solubilized dye molecules reach the fiber through the carrier droplets emulsified into the dye-bath. Increasing the temperature N-Met diffuse from the fiber surface to the inner fiber and creates voids in which the dye molecules can penetrate. This phenomenon is pronounced both at high dyestuff concentration and high carrier concentration. Then, 40% o.w.f. of N-Met is not enough to reach a good dye uptake especially at high initial dye amount (from 5% o.w.f. or 2.5 g/l), however at low dye concentration (0.5% and 1% o.w.f.) is not necessary to use more then 40% of N-Met to reach a good uptake.

5% dye; 40% N-Met   5% dye; 60% N-Met   5% dye; 80% N-Met

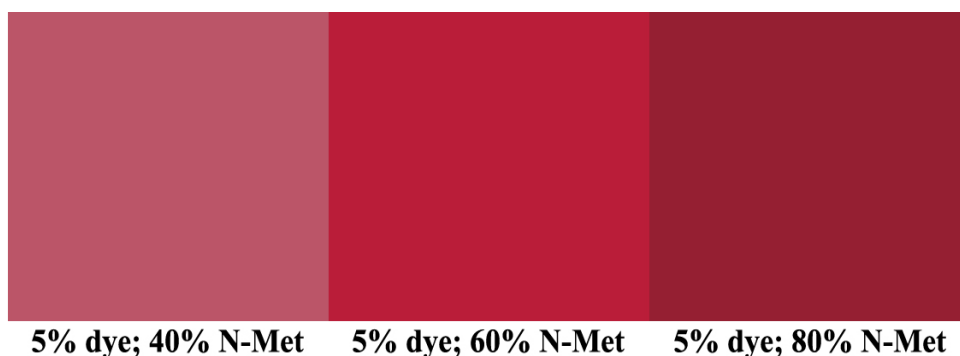Figure 21. Hues obtained by colorimetric coordinates (Lab*) analysis, using different N-Met concentrations.

As far as the end product evaluation is concerned, in terms of final hue (Figure 21), the best balance between initial dye and carrier concentrations is to use at least 60% o.w.f. of swelling agent and 5% o.w.f. of DR21, exactly the same condition defined for Basic Blue 41 in previous paragraph.

3.7.2 Adsorption isotherms in emulsion case, DR21

Two different models of isotherm adsorption have been evaluated: Langmuir and Freundlich. As shown previously, Langmuir isotherm is expressed by the equation *(2)*.

In this case, the Langmuir equation can be linearized in another way, giving the best fit with the experimental data:

$$\frac{c_e}{q_e} = \frac{1}{K_L q_m} + c_e \frac{1}{q_m} \tag{7}$$

In this case, the values of q_m and K_L are then calculated from the intercepts and the slopes of the trend lines of the plot of c_e/q_e versus c_e.

The experimental data are shown in Table 9, the Langmuir linearized plot in Figure 22.

N-Met Conc. (% o.w.f.)	Initial Dye Conc. (% o.w.f.)	Initial Dye Conc. (mg/l)	c_e (mg/l)	q_e (mg/g)
	0.5	249	144.00	2.10
	1.0	498	283.00	4.30
40%	2.0	1011	684.00	6.54
	5.0	2496	2012.00	9.68
	10.0	5007	4391.00	12.32
	20.0	10007	9295.50	**14.23**
	0.5	252	91.50	3.21
	1.0	508	216.50	5.83
60%	2.0	1009	445.50	11.27
	5.0	2508	1517.00	19.82
	10.0	5007	3780.50	24.53
	20.0	10008	8636.50	**27.43**
	0.5	251	52.00	3.98
	1.0	507	175.00	6.64
80%	2.0	1015	353.50	13.23
	5.0	2507	1410.00	21.94
	10.0	5001	3600.50	28.01
	20.0	10008	8402.50	**32.11**

Table 9. Experimental data used for adsorption isotherms, found at different carrier concentrations.
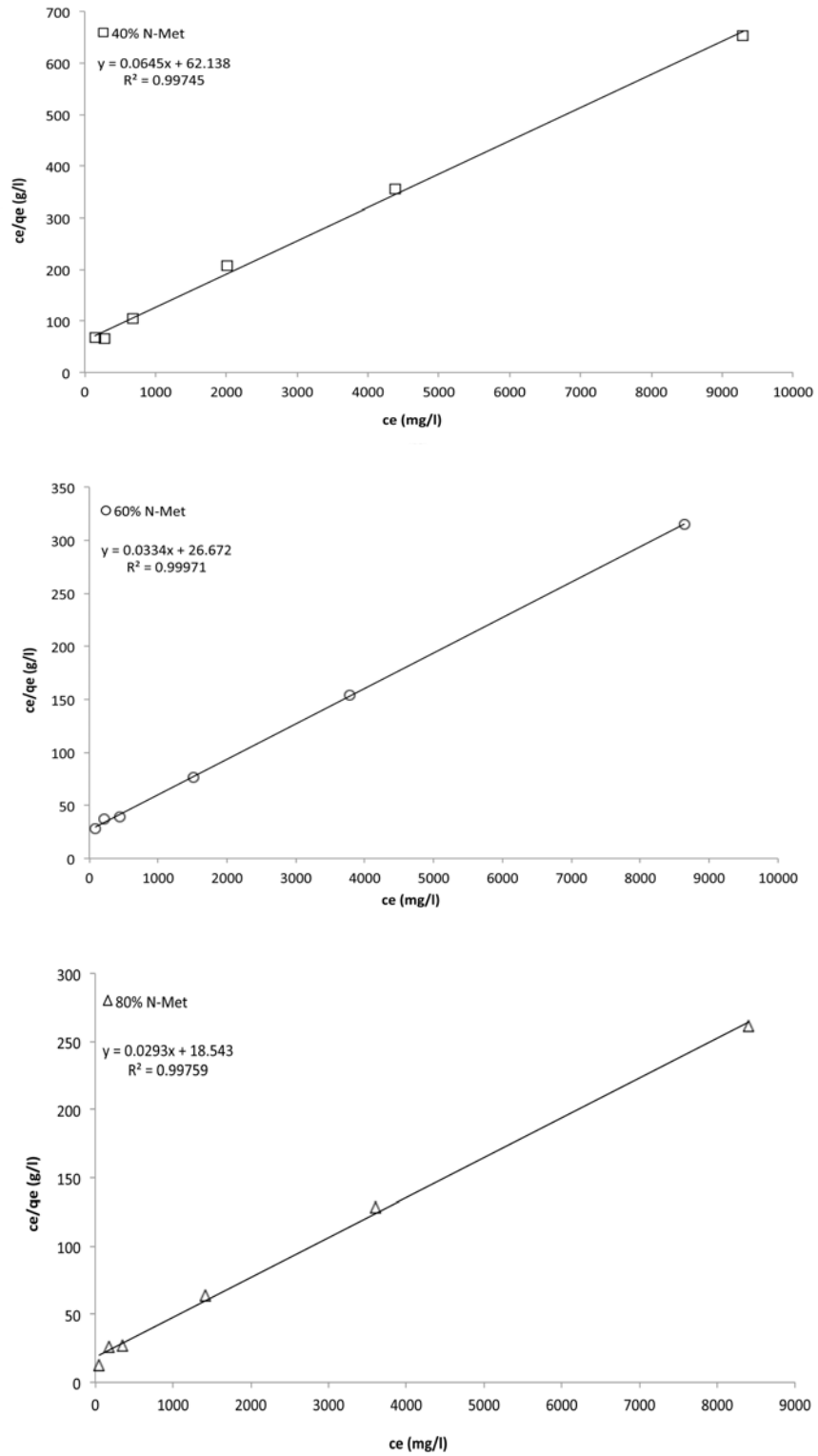
Figure 22. Plots of c_e/q_e versus c_e given by Langmuir linearized equation.

Where the slope is equal to $1/q_m$ and the intercept is equal to $1/(K_L q_m)$. Values of q_m and K_L are reported in Table 10 for the three different N-Met concentrations.

	q_m(mg/g)	K_L(l/mg)	R^2
40% N-Met	15.50	$1.04*10^{-3}$	0.997
60% N-Met	29.94	$5.38*10^{-4}$	0.999
80% N-Met	34.13	$4.72*10^{-4}$	0.997

Table 10. Parameters of Langmuir isotherm plot, including the R^2 of the trend lines.

In this case, experimental data found for the dyeing equilibrium study of DR21 at different initial dye concentration, fit very well with Langmuir linearized equation at all N-Met concentrations. So, it is possible to predict the hypothesis of the monolayer, confirming how Langmuir explained the dye adsorption. At all N-Met concentrations q_m, concentration at saturation, is pretty higher than the experimental one (Table 9 in bold), meaning that the fabric is almost saturated with an initial dye concentration of 10 g/l (20% o.w.f.). In Figure 23, the theoretical Langmuir curves have been built and compared against experimental results.
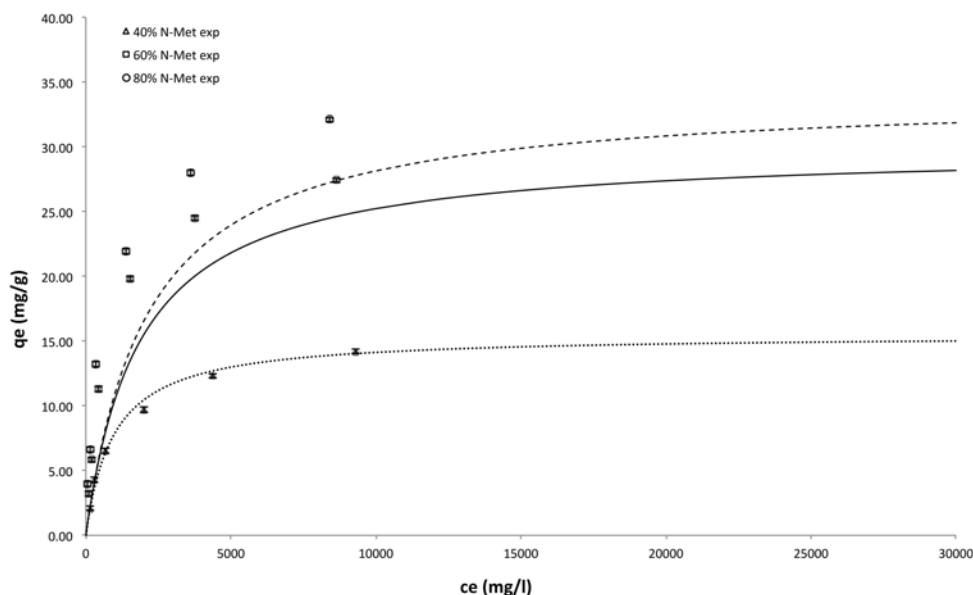

Figure 23. Experimental data compared to the theoretical Langmuir isotherms.

Even though the experimental data fit very well the Langmuir linearization (plot of c_e/q_e versus c_e), the theoretical isotherm of adsorption (build using q_m and K_L resulted from experimental data) appears to be different in comparison with the experimental trend, with the exception of the curve "40% N-Met". Looking at figure above, especially the curves of 60% and 80% o.w.f. of N-Met, seems that in the experimental pathway the fiber results more saturated (higher qe) at low initial dye concentration (from 0.5% to 5% o.w.f.) and the curve slightly decrease his slope increasing the initial dye concentration. We can say that the Langmuir isotherm curves, for 60% and 80% o.w.f. of N-Met, fit better our experimental data at high initial dye concentration then at low ones. This is confirmed by the fact that in the plot of c_e/q_e versus c_e, the first 3 points (related to 0.5%, 1%, 2% o.w.f. of initial dye concentrations) are very close to each other, reducing a lot the error of the resulting trend line (correlation coefficient very close to 1).

Plotting the obtained results using only highest initial dye concentrations (from 5% to 20% o.w.f.), with Langmuir linearization, permits to obtain new Langmuir isotherm parameter q_m and K_L.

	q_m(mg/g)	K_L(l/mg)	R^2
60% N-Met	29.94	$1.25*10^{-3}$	0.9999
80% N-Met	35.59	$1.10*10^{-3}$	0.9998

Table 11. Parameters of Langmuir isotherm plot with highest initial dye concentrations (from 2.5 to 10 g/l)

In Table 11 is easy to see that q_m do not vary for 60% o.w.f. of N-Met and vary for circa 1 mg/g for 80% N-Met; however, K_L is varied for circa one order of magnitude for both. In the variation of Langmuir constant there is the explanation of the varied isotherm pathways.

The figures below (Figures 24 and 25) show the experimental data compared to the Langmuir isotherm, built using only highest initial dye concentrations.
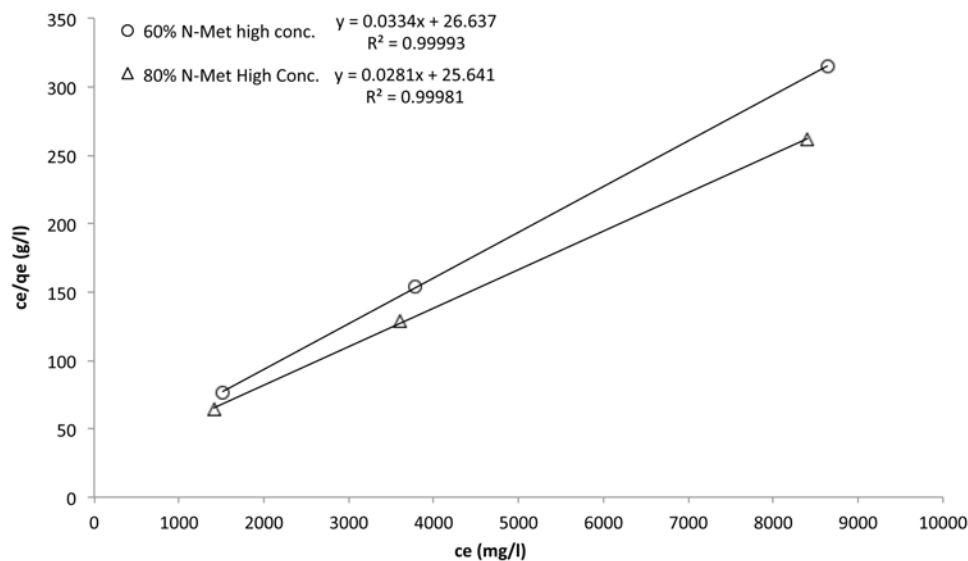
Figure 24. Plots of c_e/q_e versus c_e given by Langmuir linearized equation. Plot for high initial dye concentrations.

Figure 25. Experimental data compared to the theoretical Langmuir isotherms found for high initial dye concentrations.

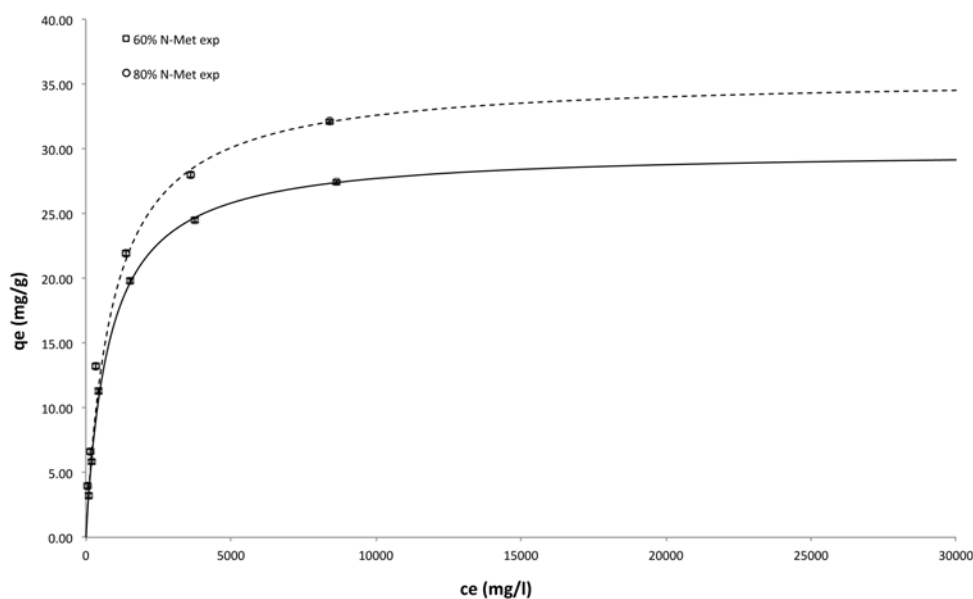Finally, in this case, it is possible to apply the Langmuir model only when the final bath concentration is very high; That is only when the concentration of dye into the fiber is very low (almost negligible) compared to the dye remained into the bath at the end of the process.

The equilibrium factor (R_L) was evaluated also for DR21 adsorption. Experimental Langmuir constant K_L and initial adsorbate concentration in the solution c_o were used to calculate R_L using the same equation *(7)* used in BB41 adsorption study.

As given in Table 12, it can be seen that the adsorption of DR21 onto X-Fiper fiber is highly favorable:
R_L values, calculated for all experimental data, are between 0 and 1. With c_o of 250 mg/l and 60% and 80% of N-Met, the adsorption in very close to be linear.

N-Met Conc. (% o.w.f.)	c_o (mg/l)	K_L (l/mg)	R_L
40%	249	0.001038	0.7946
	498	0.001038	0.6592
	1011	0.001038	0.4879
	2496	0.001038	0.2785
	5007	0.001038	0.1614
	10007	0.001038	0.0878
60%	252	0.000538	0.8807
	508	0.000538	0.7855
	1009	0.000538	0.6484
	2508	0.000538	0.4259
	5007	0.000538	0.2709
	10008	0.000538	0.1568
80%	251	0.000472	0.8942
	507	0.000472	0.8071
	1015	0.000472	0.6763
	2507	0.000472	0.4583
	5001	0.000472	0.2978
	10008	0.000472	0.1749

Table 12. Equilibrium factor (R_L) calculation for Langmuir adsorption isotherm of DR21.

Freundlich adsorption isotherm model was also used trying to fit the experimental adsorption data of DR21. The linearization , starting from the empirical Freundlich equation (5), was the same that has been used for adsorption of BB41. The logarithm of the experimental adsorption data of DR21 at different N-Met concentrations, $\ln q_e$ and $\ln c_e$, were plotted.

The plot of $\ln q_e$ versus $\ln c_e$ is shown in Figure 26, Freundlich constants are given in Table 13. K values are equal to the exponential of the value of the ordinate at the origin of the trend line and $n = 1/(\text{line slope})$.
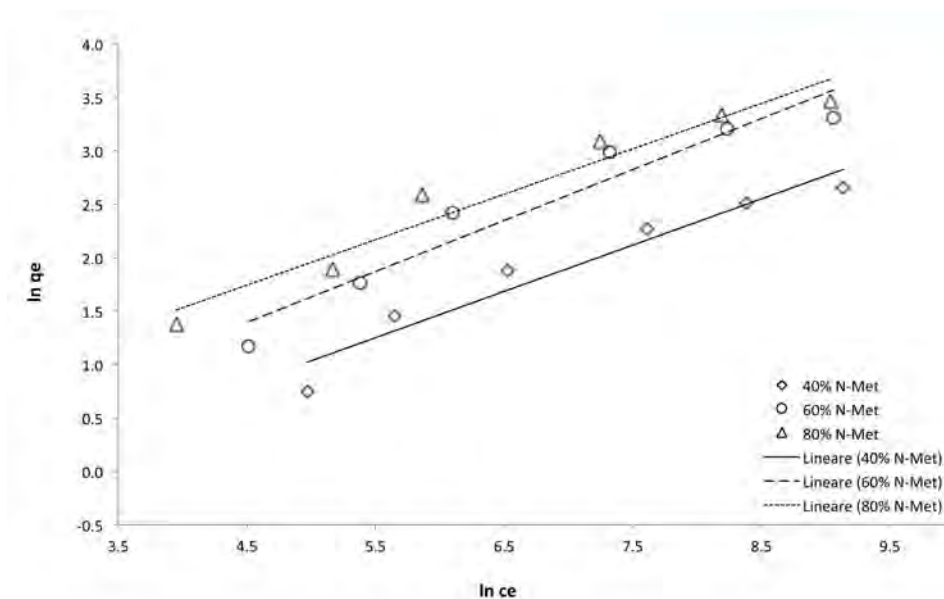

Figure 26. Plot of $\ln q_e$ versus $\ln c_e$ given by Freundlich linearized equation.

N-Met Conc. (% o.w.f.)	K (l/mg)	n	R^2
40%	$3.22*10^{-2}$	2.31	0.934
60%	$4.71*10^{-2}$	2.10	0.931
80%	$8.43*10^{-2}$	2.35	0.951

Table 13. Values of Freundlich constant (K), n exponent and R^2 at different N-Met concentrations.

The extent of the exponent $1/n$ can give an indication of the favorability and capacity of the adsorbent/adsorbate system, where $n > 1$ represents, as seen previously favorable adsorption conditions. Anyway, in the case of DR21 using 40% and 60% o.w.f. of N-Met, experimental data don't fit well with Freundlich linearized equation, then calculating n values is not significant in terms of favorable adsorption of the dye. The only acceptable correlation factor (R^2 over 0.95) is obtained for 80% o.w.f. of N-Met. The high concentration of carrier, can better diffuse into the fiber, allowing the dye molecules to deeper penetrate into the core of the fiber.

3.7.3 Pretreatment case

In the pretreatment case, the fiber was dipped into pure carrier and pneumatically squeezed reaching the desired amount of swelling agent. Namely, this amount was 20%, 40%, 60% and 80%. After the pretreatment, fiber was dyed using the same experimental condition used for the emulsion case.
Taken for granted (by the emulsion case study) that the thermodynamic equilibrium had been reached, the dye uptake of DR21 was studied. The dye uptake of DR21 at different initial dye concentration, using different amount of carrier, is shown in figure below. All the final concentrations values derived from a mean of 3 values and the error is about 0.50 mg/g of fiber.
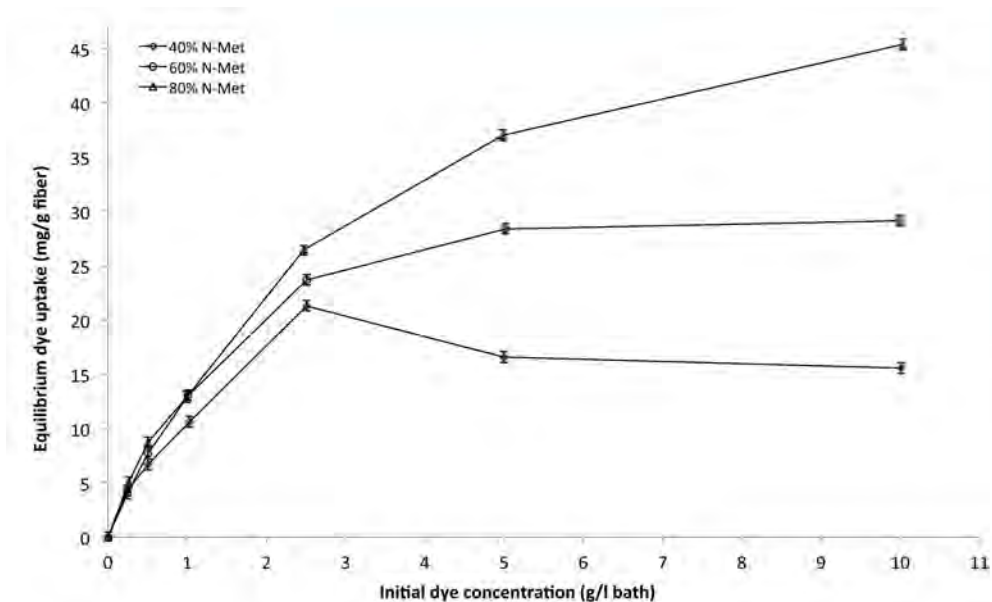

Figure 27. DR21 equilibrium dye uptake onto X-Fiper at different N-Met concentrations.

The final dye uptake of DR21, pretreating the fabrics with N-Met, is always higher then the one found for emulsion at all N-Met concentrations. The fiber swelling, applying the swelling agent as a pretreatment is probably increased even at 40% o.w.f. of N-Met; carrier is already on fiber surface when process begins, it doesn't have to diffuse from the bath to the fiber. The dye molecules, diffusing from the dye bath to the fiber, can penetrate more deeply into the fiber pores that are more accessible due to the higher swelling, especially for excess of dye using high concentration of N-Met (higher then 40%o.w.f.).

However, the trend observed appears to be weird if compared to the other curves with N-Met in emulsion. Using 40% o.w.f. of swelling agent a maximum of dye adsorption is shown for 2.5 g/l of initial dye; however, an increase of the dyestuff liquor concentration is followed by a decrease of dye uptake. Using 80% o.w.f. of N-Met and 10% of initial dye, the final dye uptake is much higher than the saturation concentration predicted by Langmuir model for the emulsion case; probably, applying the carrier as pretreatment, the total fiber swelling is greater than applying it in emulsion. Moreover, using higher concentration of swelling agent into the fiber, the adsorption follows a typical pathway even though, especially for 80% o.w.f. of carrier, the equilibrium is likely not reached, as the dye uptake is still growing. Unfortunately, with this kind of adsorption trend has not been possible to fit our experimental data with any adsorption model.

Therefore, other experiments have been carried out in order to find some possible explanations about this non-ordinary behavior.

Adsorption of DR21, pretreating the fiber with 20% of carrier and without any carrier, has been analyzed; the results are shown in Figure 28.

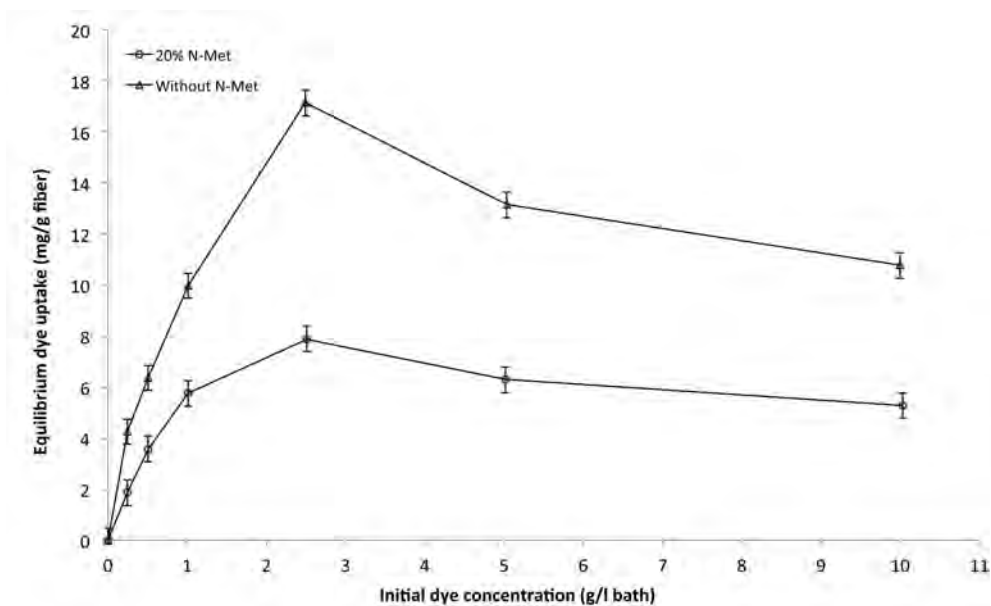Figure 28. DR21 dye uptake onto X-Fiper at 20% N-Met o.w.f. and without N-Metq.

The uptake, found for the lower quantity of carrier (40% o.w.f.), is confirmed by the last experiments. Using low quantity of N-Met to pretreat the fiber, or not even use it, causes a decreasing of dye uptake at high concentration of initial dye (higher then 5% o.w.f.). The reason can be explained by the low solubility of disperse dye in water.

As mentioned previously, dyeing with disperse dyes takes place thanks to the dissolved dye molecules; their poor water solubility promotes the formation of dye clusters or aggregates. So, the dispersion plays a crucial role during the dyeing process. In our case, at low dye concentration, from 0.25 g/l to 2.5 g/l, the dispersion can be satisfied by the great water content and with the good stirring provided by the dyeing machine even if the quantity of swelling agent is lower then 40% o.w.f.. Increasing the initial dye concentration, the cluster formation is very favored, especially at the lower swelling agent concentrations. If the N-Met concentration is increased (60% and 80% o.w.f.), the excess part of swelling agent present onto the fiber migrates into the dye bath helping the dispersion of dye molecules and reducing the dye-cluster formation. Finally, the carrier-dissolved dye molecules diffuse into the fiber as well as it happened in the emulsion case. Moreover, if the swelling agent amount into the fiber is in great excess (80% o.w.f. or more), equilibrium dye uptake has not been achieved even with an initial DR21 concentration of 10 g/l.

Obviously the dyeing mechanism, using DR21 and N-Met pretreatment of X-Fiper fiber, needs further investigation in order to confirm the formulated hypothesis based only to a dye uptake investigation.

Finally, from a technological ad industrial point of view, in terms of both end product hue and chemicals consumption, the best dyeing condition have been found concerns certainly the use of 40% o.w.f. of N-Met with an initial dye concentration of 2.5 g/l. This represents an important footstep toward a greener m-aramid dyeing process. Using 40% of carrier through the pretreatment way, it is possible to reach a dye uptake positioned (in terms of mg of dye/g of fiber) exactly in the middle of the values reached using 60% and 80% o.w.f. of swelling agent through the emulsion way.

As will be shown in the evaluation of end products paragraph, the used of pretreatment must be investigated better aiming to find the best pretreatment condition, such as dipping, squeezing, temperature of treatment etc…

3.8   Dyeing kinetics experiments and simulation

After having investigated to thermodynamics equilibrium of the emulsion dyeing with DR21, the dyeing kinetics were studied and the diffusion coefficient of the dye has estimated from the kinetics data, assuming the carrier-fiber to be a pseudo homogeneous system, by a fluid dynamic simulation using COMSOL Multiphysics® software.

The kinetics curves of dye absorption have been built, using 5% o.w.f. of initial DR21 concentration which is found to be the optimal one in the dyeing equilibrium tests. The dyeing time was set to 15-30-45-60-90-120 minutes, until the thermodynamic equilibrium was reached. All the final concentrations values derived from a mean of three values and the error is about 0.002 mol/kg of fiber for 60% and 80% N-Met curves; while for 40% N-Met and No Carrier curves the error is 0.01 mol/kg of fiber.
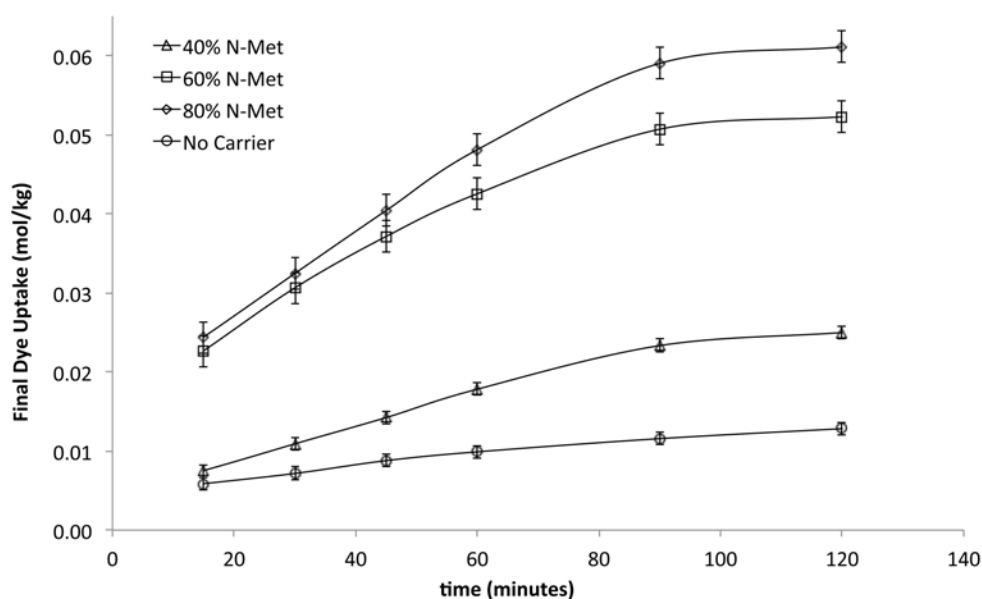

Figure 29. Kinetic curves at different N-Met concentrations and without carrier.

COMSOL Multiphysics a Finite Element Analysis Simulation software used for the description of various physics and engineering applications, especially those involving coupled phenomena or multiphysics. In our case the Transport of diluted Species Interface (chds) has been used. This interface is commonly used to compute the concentration field of a solute in a solvent. The driving forces for the solute transport is the diffusion by Fick's law and convection, when a fluid flow pattern is present. The dependent variable is the molar concentration of the solute [21].

The simulations have been carried out considering one single fiber in a fluid volume much bigger then the fiber itself.
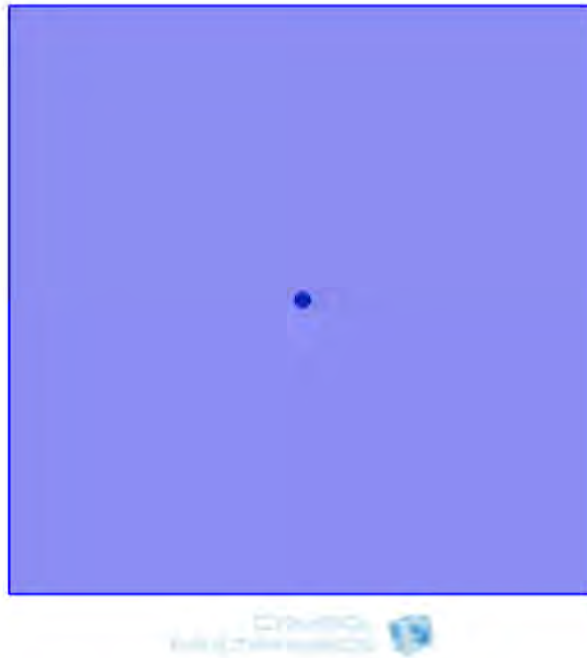

Figure 30. The mono-fiber immerse in the fluid volume.

The diffusion coefficient D_f in the liquid volume (water) for DR21, was found in literature and equal to $1.1*10^{-5}$ m^3/s.
As boundary condition, the initial concentration (t=0) of dye both into the fiber and into the liquid has been assumed equal to zero (C_0=0).
The effective diffusivity of the dyestuff onto the fiber, considered as a porous media, has been calculated by the following equation:

$$10) \; D_e = D_f \frac{\varepsilon}{\tau}$$

Where ε is the porosity, while τ represent the tortuosity.
The value of tortuosity was found in literature and was set at 1.8. Unfortunately no data for the porosity of the m-aramid fiber was found in literature, for that reason a first set of simulations has been done changing the ε value until the simulated curve fitted the experimental data of the kinetic conducted without the assistance of N-Met. The porosity was finally set at the value of $1.5*10^{-7}$.

Simulating this process, two different steps have been considered:

1) The transport of the dye from the bath to the inner fiber.
2) The adsorption of the dye onto the fiber.

In the liquid domain, a constant dye concentration of 6.62 mol/m^3 (exactly the concentration used for experimental kinetics: 5% o.w.f.) has been set. The concentration was considered constant due to its large excess compared to the concentration found into the fiber at the end of the dyeing process.

When the dye enters into the fiber, the solid matrix adsorbs it. To represent this adsorption another differential equation has been added: the Langmuir equation. This equation has been used for the adsorption step.

3.8.1   Definition of the three process parameters

A-Parameter

Assuming that experimental kinetic curves differ only for the different N-Met concentration, the hypothesis that D_e could be modified by the presence of carrier (thanks to previous experimental results) has been done. For this reason a first parameter, called "A-Parameter" was introduced. A novel set of simulation has been done as soon as the fitting with experimental data for "40% N-Met" was obtained.

Looking at experimental data in Figure 26 it can be observed that the curves at "60% N-Met" and "80% N-Met" are very similar to each other, while the curve of "40% N-Met" differs much if matched with. On the contrary, "40% N-Met" curve has a similar pathway of "No Carrier" curve. Based on these observation it has been hypothesized that the carrier gives rise to two different behaviors. Until circa 15-20 g/l (30-40% o.w.f. with a liquor ratio of 1:20) N-Met is almost completely water-soluble. Dissolved in water, N-Met, help solubilizing and dispersing the dye, but, at least initially, it doesn't swell the fiber.

B-Parameter

Increasing the swelling agent concentration to 60% o.w.f., some N-Met will be emulsified into the solution. Due to the great affinity between carrier and fiber, the emulsified droplets of N-Met go to the fiber surface and they begin to swell it starting from the surface. So, another parameter was defined as "B-Parameter" and the third set of simulations have been carried out. Maintaining constant A-Parameter, B-Parameter was varied until the calculated (by simulations) curve fitted with experimental data.

C-Parameter

The experimental curve of "80% N-Met" is very similar to the "60% N-Met" one in the initial part, but the equilibrium concentration value differs a lot. For this reason it was necessary to hypothesize another mechanism of action of the carrier. Being the carrier, at 80% o.w.f., presents in large excess, the dye solubilization effect and the superficial swelling effect are now followed by a deeper fiber swelling due to the carrier diffusion from the solution to the fiber. However, this action is remarkable after circa 40-60 minutes. After these considerations, a third parameter was introduced as "C-Parameter". The last set of simulation has been carried out keeping now constant both A-Parameter and B-Paramenter, until the calculated curve fitted the experimental data of "80% N-Met".

- A-Parameter was named SOLUBILIZING FACTOR.
- B-Parameter was named PRIMARY SWELLING FACTOR
- C-Parameter was named SECONDARY SWELLING FACTOR

Finally, when the value of the three parameters were defined, the last set of simulation has been carried out in order to find the three different parameters for each different N-Net concentration. The final values of the parameters are given in Table 13.

N-Met concentration	*Parameter*	*Value*
Water Only (WO)	A	1
	B	1
	C	1
40% o.w.f.	A	1.2
	B	1
	C	2.5
60% o.w.f.	A	1.2
	B	4
	C	1.8
80% o.w.f.	A	1.2
	B	4
	C	2.1

Table 13. Values of the three parameters changing N-Met concentration.

Using 40% o.w.f. of N-Met it has been found that the "solubilizing factor" increase about 20% if compared with the kinetic conducted without carrier. This value, 1.2, is not changed increasing the

swelling agent concentration; the maximum carrier solubility in water is already reached using the 40% o.w.f. of it. The initial "primary swelling factor" is not significant for the lower concentration of carrier, but has a value of 4 for the higher concentration. The value doesn't change increasing the N-Met concentration from 60% to 80% o.w.f., because the fiber surface has been already considered carrier-saturated with 60%. The last factor (C-Parameter), probably the most important in terms of dyeing mechanism, has the maximum value for 40%, an intermediate one for 80% and the lowest value for 60%. With 40% B-Parameters doesn't help the fiber swelling, but as soon as the carrier reach the fiber (40-60 minutes) the secondary swelling occurs stronger then using more carrier, just because is the only swelling effect.

With 60% of N-Met the total fiber swelling, in absolute value, is higher then using 40%, therefore C-Parameter is lower in compared to the total swelling. Same thing happened using 80% o.w.f. of carrier, in this case the "internal swelling factor" is higher then the value for 60% N-Met only for the increased total quantity of carrier. The final simulations obtained are shown in Figure 31.
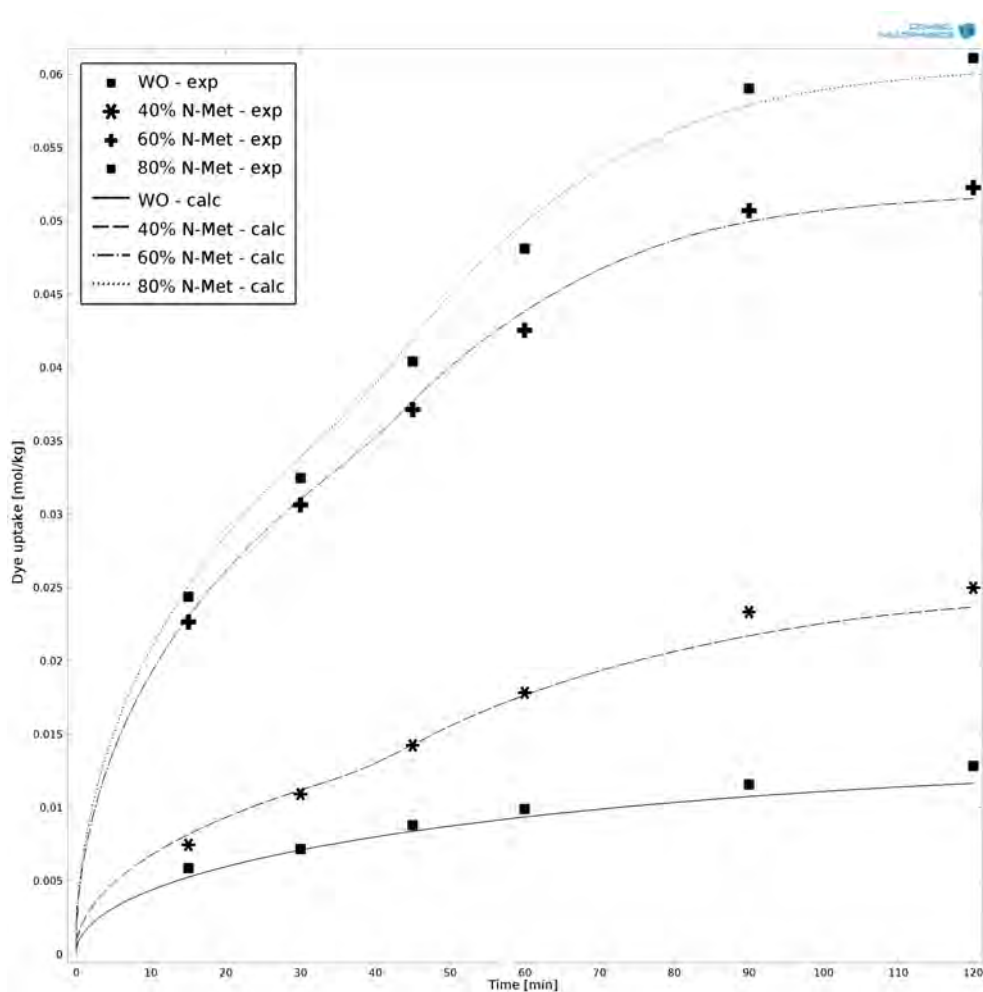

Figure 31. Simulation curves compared to the experimental data.

Looking at the "WO" graph we can see that there are no remarkable effects given by the carrier. The solubilizing factor is visible in the first point of the kinetics. The big initial difference between the first two curves and the other two is given by the surface swelling factor. Finally, from 40 to 60 minutes, is clearly visible the "stair" given by the third parameter: the internal swelling factor.
In the figure below a 2D plot of one of the simulations is shown.
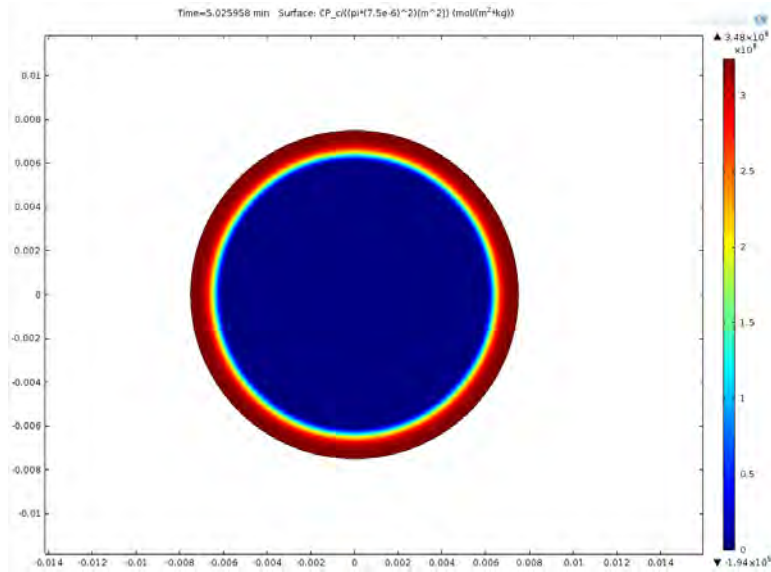

Figure 32. COMSOL 2D plot at circa 5.0 minutes of simulation.

3.9   Evaluation of the end products quality

The quality of end product was evaluated in terms fastness to wash according to the UNI EN ISO 105 C01 standard, and fastness to wet rubbing according to UNI EN ISO 105 X12 standard.

3.9.1   BB41 end products fastness and hue

Figure 33 shows satisfactory fastness for all dyeing experiments. The dyed samples did negligibly transfer color to reference samples made of wool, acrylic, polyester, polyamide, cotton and acetate both in the rubbing fastness and the washing fastness tests. Fastness ratings were assigned by using grey scale for color change and grey scale for color staining. The ratings for rubbing fastness were found 4/5, that means that the dyed materials possess good rubbing fastness property. The ratings for washing fastness both in terms of color change and color staining ranges from 4 to 4/5, that means satisfactory to good. The fastness values to rubbing and washing suggest that the dye molecules were able to penetrate in the core of the fiber.
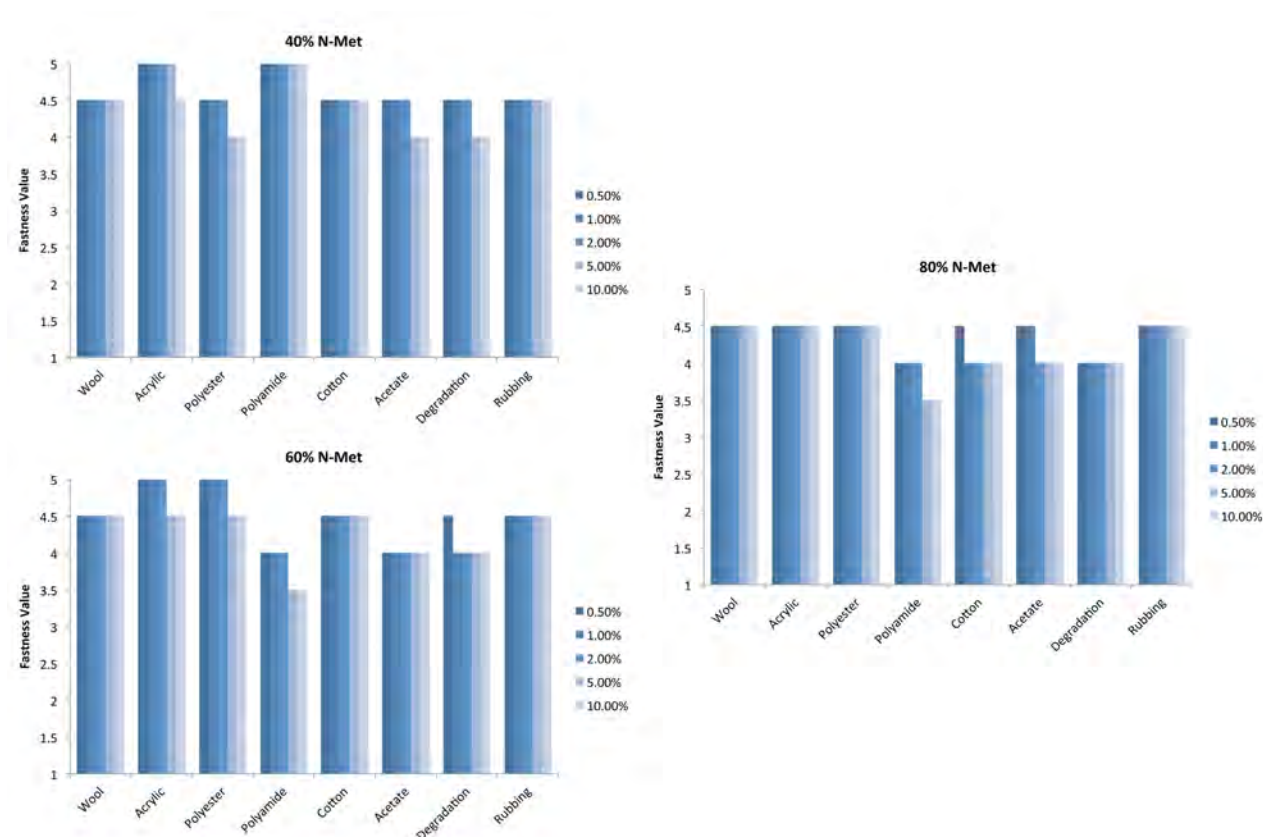
Figure 33. Fastness to wash according to UNI EN ISO 105 C01, and rub according to UNI EN ISO 105 X12.

It is worth noting that the better fastness to washing observed at 40% o.w.f. N-Met concentration were due to the light hue of the fabrics dyed with 40% of carrier: the hue was much less deep at 40% carrier concentration with respect to 60 and 80% and this makes that dyeing less prone to color fading.

As shown in Figure 34, satisfactory dyeing evenness was obtained at all swelling agent concentrations. However, at any dyestuff concentration, using 40% o.w.f. N-Met in the dyeing bath, the hue was not deep enough to make clothing commercially acceptable. On the contrary, at 60% and 80% o.w.f. of N-Met concentrations, adequate color deepness has been achieved starting from 5% o.w.f. BB41 concentration. At dyestuff concentrations lower than 5% o.w.f., the hue never reached industrial standards at any N-Met concentration. In conclusion, as far as the dyeing bath composition is concerned, the recipe for the optimal dyeing of the tested m-aramid fiber consists in 5% o.w.f. of BB41 concentration and 60% o.w.f. of N-Met concentration.

Figure 34. Hue of end products with 2.5 g/l of initial dye at different N-Met concentrations.

3.9.2   DR21 end products fastness and hue

As shown in Figure 35, rubbing fastness of X-Fiber dyed with DR21 decrease with increasing of both initial dye and N-Met concentrations. Acceptable to good values are obtained with 40% of N-Met at all dye concentrations, using 60% the maximum dye concentration that is possible to used obtaining acceptable results is 5% o.w.f.. With 80% of N-Met dyeing, only dye concentration lower than 5% o.w.f. are permitted to obtain satisfactory rubbing fastness. Fastness to wash in terms of degradation and staining, show quite the same trend. Although degradation is adequate for all dyeing experiments, staining represents a trouble. Especially for polyamide and acetate staining value are very poor at all dye and N-Met concentrations. With 60% and 80% o.w.f. of N-Met, staining is decreased for low initial dye concentration; however, increasing concentration higher then 2% o.w.f. of dye don't give satisfactory results.
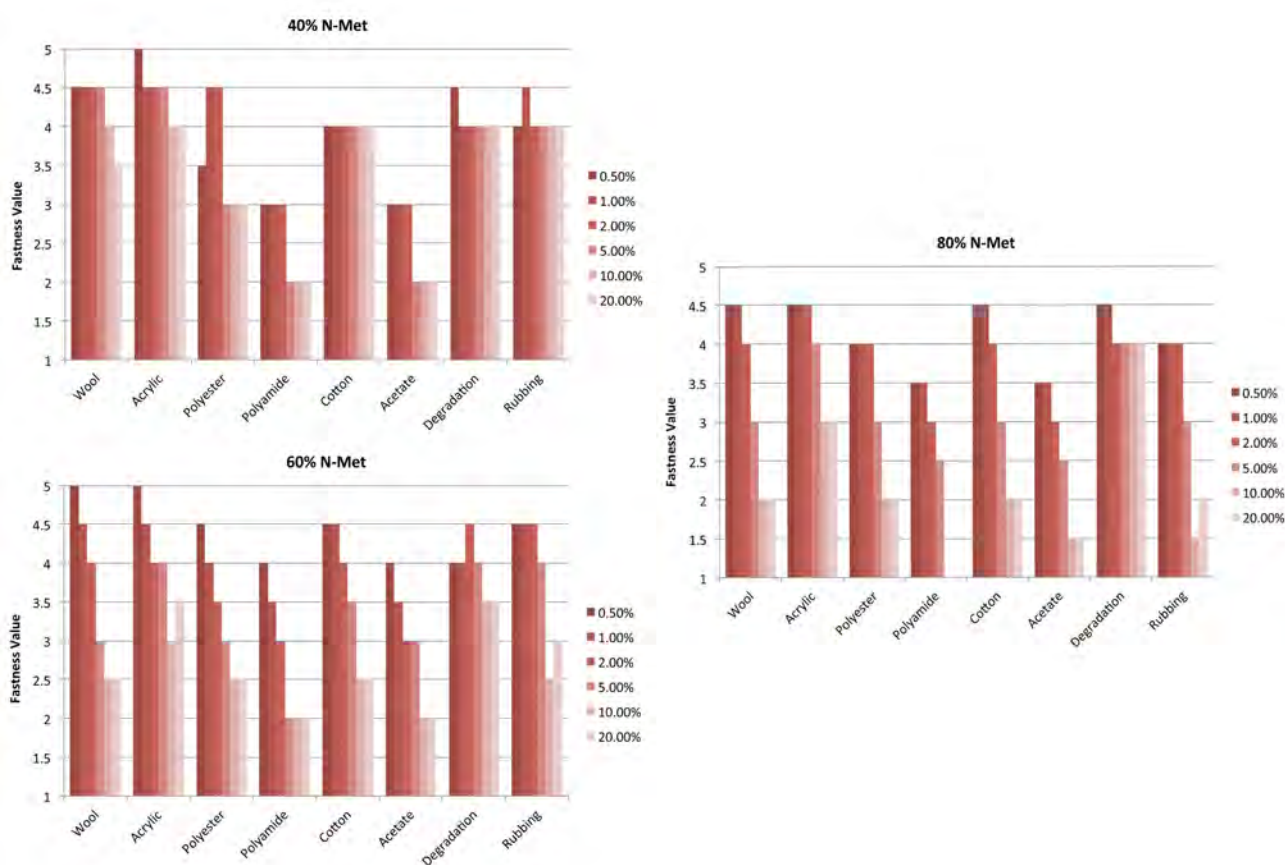

Figure 35. Fastness to wash according to UNI EN ISO 105 C01, and rub according to UNI EN ISO 105 X12.

As far as the pretreatment experiments are concerned, the obtained results are almost the same that have been observed in the emulsion case. In pretreatment, staining and degradation at initial dye

concentrations higher then 2% o.w.f. and N-Met concentration of 60% and 80% o.w.f. are even worse. From a commercial point of view, these ratings of fastness to wash would not be admitted by the market.

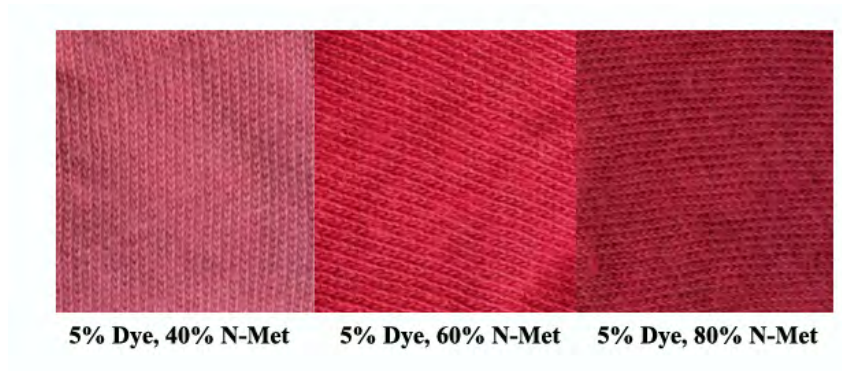**5% Dye, 40% N-Met   5% Dye, 60% N-Met   5% Dye, 80% N-Met**

Figure 36. Hue of end products with 2.5 g/l of initial dye at different N-Met concentrations in emulsion case.

As shown in Figure 36, satisfactory dyeing evenness was obtained only using N-Met concentration higher then 40% o.w.f.. Moreover, using 40% o.w.f. of N-Met in the dyeing bath at any dye concentration, does not allow to reach a hue deep enough to make clothing commercially acceptable. On the contrary, at 60% and 80% o.w.f. of N-Met concentrations, adequate color deepness has been achieved starting from 5% o.w.f. DR21 concentration. At dyestuff concentrations lower than 5% o.w.f., only using 80% o.w.f. of N-Met is possible to have hues that reach industrial standards, but the consequence is high decrease in evenness. In conclusion, as far as the dyeing bath composition is concerned, the recipe for the optimal dyeing of the tested X-Fiper m-aramid fiber consists in 5% o.w.f. of DR21 concentration and 60% o.w.f. of N-Met concentration.

In the pretreatment case, as told previously, with 40% o.w.f. of N-Met is possible to reach a dye uptake situated exactly in the middle of values obtained using 60% and 80% o.w.f. in the emulsion case. However, the evenness of these dyeing is very low and the hue is shifted to blue compared to the emulsion case (Figure 37).
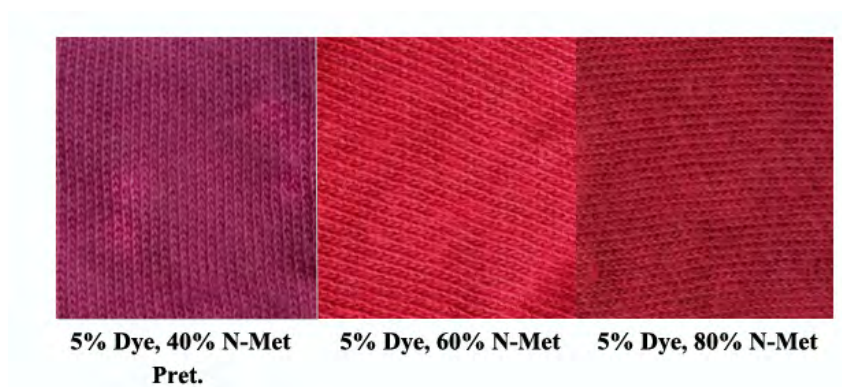

5% Dye, 40% N-Met   5% Dye, 60% N-Met   5% Dye, 80% N-Met
Pret.

Figure 37. Hue of end products with 2.5 g/l of initial dye at different N-Met concentrations and applications.

References

[1] H.H. Yang, Handbook of Fiber Science and Technology: Vol. III, High Tech. Fibers – Part C

[2] Y. Dong, J. Jang, Color. Tech., 2011, Vol. 127, pag. 173-178.

[3] J. Cegarra, P. Puente, J. Valldeperas, *The Dyeing of Textile Materials*, Paravia, Torino, 1988.

[4] E. I. Du Pont, Technical Guide for NOMEX® Brand Fiber, H-52720 Revised July, 2001.

[5] W. Ingamells, *J. Soc. Dyers and Colour.*, 1980, Vol. 96, pag. 466-474.

[6] W. Ingamells, K. V. Narasimhan, *J. Soc. Dyers and Colour.*, 1977, Vol. 93, pag. 306-312.

[7] W. Ingamells, A. M. Yabani, *J. of Appl. Polym. Sci.*, 1978, Vol. 22, pag. 1583-1592.

[8] A. Nechwatal, V. Rossbach, *Textile Res. J.*, 1999, 69, pag. 635.

[9] H. Herlinger, D. Fiebig, *Textile Prax. Int.*, 1983, Vol.38, pag. 583-593.

[10] B. Noroozi, G. A. Sorial, H. Bahrami, *Dyes and Pigments*, 2008, 76 (3), pag. 784-791.

[11] M. Roulia, A. A. Vassiliadis, *Microporous and Mesoporous Mat.*, 2009, 122 (1-3), pag. 13-19.

[12] B.H. Hameed, A.T.M. Din, A.L. Ahmad. *J. Hazard. Mater.*, 2007, 141, pag. 819–825.

[13] I.A.W. Tan, B.H. Hameed, A.L. Ahmad, *Chem. Eng. J.*, 2007, 127, pag. 111–119.

[14] M. Roulia, A. A., *Microporous and Mesoporous Mat.*, 2008, 116, pag. 732–740.

[15] Langmuir I., *J. Am. Chem. Soc*, 1918, 40, pag. 1361–1403.

[16] S.J. Allen, G. Mckay, J.F. Porter, *J. of Colloid and Interface Science*, 2004, 280, pag. 322–333.

[17] B.H. Hameed, D.K. Mahmoud, *J. of Hazardous Materials*, 2008, 158, pag. 65–72.

[18] P. Manoj, K. Reddy, *et al.*, *Environ Sci. Pollut. Res.*, 2013, 20, pag. 4111–4124.

[19] K.A. Guimarães Gusmãoa, L.V. Gurgelb, *et al.*, *Dyes and Pigments*, 2012, 92, pag. 967-974.

[20] Freundlich H., Z. Phys. Chemie, 1906, 57, pag. 384–470.

[21] http://en.wikipedia.org/wiki/COMSOL_Multiphysics; COMSOL Multiphysics user guide.

Chapter 4

4. Ultrasounds assisted X-Fiper® dyeing using DR21

The aim of this chapter is to introduce the concept of ultrasounds assisted dyeing of m-aramid fiber (X-Fiper®) using the Disperse Red 21 dyestuff. A short introduction about the theory ultrasounds will be followed by the experimental part in which will be evaluated the double effect of the carrier fiber swelling and the effect of US (ultrasounds) dye bath pretreatment. This chapter is based on a thesis carried out in 2012.

4.1 Introduction to ultrasounds

As well known, dyeing processes implies the consumption of large amount of water, electricity and thermal energy. Moreover, they involve the use of chemical additives for assisting, accelerating or retarding their rates. They also must be carried out at elevated temperature in order to transfer mass of dye from the processing liquid medium across the surface of the textile material in a reasonable time. These transport processes, like every chemical process is time and temperature dependent. In order to overcome these difficulties, many non-traditional techniques have been put forward to conserve energy in wet processing of textile.

Sound is the auditory perception given by the vibration of a body that oscillates; such vibration propagates in any elastic medium until reaching the ear, where a complex internal mechanism creates the auditory sensation. All sounds can be divided, according to their frequency in three categories: main infrasound, audible and ultrasound [1].
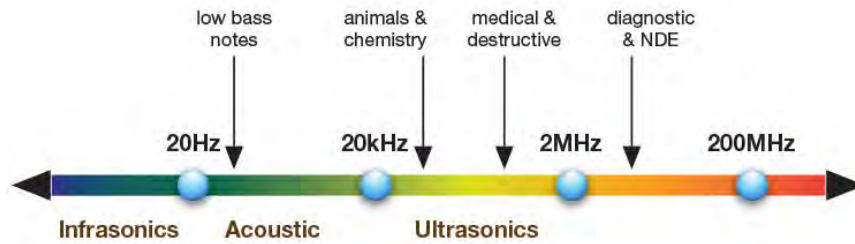
Figure 1. The ultrasonic range diagram

Nowadays they exist many application fields that take advantages ultrasounds, for example in the medical field they are used in scanning techniques, in chemical industry in order to accelerate chemical reactions otherwise too slow or in naval application to probe the different levels of seabed (Sonar). Being the ultrasound a wave phenomenon, it will be subject to refraction, diffraction, reflection, absorption and transmission. Moreover, related to it, are defined frequency (f), wavelength (λ), propagation speed (V), intensity (I) and the attenuation (due to the acoustic impedance of the medium traversed). The acoustic wave generation is due to the improper term "transducers" (also called emitters or converters) that transform electrical power, given by a generator, in mechanic vibrational energy (sound energy).

The vibrational element is a piezoelectric. Usually, this element is a ceramic material showing a particular property: it is able to produce a potential difference when subjected to a mechanical deformation and, vice versa, if subjected to an electric field, it deforms mechanically. The entity of this phenomenon is observed in micrometrical scale. Therefore, applying a potential difference to the crystal, it expands or contracts itself along a specific axis, causing a vibration of the transducer. The volumetric expansion is easily controllable and electrical stimulation dependent.

The generator provides an electrical tension showing a sinusoidal wave type: the tension is alternatively on positive and negative field. The piezoelectric ceramic is affected by this variation, stretching in positive field and shortening in negative field. Consequently, if the transducer is in contact with an elastic media, the propagation of vibration is then is possible. The amplitude of the deformation of ceramic material can vary depending on the generated power, generally it is between 5 and 25 μm.

Ultrasounds propagate in bodies thanks to the elastic vibration of its atoms and molecules, in same manner of sound. However, transmission mechanism is different compared to the propagation mechanism because it needs an elastic transport to propagate. This allows understanding the reason why sound cannot propagate in vacuum. The vibration transfer speed is function of the propagation medium. Therefore, propagation speed is high influenced by mechanical characteristics of the crossed medium. Moreover, due to imperfection of the medium, dispersion phenomena, that cause sound wave attenuation, are very probable. Propagation of ultrasonic waves can occur in 2 different modalities: by longitudinal and transversal waves. The difference is in the propagation direction of the waves: for the longitudinal ones oscillation of the particles is parallel to the direction of wave

propagation, for those transversal occurs orthogonally. Sound waves, independently of their frequency (*f*), propagate in material under a local pressure, called sound pressure (P_s), which represents the overpressure by which atoms and molecules are subjected with respect to the standard atmospheric pressure.

$$P_s = P_A \sin \omega t \qquad (1)$$

$$\omega = 2\pi f \qquad (2)$$

P_A is the ultrasonic wave amplitude. Since waves propagate in a sinusoidal way, they are time (*t*) dependent. Important characteristic of medium is represented by acoustic impedance (*Z*), it expresses the ratio between sound pressure that propagate into medium and speed of particles. The acoustic impedance characterizes the sound behavior in the propagation medium, it has been shown that there is correlation linking material properties (density ρ) and propagation speed of the particles (*V*):

$$Z = \rho V \qquad (3)$$

In Table 1 are reported some *Z* values of some materials.

	ρ (kg/m3)	*V* (m/s)	*Z* (kg/m2*s)
Water	1000	1480	$1,5 \cdot 10^6$
Air	1,3	330	429
Steel	7500	5900	$44.3 \cdot 10^6$

Table 1. Z values of some common materials.

The parameters that characterize materials are: adsorption coefficient (α), transmission coefficient (τ) and reflection coefficient (χ). They are linked by the following relationship:

$$\alpha + \tau + \chi = 1 \qquad (4)$$

Poisson has formulated the fundamental relationship, which governs reflection of an ultrasonic wave, in the nineteenth century. The relationship links the acoustic impedances of the two media (Z1 and Z2) separated by a flat interface:

$$\chi = \left(\frac{Z_2 - Z_1}{Z_2 + Z_1} \right)^2 \qquad (5)$$

Similarly to the previous equation, the relationship between impedances for the obtaining of the transmission coefficient is the following:

$$\tau = \frac{4Z_2}{(Z_2 + Z_1)^2} \qquad\qquad (6)$$

Looking at Table 1, it's interesting to observe that acoustic impedance is very low in gases. For this reason is not possible to propagate acoustic waves through gases because they are mainly reflected in their same propagation direction.

One of the most important phenomenon due to ultrasound wave's propagation in a liquid medium is the "cavitation phenomenon": in liquids, longitudinal vibration of molecules generate compression and rarefaction forming areas of high pressure and low atmospheric pressure. In liquid medium these high frequencies cause the formation of microscopic bubbles or cavities, which expand and finally, during the compression phase, collapse. The collapse explosion generates tiny, but powerful, shock waves and severe shear forces capable to break chemical bonds.

The bubbling phenomenon (formation and collapse) is generally considered responsible for most of ultrasonic physical and chemical effects observed in solid/liquid or liquid/liquid systems. The total energy released by the cavitation effect can improve mass transport phenomena (e.g. between the bath and dyeing the textile article) and allows greater destruction of molecular aggregates dispersed in the liquid (e.g. of dyes) reducing the dimensional distribution and improving the diffusive transport. Is possible to distinguish three kind of cavitation: acoustic cavitation, hydrodynamic cavitation and optical cavitation. Those are resulting to a pressure change in a liquid when the ultrasonic waves pass through it.

In the context of acoustic cavitation can also be defined two types of phenomenon:

1) Stationary when bubbles change in their size, often not linear, around a balance dimension.
2) Transient when, applying a sound field pressure sufficiently intense, the bubbles have a first phase of rapid expansion followed by a violent collapse during the compression phase of the acoustic pressure.

Solokov and Tumansky presented first studies regarding ultrasounds assisted dyeing process in 1941. After them, numerous papers are shown in literature in which are presented works whose results were obtained through the use of ultrasound at high and low frequencies.

The use of ultrasounds in textile field leads to many advantages such as a reduction of temperature at which dyeing processes are conducted, maintaining intact some fiber properties that can degrade with high temperature. Also an increase of dye diffusion can occur (increasing in mass transfer), increasing the final bath exhaustion; by a kinetic point of view, the increased diffusion, is due to an increase in mobility of the amorphous regions with a consequent increase of diffusion speed of dye within the fiber.
Thanks to the disintegrating action of ultrasonic waves, the use of dispersing agents, which avoid the aggregation of the dye, may be reduced significantly [2-6].

4.2   Experimental

4.2.1   Planning the tests

This experimental work is based on the combined use of a carrier (N-Met) for the swelling of the X-Fiper fibers and a pretreatment of the dye solution, through the use of ultrasounds. The swelling agent, as we know, is used with the purpose of swelling the amorphous part of the polymer, which is located into the crystalline polymer chains, in order to increase the pores dimensions of the fiber allowing a better diffusion of dye molecules within the same; ultrasonic pretreatment arises instead the purpose of promoting the disaggregation of cluster of dye, and then move the particle size distribution curve towards the fine particles, in order to facilitate the insertion of the dye in the pores of the fiber. The process is carried out taking into account the different variables that may influence this dyeing process, and in particular:

1) Power of US in the pretreatment (W).
2) Time of pretreatment with US (min).
3) Time of dyeing (min).
4) Concentration of dye (% over weight of fiber).
5) Concentration of swelling agent (% over weight of fiber).
6) Liquor ratio (L/R).

The final concentration of dye adsorbed onto the fiber was, in this case, calculated indirectly from the exhausted dye bath. This evaluation in typical in textile world and is better knows as final exhaustion percentage (E%). The segregation of the dye from the carrier has been overcome diluting the exhausted dye bath with acetone. The E% has been calculated as follows:

$$E\% = \frac{[Dye]_{initial} - [Dye]_{final}}{[Dye]_{initial}} \cdot 100 \qquad (7)$$

where:

$[Dye]_{initial}$: dye concentration at the beginning of the process.
$[Dye]_{final}$: dye concentration at the end of the process.

In table below is shown a list of the planned test in which different process variables has been used.

US Power (W)	Dyeing time (min)	Dye Conc. (% o.w.f.)	Carrier Conc. (% o.w.f.)	US Pretr. Time (min)	L/R
600	120	1	60	0	1/20
600	120	1	60	60	1/5
600	120	10	60	0	1/5
600	120	10	60	60	1/20
600	120	10	20	0	1/20
600	120	1	20	60	1/20
600	120	1	20	0	1/5
600	120	10	20	60	1/5
300	60	10	20	0	1/20
300	60	1	20	0	1/5
300	60	1	60	0	1/20
300	60	1	20	60	1/20
300	60	10	20	60	1/5
300	60	10	60	0	1/5
300	60	10	60	60	1/20
300	60	1	60	60	1/5
300	120	1	60	0	1/5
300	120	10	60	0	1/20
300	120	10	20	60	1/20
300	120	10	20	0	1/5
300	120	10	60	60	1/5
300	120	1	20	0	1/20
300	120	1	60	60	1/20
300	120	1	20	60	1/5
600	60	1	60	0	1/5
600	60	1	20	0	1/20
600	60	10	20	60	1/20
600	60	10	60	60	1/5
600	60	1	60	60	1/20
600	60	1	20	60	1/5
600	60	10	60	0	1/20
600	60	10	20	0	1/5

Table 2. Table of tests

It has been used two different ultrasound applied power (1st column) as well as two different dyeing time (2nd column), for this reason we divided the tests into 4 groups of 8 tests each one. The equipment used (Mathis Labomat-8 laboratory-dyeing machine) allows running 8 samples together. Moreover, is not possible to pretreat at the same time different dye bath at different US power varying the dyeing time for each run.

4.2.2   Dyeing recipe

Usually, m-aramid dyeing is performed at 120-130 ºC (in chapter 3 dyeing temperature was 125 ºC). In this case, in order improve the sustainability of the process and thanks to the application of ultrasounds, the dyeing operative temperature was set at 105 ºC. For same reason it has been tried to decrease the liquor ratio at 1:5 (not that used in exhaustion dyeing of fabrics) reducing the water consumption. The used dye was the same used in chapter 3, the C.I. Disperse Red 21.
All these improvements have been thought in order to realize a greener process looking toward the eco-sustainability in textile.

Feature of the new dyeing recipe:

- Liquor ratio (R/B): 1/5 or 1/20.
- Dyeing bath volume: 200ml (water + carrier).
- Concentration of dye (DR21): 1% or 10% o.w.f.
- Concentration of swelling agent: 60% or 20% o.w.f.
- Weight of fiber: 40g for liquor ratio 1:5 and 10g for liquor ratio 1:20.

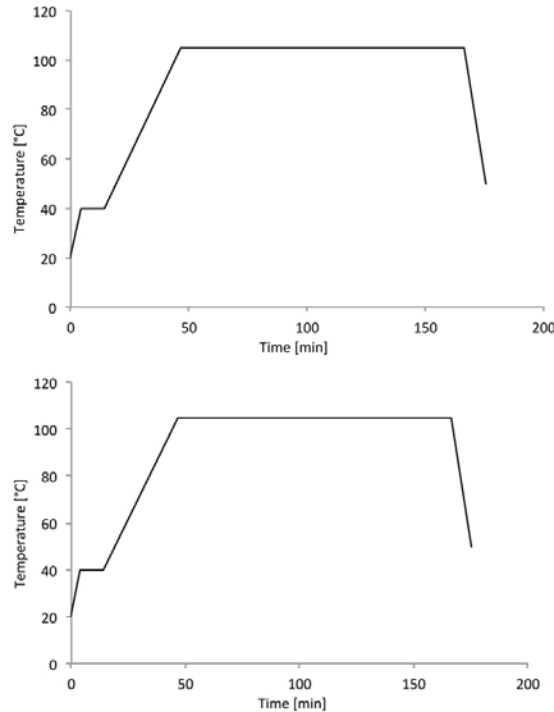In Figure 2 the time/temperature diagrams are reported.

Figure 2. Time/Temperature diagrams for 60 and 120 minutes of dyeing.

4.2.3   Ultrasound bath-pretreatment equipment

As analyzed in the previous chapter, one of the most important trouble found in this kind of dyeing processes is the formation of dye aggregates or clusters, especially with high initial dye concentration followed by low initial swelling agent concentrations. In order to reduce the dye particle size with ultrasound irradiation and consequently avoid the aggregation, was used a pilot plant equipment for the dyeing process of hanks, fabrics or garments. It is a laboratory apparatus that allows reproducing in smaller scale the dyeing process. The equipment consists in a stainless steel tank equipped with a circulation pump and an electrical resistance for heating the liquor. On the system can be positioned two geometric configurations of transducers for the emission of ultrasounds: flat and cylindrical. What we use is the flat one, as you can see in Figure 3, called "Sonoplate®" emitting device, made by "Weber Ultrasonics GmbH". It is positioned on the bottom of the vessel, because is possible also to put it in vertical position on one side. The Sonoplate® is 40 cm length and 30 cm width while the vessel is 50 cm length and 40 cm width. This flat Sonoplate consists of a series of eight piezoelectric transducers glued to the plate by means of a resin and connected in series to the generator.

Figure 3. Picture of the Sonoplate®.

The applied procedure is very simple: after weighing the desired amount of DR21 in each beaker and after the addition of the necessary swelling agent, we put in each beaker 100 ml of water and we stirred the whole for few minutes. After that, the beakers have been put on the vessel water filled until water reaches the middle height of them; Machinery has been switched on and set up at the required ultrasounds power for the desired pretreatment time.
For the dyeing process the same laboratory equipment used use in chapter 3 was utilized: MATHIS LABOMAT «BFA-8».

4.3 Results and discussion

The results of the tests are reported in Table 3 in terms of exhaustion percentage.

Entry	US Power (W)	Dyeing time (min)	Dye Conc. (% o.w.f.)	Carrier Conc. (% o.w.f.)	US Pretr. Time (min)	L/R	E%
1	600	120	1	60	0	1:20	**66.37**
2	600	120	1	60	60	1:5	**91.44**
3	600	120	10	60	0	1:5	**86.67**
4	600	120	10	60	60	1:20	**57.40**
5	600	120	10	20	0	1:20	**28.86**
6	600	120	1	20	60	1:20	**26.61**
7	600	120	1	20	0	1:5	**89.10**
8	600	120	10	20	60	1:5	**51.23**
9	300	60	10	20	0	1:20	**20.81**
10	300	60	1	20	0	1:5	**89.22**
11	300	60	1	60	0	1:20	**64.58**
12	300	60	1	20	60	1:20	**37.68**
13	300	60	10	20	60	1:5	**43.90**
14	300	60	10	60	0	1:5	**46.06**
15	300	60	10	60	60	1:20	**48.21**
16	300	60	1	60	60	1:5	**90.78**
17	300	120	1	60	0	1:5	**91.48**
18	300	120	10	60	0	1:20	**60.85**

19	300	120	10	20	60	1:20	**22.25**
20	300	120	10	20	0	1:5	**67.13**
21	300	120	10	60	60	1:5	**84.99**
22	300	120	1	20	0	1:20	**32.66**
23	300	120	1	60	60	1:20	**65.72**
24	300	120	1	20	60	1:5	**88.56**
25	600	60	1	60	0	1:5	**91.69**
26	600	60	1	20	0	1:20	**28.99**
27	600	60	10	20	60	1:20	**34.60**
28	600	60	10	60	60	1:5	**83.79**
29	600	60	1	60	60	1:20	**66.77**
30	600	60	1	20	60	1:5	**88.99**
31	600	60	10	60	0	1:20	**60.08**
32	600	60	10	20	0	1:5	**58.03**

Table 3. Final results in terms of E%.

The influence of the process parameters on the exhaustion is reported in Figure 4.
The two levels are shown for each variable and each level value is the mean value obtained of all the samples dyed at same conditions.
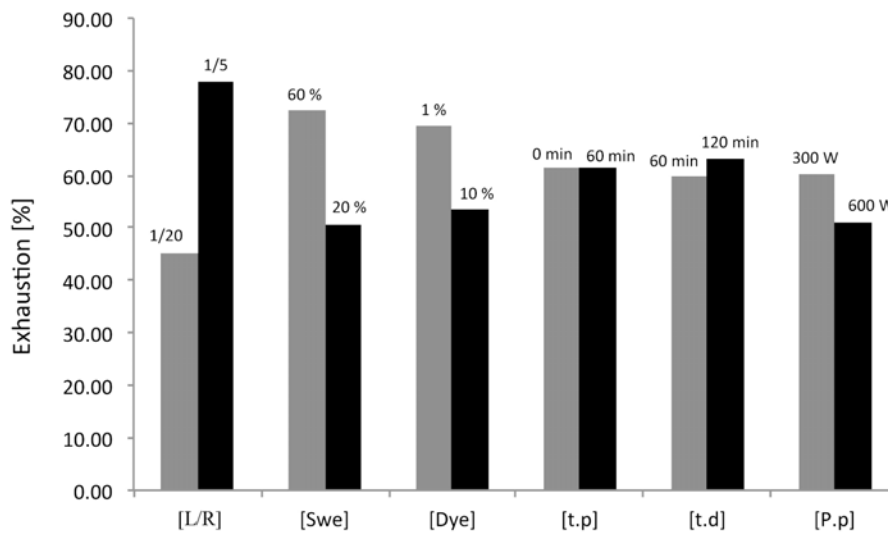

Figure 4. Influence of process parameters on E% results.

Legend:

- [L/R]: liquor ratio
- [Swe]: N-Met concentration
- [Dye]: dye concentration
- [t.p]: ultrasounds pre-treatment time
- [t.d]: dyeing time
- [P.p]: Ultrasounds pre-treatment power

As shown in graph above it appears that US pre-treatment intensity and time does not have a relevant influence on the exhaustion values. It is possible to notice that exhaustion value obtained with 10% dye concentration is lower than that obtained with 1% concentration, while considering the amount of dye adsorbed inside the fiber sample is higher in case of dye concentrations of 10% (Figure 5).

This led us to conclude that exhaustion percentage values are not appropriate for our evaluations because of the equilibrium between the two phases.

In order to avoid these erroneous conclusions, the amount of dye adsorbed by the fiber was referred to the sample weight and reported in Table 4.

Entry	US Power (W)	Dyeing time (min)	Dye Conc. (% o.w.f.)	Carrier Conc. (% o.w.f.)	US Pretr. Time (min)	L/R	Dye uptake (g_{dye}/g_{fib})
1	600	120	1	60	0	1:20	0.007
2	600	120	1	60	60	1:5	0.009
3	600	120	10	60	0	1:5	0.087
4	600	120	10	60	60	1:20	0.057
5	600	120	10	20	0	1:20	0.029
6	600	120	1	20	60	1:20	0.003
7	600	120	1	20	0	1:5	0.009
8	600	120	10	20	60	1:5	0.051
9	300	60	10	20	0	1:20	0.021
10	300	60	1	20	0	1:5	0.009
11	300	60	1	60	0	1:20	0.006
12	300	60	1	20	60	1:20	0.004
13	300	60	10	20	60	1:5	0.044
14	300	60	10	60	0	1:5	0.046
15	300	60	10	60	60	1:20	0.048
16	300	60	1	60	60	1:5	0.009
17	300	120	1	60	0	1:5	0.009
18	300	120	10	60	0	1:20	0.061
19	300	120	10	20	60	1:20	0.022
20	300	120	10	20	0	1:5	0.067

21	300	120	10	60	60	1:5	0.085
22	300	120	1	20	0	1:20	0.003
23	300	120	1	60	60	1:20	0.007
24	300	120	1	20	60	1:5	0.089
25	600	60	1	60	0	1:5	0.009
26	600	60	1	20	0	1:20	0.003
27	600	60	10	20	60	1:20	0.035
28	600	60	10	60	60	1:5	0.084
29	600	60	1	60	60	1:20	0.007
30	600	60	1	20	60	1:5	0.009
31	600	60	10	60	0	1:20	0.060
32	600	60	10	20	0	1:5	0.058

Table 4. Final results in terms of final Dye uptake (g_{dye}/g_{fib}).
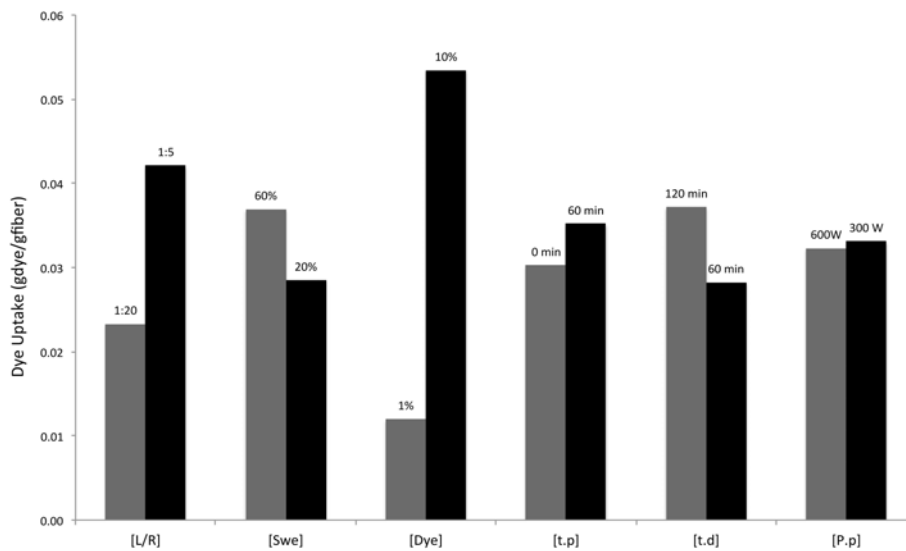
Figure 5. Influence of process parameters on Dye uptake (g_{dye}/g_{fib}) results.

Obviously, the amount of dye absorbed into the fiber depends on its initial concentration in the liquor, even though is not proportionally. To help understanding the effect of the different parameters two graphs obtained from Minitab (a software for statistical analysis of experimental data) are reported; the first one (Figure 6) is the "Pareto Chart of the Effects", that shows which are the most important parameters for our process; α is the level of significance and its value was obtained by ANOVA analysis of variance. The second one (Figure 7) gives the "Main Effects Plot", that shows the magnitude of each parameters.
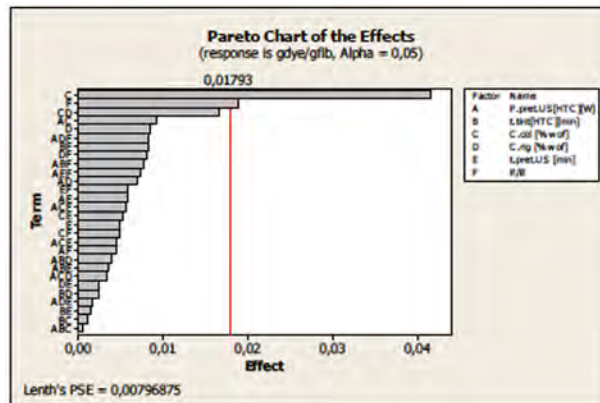
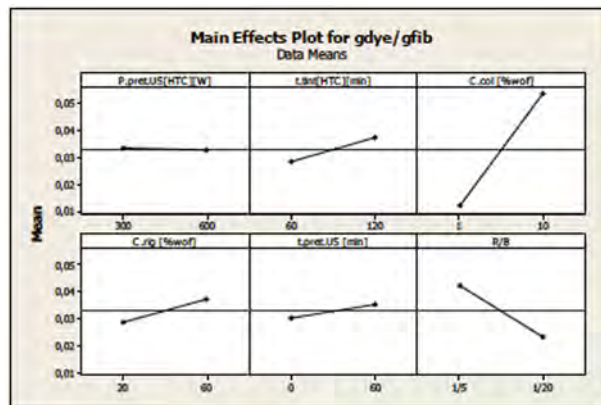Figure 6. The Pareto Chart of the Effects given by the Minitab output.

Figure 7. The Main Effects Plot given by the Minitab output.

As we can see in Figure 6, only the dye concentration and the liquor ratio are relevant variables for a dyeing process. In Figure 7 we can see that the swelling agent concentration, dyeing time and pre-treatment time have only a minor influence on dyeing while pre-treatment power has no influence at all. The low effect of the swelling agent concentration leads to the conclusion that is very important to evaluate its influence on disperse dye use (by selecting dyes with different characteristics, temperature, etc…) to minimize the carrier consumption. In our tests US pre-treatment has only a small influence on the process and this is probably due to the dye characteristics; in fact, Disperse Red 21 is one of the smallest disperse dyes and also its aggregates are quite small. Probably using disperse dyes with higher molecular weight, US pre-treatment could increase his effect.

In the end, thanks to ultrasounds, the dye diffusion into the fiber was made easier, let the dye to reaching the fiber pores more easily and, subsequently, the dye molecules undergo easier entrapping.
Two different pretreatment time-lengths were applied and two different intensities of US pretreatment were used to define whether and to what extent duration and power affected the dyeing

properties. The statistical method, based on the Minitab procedure, has provided well-defined results, thanks to which is possible to interpret the results more effectively. The most significant parameter, to obtain a good exhaustion and to enhance it, is the liquor ratio. Also the dye concentration and the swelling agent have displayed a certain effect: with a mass ratio of 60% o.w.f. of the swelling agent, an optimal exhaustion was reached; which is a value consistent with previous findings. On the contrary, the dyeing time and the pretreatment length do not seem to have influence on the results. As a general conclusion, it is expected that an ultrasound pretreatment may show their full potential with dyes characterized by a high molecular weight: in this case their aggregation would be undoubtedly critical to conceive a massive fiber uptake. The experimentation presented was carried out with small dyes. Therefore, it is possible to infer that the dye used in the tests presented, which is the one typical of the current production procedure, could not throw full light on these dyeing mechanisms.

However, in terms of quality of dyed materials, the ultrasound pretreatment allows to obtain more uniform hues, without any strikethrough or defective results if compared to the end products obtained without ultrasounds pretreatment.

References

[1] http://www.sonochemistry.info/introdution.htm

[2] A.I. Sokolov, S.S. Tumansky, Journal of Applied Chemistry, 1941, Vol. 14, pag. 843-848

[3] C. Udrescu, F. Ferrero, *Ultrasonics Sonochemistry*, 2014, Vol. 21, pag. 1477-1481.

[3] F. Ferrero, M. Periolatto, *Ultrasonics Sonochemistry*, 2012, Vol. 19, pag. 601-606.

[4] S.J. McNeil, R.A. McCall, *Ultrasonics Sonochemistry*, 2011, Vol. 18, pag. 401-406.

[5] D. Sun, Q. Guo, X. Liu, *Ultrasonics*, 2010, Vol. 50, 441-446.

[6] S.M. Burkinshaw, D.S. Jeong, Dyes and Pigments, 2012, Vol. 92, pag. 1025-1030.

Chapter 5

5. Application of Capillary Electrophoresis in basic dyes mixture separation

In this chapter an analytical separation method is applied for the separation of single components from a complex mixture of different basic dyes. This experimental work has been carried out during the abroad experience of my Ph.D, at the analytical chemistry Dept. of the University of British Columbia (U.B.C.), Vancouver, CANADA. The Capillary Electrophoresis technique has never been applied for this kind of molecules and represents a real novelty in wastewater treatment deriving from exhausted dye bath.

5.1   Introduction

The most common dyes used in the dyeing of *m*-aramid fibre, as previously mentioned in chapter 3 of this thesis, belong to the class of Basic Dyestuffs. These dyes are organic molecules soluble in water due to their cationic behaviour. These dyes have also relatively low molecular weight, an important feature to penetrate inside the small pores of the *m*-aramid fibre. Studying the kinetics with which these molecules reach the fibre could be an important step in improving our new process and the dyeing of aramid in general as well as for the E% extrapolation. Nevertheless, several concerns have to be considered:

1) The dyes are provided by International Companies that, in most cases, don't provide the molecular structure or the real structure of the molecules.
2) Usually, in a dyeing process, a tern of dyestuffs (blue, yellow and red) is used to reach the desired final colouration. In our case the final colouration depends on the ability of each dye to penetrate into the fibre and that depends primarily on their structure. When the dyes are finally extracted from the fibre calculating the E%, all the molecules are mixed and it is impossible to figure out the amount of the single dye that has been absorbed by the fibre.

For that reason is necessary to use some particular analytical techniques that allow in first instance to separate and quantify the different molecules from a complex mixture, and then to discover the real structure of these organic compounds.

In this regard, the team of Professor David Chen located in Chemistry Department of U.B.C. (University of British Columbia, Canada) is well known as expert in Capillary Electrophoresis (CE) using Mass Spectroscopy (MS) as detector.

The CE is an instrumental analysis that, in a few words, allows separating a complex mixture applying a voltage across a capillary in which analytes migrate. The separation takes place thanks to the different mass/charge ratio of the different molecules present in the mixture. Therefore, using the CE technique permits to separate the complex mixture of analytes [1].

5.2   Experimental

In order to analyse these particular substances, standard silica capillary was coated using a triple layer coating called PB-DS-PB (PolyBrene-DextraneSulfate-Polybrene) [2]. With this procedure a positive surface was given to the capillary and the analysis of cationic dyestuff molecules have been carried out. Five different dyes were then analysed:

1) Basic Yellow 21 (BY21)
2) Basic Yellow 28 (BY28)
3) Basic Blue 41 (BB41)
4) Basic Blue 03 (BB03)
5) Basic Red 23 (BR23)

These compounds were studied alone in first instance, figuring out the best operative condition of the machine and to develop an analysis method. The PDA detector (PolyDiodArray) was used for these analyses.

Methods used:

BY21: rinse with pressure for 5.0 min. at 20.0 psi of pressure, injection with pressure for 30 s at 1.0 psi of pressure, separation with voltage at 10.0 kV for 20.0 min.
BY28: rinse with pressure for 5.0 min. at 20.0 psi of pressure, injection with pressure for 30 s at 1.0 psi of pressure, separation with voltage at 10.0 kV for 20.0 min.
BB41: rinse with pressure for 5.0 min. at 20.0 psi of pressure, injection with pressure for 90 s at 1.0 psi of pressure, separation with voltage at 15.0 kV for 20.0 min.
BB03: rinse with pressure for 5.0 min. at 20.0 psi of pressure, injection with pressure for 60 s at 1.0 psi of pressure, separation with voltage at 10.0 kV for 20.0 min.

<u>*BR23*</u>: rinse with pressure for 5.0 min. at 20.0 psi of pressure, injection with pressure for 90 s at 1.0 psi of pressure, separation with voltage at 15.0 kV for 20.0 min.

A solution of 1% of HCOOH in water was used as mobile phase.

The results, presented in the following figures, showed that the dyestuffs are pure molecules with a well-defined peak having a maximum of Absorbance in typical wavelengths.
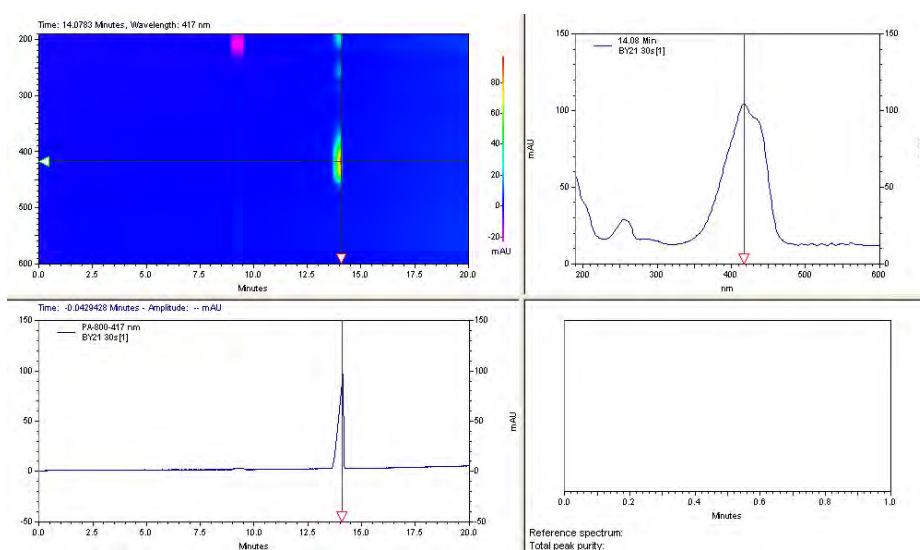

Figure 1. BY21 analysis: top left 3D graph, top right UV spectrum, bottom left electropherogram.

MAX of Absorbance for BY21: 254 nm; 417 nm.
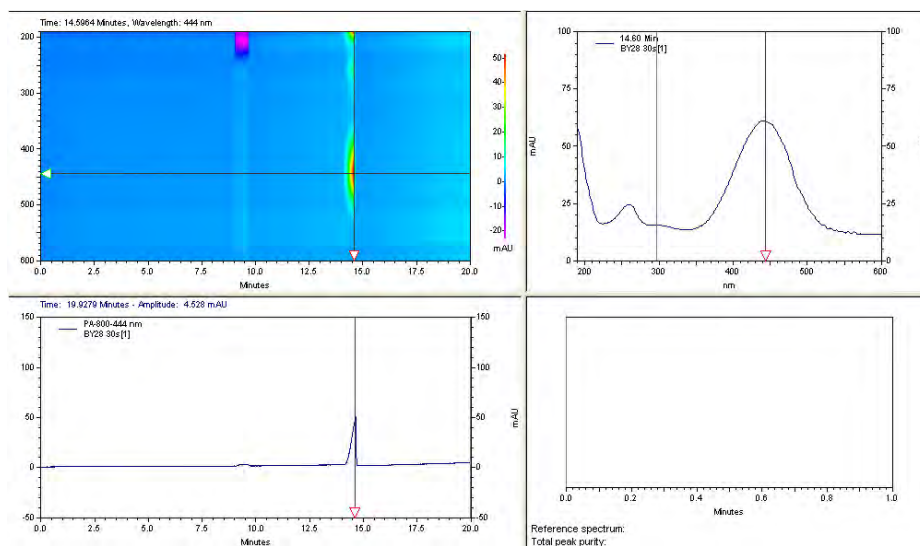
Figure 2. BY28 analysis: top left 3D graph, top right UV spectrum, bottom left electropherogram.

MAX of Absorbance for BY28: 258 nm; 444 nm.
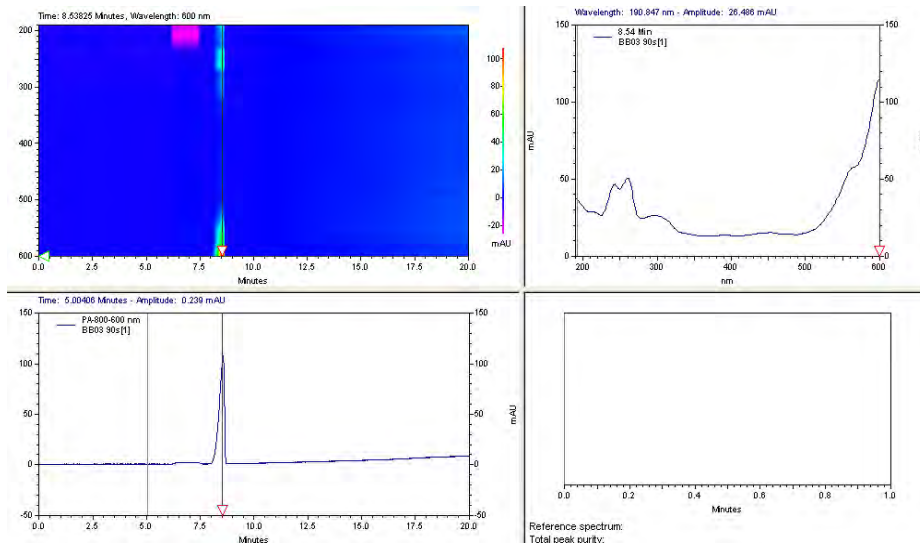
Figure 3. BB03 analysis: top left 3D graph, top right UV spectrum, bottom left electropherogram.

MAX of Absorbance for BB03: 259 nm; 599 nm.
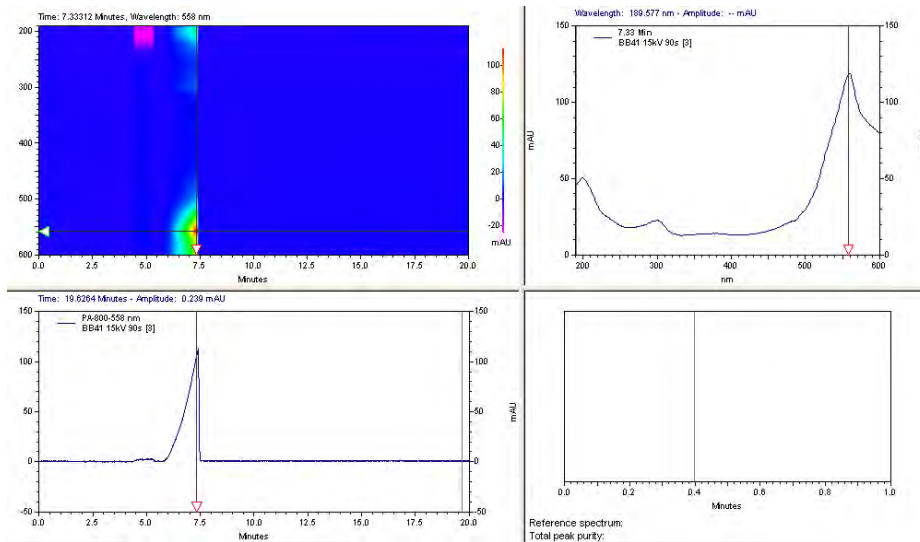
Figure 4. BB41 analysis: top left 3D graph, top right UV spectrum, bottom left electropherogram.
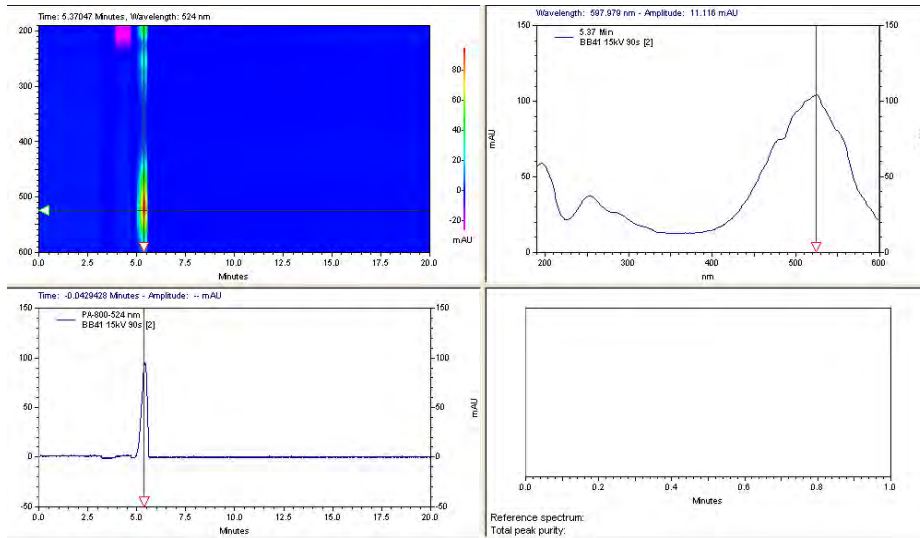
MAX of Absorbance for BB41: 195 nm; 557 nm.

Figure 6. BR23 analysis: top left 3D graph, top right UV spectrum, bottom left electropherogram.

MAX of Absorbance for BR23: 250 nm; 524 nm.

Thanks to these good results, it was possible to continue our studies with the construction of a calibration curve for each dye. For both the yellows the calibration curves perfectly fit the experimental results ($R^2 > 0.99$), for the other three dyes the R^2 of could be acceptable (Figure 7,8 and 9).
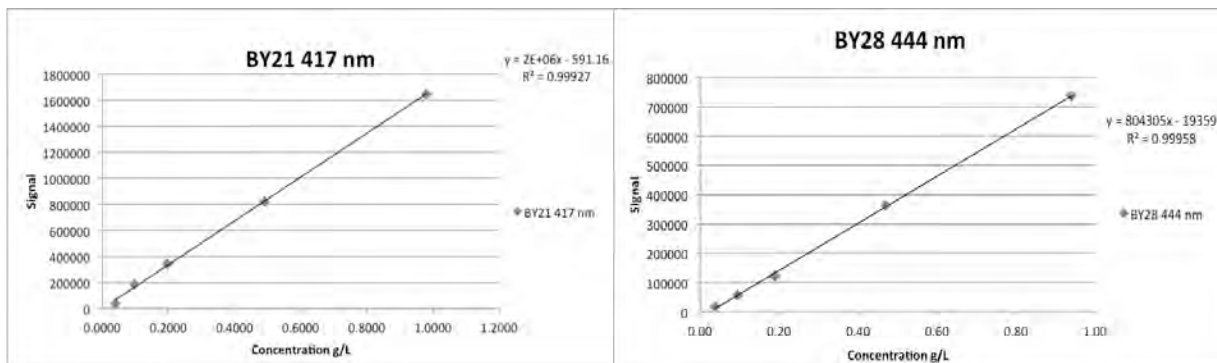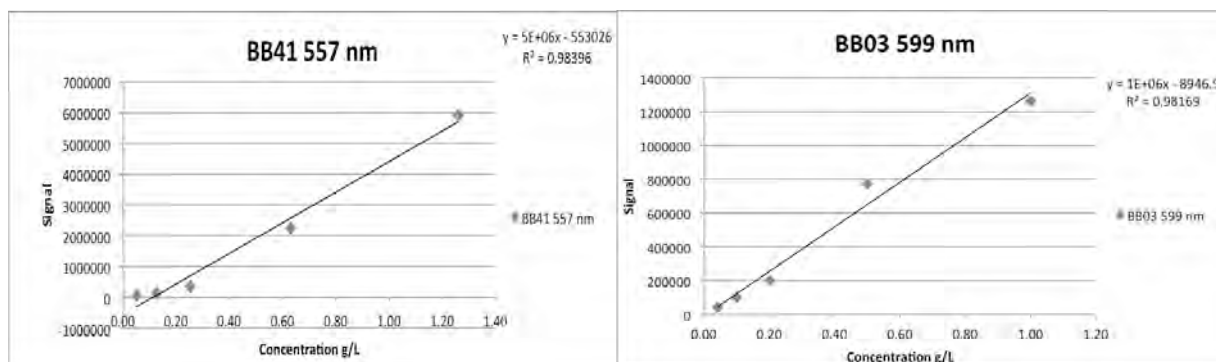

Figure 7. Calibration curves of BY21 and BY28.
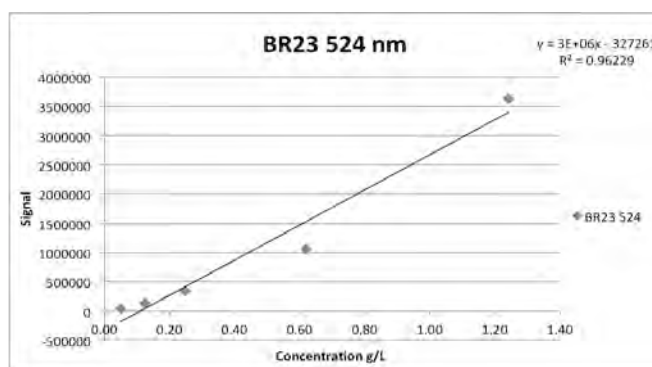
Figure 8. Calibration curves of BB03 and BB41.

Figure 9. Calibration curves of BR23.

After that, several mixtures were prepared and then separated using CE with triple layer coated capillary:

1) MIX 1: BY21 + BB41 + BR23 (rinse-pressure: 5.0 min 10.0 psi; injection-pressure: 90s, 1.0 psi; separation-voltage: 10 kV, 20.0 min.).
2) MIX 2: BY28 + BB41 + BR23 (rinse-pressure: 5.0 min 10.0 psi; injection-pressure: 60s, 1.0 psi; separation-voltage: 15 kV, 20.0 min.).
3) MIX 3: BY28 + BY21 (rinse-pressure: 5.0 min 10.0 psi; injection-pressure: 30s, 1.0 psi; separation-voltage: 10 kV, 20.0 min.)
4) MIX 4: all five (rinse-pressure: 5.0 min 10.0 psi; injection-pressure: 60s, 1.0 psi; separation-voltage: 15 kV, 20.0 min.)

The figures below described only the results of MIX 1 and MIX 2 as formed by mixing a tern of dyes (important in dyeing industry to reach all the possible colouration).
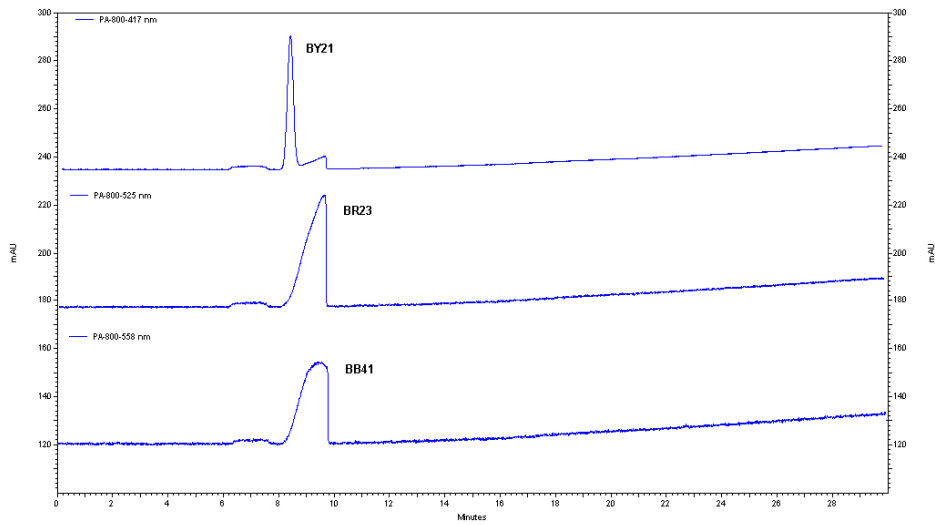
Figure 10. MIX 1 Electropherogram of the three peaks related to the three dyes used.
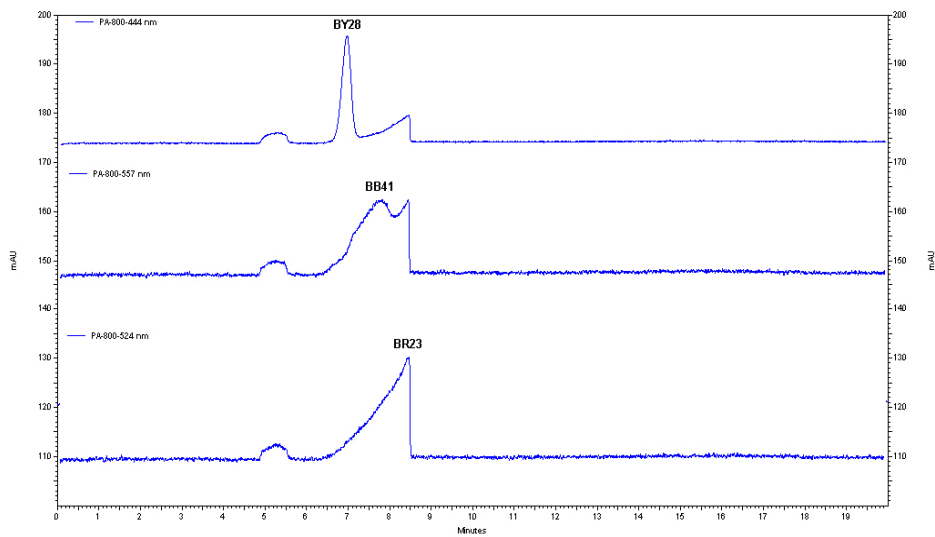

Figure 11. MIX 2 Electropherogram of the three peaks related to the three dyes used.

Looking at the figure relative to the first mixture we can say that the peak of the BY21 is well separated from the other 2, however the peaks of BB41 and BR23 are a little bit overlapped. Probably, increasing the applied voltage the overlapping could disappear. Otherwise, in MIX 2 the three peaks are well separated (separation with 15.0 of applied voltage).

The next step will be the MS analysis but unfortunately the results are not yet ready.

5.3   Final considerations

In conclusion the CE method could be used for the separation and single component quantification of complex dyes mixtures. Knowing the concentration of single components of the mixture helps to find out the kinetics mechanisms that occur during the dyeing process using more than one dye. Knowing at the beginning how much dye will penetrate and bond the fiber allows easy prediction of what will be the final coloration.

Furthermore, these colored organic molecules are used in big quantity in the dyeing of aramids and only a small percentage of these can reach the fiber, the rest is collected in waste water and has to be treated. Once again, the sustainability of the process is not compromised because knowing these parameters allows the optimizing of the initial concentrations, saving a large amount of dyes.

References

[1] James P. Landers, Handbook of Capillary and Microchip Electrophoresis and Associated Microtechniques, Chapter 1, 3rd Edition, 2008, CRC Press-New York.
[2] Ramautar R., *Electrophoresis*, 2010, Vol. 31, pag. 2319.

Conclusions

The first part of the present work has allowed defining the behavior of X-Fiper® m-aramid fiber when put in contact with a dyeing carrier, called swelling agent, which use is mandatory in obtaining acceptable results in terms of dyed product. Physical and chemical surface and bulk properties of the fiber were evaluated in order to define if some changes on these features occurred after the fiber-carrier contact during the dyeing process. No serious modifications of the fiber surface and structure have been found after testing with the two selected swelling agents (1-phenoxy-2-propanol and N-methyl formanilide). The surface morphology, tested by FT-IR and SEM, has not been altered except some roughness that, however, does not change the final hand of the fabric. Thermal properties evaluations by DSC analysis have shown important modification in the Tg pathway, this modification in higher if the carrier is still present into the fiber when the thermal analyses begin. Increasing the chain mobility, the carriers, act as plasticizers and, causing the swelling of the fiber, they change the Tg trend of the polymer. The chemical resistance of X-Fiper, after carrier treatments, is not varied. Also Tensile and mechanical properties of the yarn are maintained after any kind of treatment. However another important modification occurred in terms color alteration of the fiber, especially using N-methyl formanilide there is an accentuated "red shift" in fiber final coloration.

In Chapter 3 the dyeing process of the X-Fiper® fiber was considered in terms of thermodynamic equilibrium and kinetic studies. Two different dyes were tested: Basic Blue 41 and Disperse Red 21.
In the emulsion case, applying N-Met directly into the dye bath two different adsorption isotherm models have been applied: Langmuir and Freundlich. It has been discovered that the absorption model that better describe the adsorption of Basic Blue 41 on X-Fiper was the Freundlich one, suggesting a heterogeneous distribution of the adsorption sites that promote the development of local multilayers on the fiber. Unfortunately the kinetic study was not possible due to dye degradation, assisted by both carrier and temperature, at high initial dye concentrations. As far as the dyeing bath composition is concerned, the recipe for the optimal dyeing of the tested m-aramid fiber consists in 5% o.w.f. of BB41 concentration and 60% o.w.f. of N-Met concentration.
The dyeing process using Disperse Red 21 was evaluated applying the swelling agent as emulsion and as fiber pretreatment. For the emulsion case, the semi-empirical isotherm, proposed by Langmuir, is the most accredited in explaining the dyeing equilibrium adsorption, but only for

initial dye concentration higher than 2% o.w.f.. The recipe for the optimal dyeing of X-Fiper m-aramid fiber consists, in this case, in 5% o.w.f. of DR21 concentration and 60% o.w.f. of N-Met concentration.

A kinetic study, followed by a simulation using COMSOL Multiphysics, has been carried out in order to find some explanation about the dyeing mechanism of the studied system. Three dyeing parameters have been calculated for each initial concentration of N-methyl formanilide.

These parameters have been called:

1) SOLUBILIZING FACTOR, due to the solubilized carrier that helps the dye solubilization.
2) PRIMARY SWELLING FACTOR, due to the part of swelling agent not water solubilized that reaches and swells the fiber surface.
3) SECONDARY SWELLING FACTOR, after 40-60 minutes of dyeing the swelling agent diffuse from the solution to fiber surface starts a deeper fiber swelling, allowing more dye molecules to penetrate.

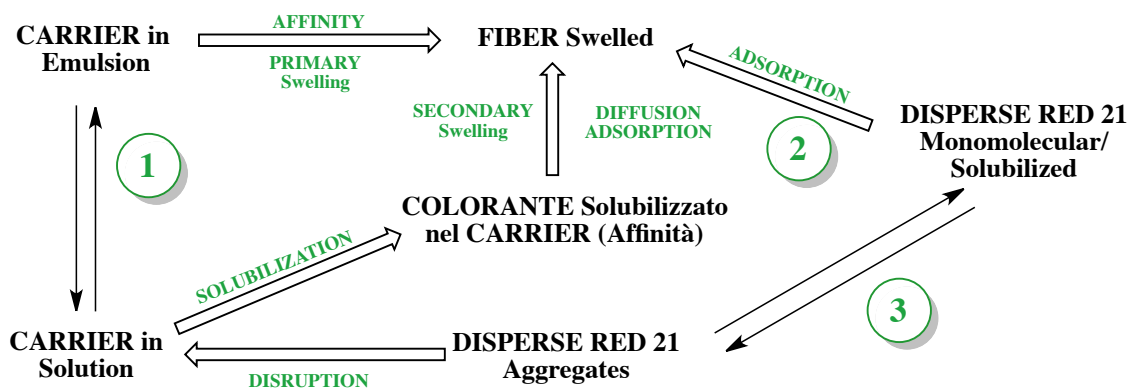After these studies a dyeing mechanism was proposed (Figure 1).

Figure 1. Proposed dyeing mechanism in the emulsion case

The first equilibrium is regulated by the initial N-Met concentration; the second by the presence of the primary swelling due to the excess of carrier (over 40% o.w.f.); the third by the initial dye concentration.

Applying N-methyl formanilide as pretreatment was not possible to apply any adsorption isotherm model, the reason is due to the dye aggregates formation at high initial dye concentration using carrier concentration lower than 60% o.w.f..

However, using 40% of carrier through the pretreatment way, it is possible to reach a dye uptake positioned exactly in the middle of the values reached using 60% and 80% o.w.f. of swelling agent through the emulsion way. This is very important from a technological ad industrial point of view, in terms of both end product hue and chemicals consumption.

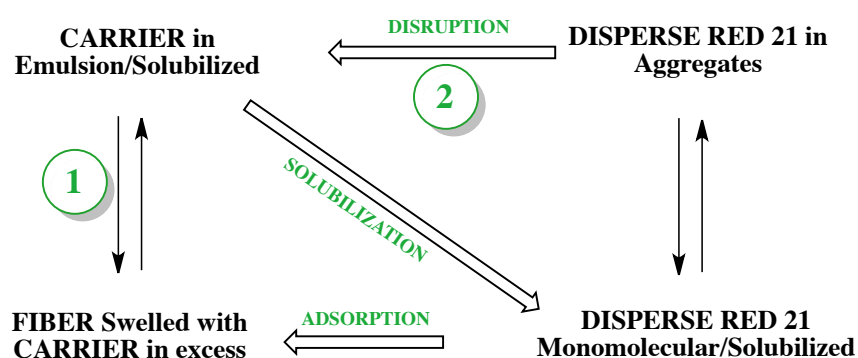A carrier mechanism of action is hypothesized and showed in Figure 2.

Figure 2. Carrier action mechanism during the process in the pre-treatment case.

The first equilibrium is regulated by the initial quantity of N-Met into the fiber, when it is in excess part of it dissolves or is emulsified into the liquor. The second equilibrium depends on the initial DR21 concentration. When the dye forms aggregates (high initial concentrations) and the N-Met is in large excess (over 40% o.w.f.), the carrier disrupts aggregates of dye favoring his solubilization and subsequently his adsorption onto the swelled fiber. The greater dye uptake, if compared to the emulsion case uptake, is explainable with the fact that the carrier, already at the beginning of the process, largely swells the fiber.

The use of ultrasounds (discussed in Chapter 4), pretreating the dyeing liquor before dyeing, can minimize the dye aggregate formation. This research work represent only a starting point and needs additional investigation and tests.
Wet processing of textiles has always had a relevant environmental impact because of important intake of pure, clean water and utilization of a variety of chemicals required to perform many functions; ultimately large volumes of problematic wastewater are produced. Over 100 years of process improvements have decreased this impact thanks to dyeing and finishing machinery upgrading (lower liquor-to-textile ratios. The textile/clothing industry remains the second largest one in the world nowadays, though we have to consider that it is progressively delocalized to underdeveloped countries, where waste treatment are inadequate, and new products, namely technical textiles, are more and more required. For this reasons the use of pretreatment, assisted by ultrasound, needs further investigation aiming to find the best pretreatments conditions.

In last chapter of this thesis, aiming also to facilitate the wastewater treatments, the use of Capillary Electrophoresis technology for the separation of complex dyes mixtures have been successfully tested.

In conclusion, the new technologies can provide the textile sector a possibility to increase its competitiveness in the European continent with new kinds of textiles in a highly engineered industrial context and contemporarily protect the surrounding environment.